Representation of color in the human retina

Brian P. Schmidt

A dissertation
submitted in partial fulfillment of the
requirements for the degree of

Doctor of Philosophy

University of Washington

2015

Reading Committee:

John (Jay) Neitz, Chair

Maureen Neitz

Fred Rieke

Program Authorized to Offer Degree:
Neuroscience

University of Washington

Abstract

Representation of color in the human retina

Brian P. Schmidt

Chair of the Supervisory Committee:
Professor John (Jay) Neitz
Department of Ophthalmology

Preceding the development of modern biological techniques, psychophysical experimentation and careful reasoning alone yielded an accurate account of human color perception predicated upon three opponent processes: blue versus yellow, red versus green and white versus black (Hurvich and Jameson, 1957). That is, when one of the opponent pairs, say blue, is perceived the other, yellow, is necessarily absent. The discovery, nearly five decades ago, by De Valois, Abramov and Jacobs of neurons early in the visual pathway with spectral characteristics similar to the theorized opponent interactions provided a plausible neurobiological substrate for hue perception (De Valois et al., 1966; Wiesel and Hubel, 1966).

In the decades since De Valois and colleagues published their seminal findings (De Valois et al., 1966), discrepancies between the properties of the lateral geniculate nucleus (LGN) cells reported and behavioral evidence have weakened the interpretation that these early visual cells directly map to human color perception (Stockman and Brainard, 2010). In particular, the contribution of S-cones to each opponent system has continued to be the subject of considerable experimental attention (Neitz and Neitz, 2011; Solomon and Lennie, 2007). On the basis of these discrepancies, De Valois and De Valois proposed a cortical transformation of LGN signals amounting to a rotation of the color axes (De Valois and De Valois, 1993).

In light of evolutionary constraints and evidence from the genetic introduction of a third class of cones to a dichromatic retina (Mancuso et al., 2009), a simplified version of the De Valois model has been proposed (Neitz and Neitz, 2011; Mancuso et al., 2010; Schmidt et al., 2014). This model posits that the spectral opponency necessary to account for hue perception is already present in a subset of midget ganglion cells. Early reports from de Monasterio et al. (1975); de Monasterio (1978) described such retinal cells, with more recent support from a large sample of LGN neurons taken by Tailby et al. (2008b). The goal of the research presented here was to directly test the hypothesis that *hue perception is mediated by a small subset of midget ganglion cells that receive S-cone input via H2 horizontal cells.*

TABLE OF CONTENTS

ACKNOWLEDGMENTS

The work presented in this document has benefited from the support of many people.

First and foremost, I am indebted to my advisors Jay and Maureen Neitz who shared with me their time, expertise and support more generously than I had any right to ask. My development as a scientist under their careful guidance can be measured in the manuscripts, presentations and grants that have resulted from the last four years of collaboration. I have developed a deep respect for them as people and scientists and will surely continue to seek their advice on matters of science and life.

I would like to thank Fred Rieke for serving on my committee and for teaching me how to think about perception from the perspective of a physicist. His skill in communicating these ideas are evident in the analysis and description of the results that follow.

In the summer of 2013 Jay and I traveled to Berkeley for a conference on myopia. Beforehand we met Austin Roorda and Ram Sabesan for lunch. Over Thai food, we (mostly Jay) pitched Ram and Austin some crazy ideas about the single cone psychophysic experiments that they had recently begun. After this meeting it was agreed that I would come down to Berkeley to participate in their studies with the hope of collecting some data that would test our ideas. The results from this collaboration are reported in Chapters 4 and 5. I am greatly in debt to Ram, Austin and Will Tuten (another student in the Roorda lab working on this project) for allowing me to take part in these exciting experiments. I have learned a great deal from all three and consider them good friends.

At the Allen Institute's Summer Course on Vision at Friday Harbor Laboratories in 2014, I had the good fortune of spending two weeks learning about the visual system from Wyeth

Bair. During that course, a fellow student, J. Patrick Weller, and I approached Wyeth with some ideas we had about using his model of the retina to study color vision. From that work Chapter 6 was born. Since those summer days, Wyeth has continued to be generous with his time as I continued to wrestle with his code.

During my time in the Neitz lab I was lucky to share the experience of being a graduate student with both Scott Greenwald and Candice Davidoff, both of whom were supportive and empathetic during the challenging times of my career as a doctoral student. I often enjoyed entertaining discussions with with Jim Kuchenbecker about vision science, life in the Neitz lab and the hoppiness of Pacific Northwest beer. I learned a great deal about retinal anatomy, physiology and Germany from sitting next to Christian Puller for the last few years of his time as a post-doc in the Neitz lab. Mike Manookin frequently answered my naive questions about retinal physiology and the early stages of a faculty career. Phanith Touch served as an excellent subject, mentee and psychophysist – together we completed the studies reported in Chapter 3. Jessica Rowlan, Toni Haun and Netta Smith collected most of the ERG and genetic data from Chapter 3 and often helped me navigate the bureaucracy of UW. To all of my lab friends, I am extremely grateful.

I'd also like to thank my past mentors, especially, Andrea Simmons at Brown University and Florian Eichler at Harvard Medical School. Both were instrumental in helping me move on to the next stage of my career and I surely would not have ever reached this stage without them.

Finally, I need to thank my family, especially my parents Cathy and Sandy who have supported nearly every decision I have made since I was a child – even when I choose the insane and vague path of pursuing a PhD in Neuroscience. And my fiancee, Anjuli Kannan who has endured all of the highs and lows of this often lonely pursuit and consistently offered me wise advice, and comic relief in exactly the right moments.

Chapter 1

INTRODUCTION

> Whether the sun's rays will be perceived as light or heat, is simply a question of whether they are perceived by the optic nerve or by the cutaneous nerves. But whether they will be perceived as light that is red or blue, and dim or bright, or as heat that is mild or intense, depends both on the nature of the radiation and the condition of the nerve. The quality of the sensation is thus in no way identical with the quality of the object by which it is aroused. Physically, it is merely an effect of the external quality on a particular nervous apparatus. The quality of the sensation is, so to speak, merely a symbol for our imagination, a sort of earmark of objective quality.
>
> - Herman von Helmholtz, Treatise on Optics Vol. II

1.1 The phenomenology of color

Color vision is the ability to distinguish a surface based on spectral content alone, independent from information about intensity. The necessary components for color vision are at least two sensors sensitive to different spectra of radiant energy and a nervous system capable of comparing the output of the two sensors. This definition is both accurate and severely impoverished.

Imagine placing your head in a smooth white sphere, with no edges or shapes, that covers your entire field of view. Now imagine that a warm red light is turned on behind you that

uniformly illuminates the sphere. You initially experience a flood of red all around you. But soon you find the redness slipping away, fading to gray; becoming dimmer and dimmer. What is happening? Why does this big ping-pong ball upturn your expectation of the perceptual world?

The situation just described is referred to as a Ganzfeld illusion (Avant, 1965), from the German for "entire field", and it serves to illustrate several important facts about color vision and human perception, in general. Firstly, the Ganzfeld illusion, like all illusions, demonstrates a scenario where the brain fails to faithfully represent the physical world. The photons that initially excited redness in your visual system were not colored red in the external world, but only in the private experience of your mind. Color, like pitch and pain, is a property of internal experience. Therefore, perception is better thought of as the brain's best guess of some physical state of the world, rather than a direct measurement as you might make in a physics experiment.

Secondly, the Ganzfeld raises an issue called adaptation or normalization. Once the red light has been turned on, the spectral content of the sphere does not change, instead the neural fibers carrying color information become less excited with each passing moment. This strategy of faithfully transmitting new, interesting information to the brain while filtering out stagnant, unchanging signals is common across sensory systems (see Webster (2011) for a review of visual adaptation, and Carandini and Heeger (2012) for a general discussion of adaptation). In the absence of new information – a change in light distribution or a moving edge – neurons tend to decrease their excitation back towards a baseline level. Adaptation focuses an organisms sensory systems on the most relevant stimuli, heightening awareness of novel information and efficiently disregarding less informative signals (Webster, 2011, 2012). The principle of normalization is critical to understanding the neural processes of color vision and will be discussed in more detail below and in Chapters 2 and 3.

There is one more lesson to take away from the Ganzfeld illusion: color vision depends

upon comparisons — in time and space. When the light was first turned on, the globe surrounding your head looked red because neurons in your visual system sensitive to long wavelengths of light were more excited than the moment before the light reached your eye. Remember color is the ability to detect changes in spectral distribution distinct from fluctuations in intensity. In other words, is there more long or short wavelength light in my visual field than a moment ago? But comparisons of spectral distribution also occur across space, as demonstrated in Fig 1.1. The same purple rectangle has been placed on two different backgrounds. On a green background, it appears brighter and pinker. The red background, by comparison, has a muted effect on the rectangle's appearance; it appears darker, deeper purple.

The explanation for why green and red backgrounds cause us to have two distinct impressions of two physically identical squares comes from the manner in which color percepts are computed by the visual system. Certain neurons are excited by long wavelengths of light and are inhibited by shorter wavelengths; producing a cell that responds robustly to red, but becomes quiet in the presence of green. The opposite scenario produces a neuron suited to signal green. The same goes for blue versus yellow cells. This principle of being excited by certain wavelengths and inhibited by others is called spectral opponency (Hurvich and Jameson, 1957; Hering, 1878) and will be elaborated in more detail below. In classical color theory the idea of spectral opponency is intertwined with the notion that there are four elementary hues – red, green, blue, and yellow – and two achromatic sensations – black and white. Each elementary color is represented in the brain by a class of neurons that compare, in time and space, the distribution of wavelengths in the world.

Continuing with this line of thinking, purple occurs when light excites both red and blue sensitive neural fibers. On a red background the spatial comparison is weak in red coding neurons; both the background and the purple rectangle contain red-inducing long wavelengths. Thus the rectangle appears dull and a deep blueish-purple. A green background

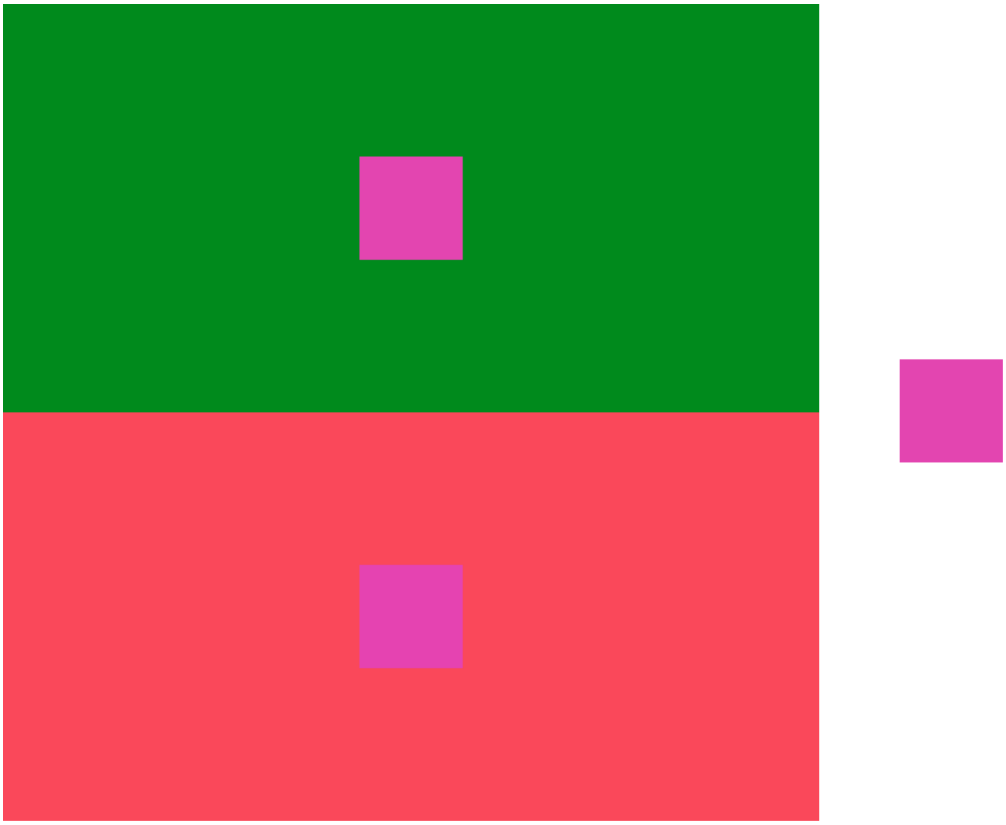

Figure 1.1: Color contrast. Two physically identical rectangles are overlaid on two background colors. Move your eyes slowly between the two. The top rectangle appears pink, while the bottom appears purple in hue. The rectangles are physically identical. The only difference is the hue of the background on which they are placed. Inspired by Albers (2013).

accentuates the redness of the center rectangle. The spatial comparison is maximized by the green background and causes the rectangle to appear less blue and more red. This example illustrates the notion of color contrast.

A final example to illustrate the basic principles of human color experience is shown in Fig 1.2. A series of alternating blue and yellow lines are overlaid on the word "vision". The letters in "vision" alternate between the red and green colors shown in the squares to the right. In other words, the light reaching your eye is the same from the letters of "vision" as from the red and green squares. However, colors you perceive are quite different. And further, the "io" in vision look different than the neighboring letters. This illusion (Shevell and Kingdom, 2008; White, 1979, 2010) calls to attention how drastically context influences the appearance of a color. The "i" and the "o" in the middle of vision appear so different from the other letters that most people would describe them as distinct colors, perhaps lime and orange, as opposed to the purple and teal of the other four letters, which themselves appear distinct from the basic red and green of the squares set on a white background. So why do these letters look so different?

One part of the explanation comes from the idea of color contrast just described above. The letters of vision are contrasted with the blue and yellow stripes. In the case of the orange "o", the letter sits above blue stripes. The contrast with blue induces some yellowness into the "o", which mixes with the red of the letter to push the color towards orange. On the other hand, the "v" and "s" of vision are contrasted with the yellow stripes underneath them, which elicits a weak sense of blue into the redness, thus yielding a purple color. The same contrast effects are also at play with the remaining green tinted letters ("i", "i" and "n"). Yet, as satisfying as this sounds, the magnitude of this contrast effect is not enough to explain the strength of the illusory colors we perceive.

The second component of the explanation for this illusion is hinted at in the color names used to describe the appearance of the letters. The pure red and green colors shown in the

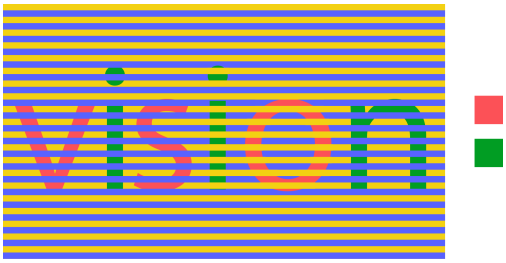

Figure 1.2: Color assimilation. The letters in vision appear to pass beneath the blue stripes and above the yellow stripes of the background. The two exceptions, the "i" and "o", are reversed and consequently take on very different color appearance. This chromatic form of the Munker-White illusion was inspired by Shevell and Kingdom (2008).

squares to the right are being mixed at some level in the brain with the blue or yellow lines that cross over the letters. This phenomenon is called assimilation and it is familiar to those in textile industry (White, 2010). When blue overlays the red and green letters, they become purple and teal, respectively, while yellow creates the orange and lime that we see in the "io". It is the synergistic effects of contrast and assimilation, acting in the same direction, that produce the strong illusory colors seen in this demonstration.

One way to demonstrate the importance of both assimilation and contrast in this illusion is to vary the size of the image. Had the same image been printed to encompass this entire page the effect of the illusion would be reduced: the "io" of vision would look more like the other letters and all of the letters would look more like pure red and green. You can prove this to yourself by zooming into the image on a digital copy of this document. As the letters and stripes become larger, the colors of the letters become more and more similar. This is because the effects of assimilation are diminished. With only the influence of chromatic contrast, the illusion becomes weaker (Anstis, 2006). The dependence of these illusory colors on spatial scale highlights the importance of this dimension to the neurons responsible for

generating color percepts.

One final, surprising aspect of this illusion is that some of the effects may be seen even if the stripes and letters are shown separately to each eye (Shevell and Kingdom, 2008). For instance, imagine that the stripes were presented to your left eye, while the letters were projected into your right eye. The information necessary to produce this illusion would, in this case, be separated in the nervous system until the signals from your two eyes are combined in cortex. That the illusion might (this has been suggested, not proven) partly persists despite this split presentation indicates that some of the neural computation necessary to produce the illusion may occur only after the signals from the two eyes are brought together (Shevell and Wei, 2000). Somewhere beyond the initial computations of color – red versus green, blue versus yellow – in the retina, the brain combines information from both eyes to produce a binocular, three-dimensional representation of the world. If it is true that the illusion persists in this split eye presentation, then the final illusory colors in Fig 1.2 are not born in the peripheral neurons of the retina, but higher up in visual processing. The focus of the current work, however, is on the earlier, simpler stages of color coding, before the murky depths of cortex season our perceptions.

1.2 Cone opsins

The illusions discussed above reveal several fundamental features of how the visual system assigns color to objects. All three examples were curious cases where our perceptions did not match the physical light impinging upon our eyes. Despite cases such as these where color appears inappropriately assigned, color vision is useful to the organisms that possess it. The most concrete proof of its utility is the prevalence of color vision across the animal kingdom (Jacobs, 2009, 2008). Although not universal, a wide variety of species possess some capacity to discriminate surfaces on the basis of spectral content alone (Jacobs, 2009).

The manner in which color vision is achieved, however, varies widely (Kelber and Osorio,

2010). The first stage of color vision is the transduction of radiant energy into chemical and electrical signals in photoreceptors of the eye. Therefore, the number of distinct photoreceptor types and their sensitivity properties are defining features of every color vision system. Some species of birds, for example, have four classes of photoreceptors. Additionally many birds have evolved oil droplets in the tips of their photoreceptors, which act as filters that could theoretically enhance color discrimination (Bowmaker et al., 1997; Vorobyev et al., 1998; Vorobyev, 2003). A genus of particularly colorful jumping spiders (family *Salticidae*, genus *Habronattus*) have four eyes, with two principle eyes that serve spatial and color vision. Like most spiders they possess two types of photoreceptors, but unlike most spiders, *Habronattus* possess a long-pass (red) filter that shifts the sensitivity of a subset of middle wavelength sensitive photoreceptors to longer wavelengths, thereby creating three classes of cones (Zurek et al., 2015). The compound eye of the fly, like birds, also contains four types of photoreceptors (Behnia and Desplan, 2015). Perhaps most varied of all are marine animals, who have adopted a wide variety of strategies to sense color in their environment depending on their ecological niche (Marshall et al., 2015). Clearly, the ability to distinguish differences in the distribution of spectral energy must provide important information for analyzing the visual environment. But exactly how the computations of color vision are carried out depends on both evolutionary happenstance and environmental demands places on the organism. The present work focuses on how humans and our primate relatives have solved the task of distinguishing colors.

Normal human vision is trichromatic. In general, any light, regardless of spectral composition, can be matched with a mixture of just three other lights. Humans and some primates have trichromatic vision because they possess three types of cone photoreceptors: long (L), middle (M) and short (S) wavelength sensitive (Fig 1.3), which are maximally sensitive to 559, 530 and 420 nm, respectively. In the case of humans and other primates with only two photoreceptors, just two lights are required to make a match to a test light and those

individuals have dichromatic vision. Today these facts are common textbook knowledge, but the scientific path towards the discovery of trichromacy in humans is an interesting story in its own right (Mollon, 2003). Skipping the history lesson for now, by the middle of the 20th century, a long progression of increasingly sophisticated thinking and experimental paradigms had led to a consensus that human color vision is mediated by three types of photoreceptors (Mollon, 2003). Direct evidence was provided by Nathans et al. (1986b) who isolated and sequenced the genes that code for the human cone opsins, which determine the sensitivity of each cone. Around the same time, Schnapf et al. (1987) used a suction electrode technique to definitively characterize the sensitivity of individual cones and demonstrated that individual cones confuse fluctuations in intensity with changes in wavelength; an idea known as the principle of univariance (Rushton, 1972). Schnapf's experiments together with Nathans' discovery greatly facilitated appreciation of the early stages of color perception and the evolution of this modality (Neitz and Neitz, 2011; Nathans et al., 1986b).

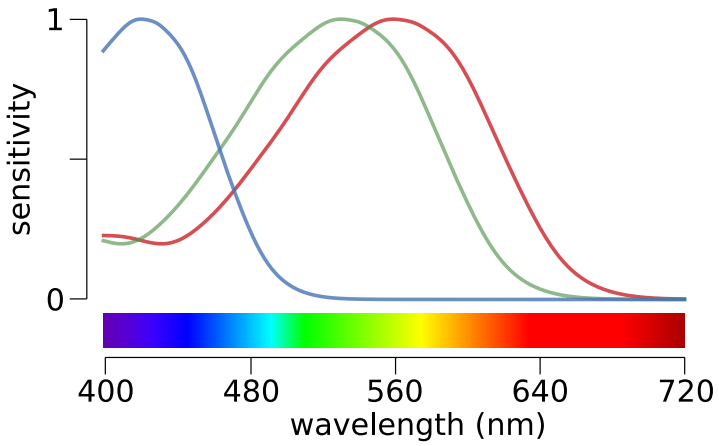

Figure 1.3: Human spectral sensitivity functions (Carroll et al., 2000). Blue line = S-cones, Green = M-cones, Red = L-cones.

The opsin genes in Old World (catarrhine) primates are now understood to represent an evolutionary lineage that diverged from New World (platyrrhine) monkeys about 30-60 million years ago (Jacobs, 2008; Neitz and Neitz, 2011; Nathans et al., 1986b; Nathans, 1999). In most New World monkeys, all males and some of the females are dichromats, while the remaining females (often around 2/3) are trichromats. The discrepancy of color vision phenotype between the sexes occurs because the genes that code for the L and M-opsins reside on the X-chromosome. Typically, three (to five) types of L/M-opsins exist in the population, each with slightly different peak sensitivities (e.g. 535, 550 and 562 nm in Cebus and squirrel monkeys) (Jacobs, 2009). Males, with their single X-chromosome, can only have one of the three genes. Along with their S-opsin, encoded on chromosome 7 (Nathans et al., 1986b), this scenario results in dichromatic vision for males. Females, on the other hand, have two L/M-opsin genes that depend on the genotype of her parents. As a result, many females end up with two L/M-opsin genes with different sensitivities, producing trichromatic color vision. In Old World primates, the L- and M-opsin genes are aligned in a head-to-tail tandem array on the X-chromosome. This arrangement is believed to have arisen from a gene duplication event several million years ago that placed two L/M-opsin genes back-to-back (Nathans et al., 1986b). Presumably, multiple types of L/M-opsin with distinct sensitivity peaks already existed in the population, as is the case with modern New World primates. The serendipitous duplication event then served to confer routine trichromacy on Old World primates (Neitz and Neitz, 2011) – both males and females suddenly had at least two L/M-opsin genes.

The evolution of distinct opsin genes sensitive to long and middle wavelengths is thought to have occurred through a series of single nucleotide base changes. In fact, as few as three nucleotide base changes in the opsin sequence are sufficient to account for the shift in peak spectral sensitivity of the M-opsin towards 530 nm (Asenjo et al., 1994; Neitz et al., 1991), where it typically sits in catarrhines. Thus, the L- and M-opsin genes share very similar

DNA sequences (98% identical) in both primate lineages (Neitz and Neitz, 2011). Combined with their arrangement on the X-chromosome in Old World primates, the homology between opsin sequences allows for frequent unfavorable polymorphisms, due to misalignments and cross-over events, during meiosis (Nathans et al., 1986a; Neitz and Neitz, 2011). Therefore the duplication event, while favorably producing routine trichromacy, did not eliminate the risk of color deficiencies.

1.3 Color deficiency

In males of European descent, the incidence of color vision deficiencies is estimated to be 7.4% (Sharpe et al., 1999). Two degrees of congenital color vision deficiency exist. Individuals that possess two normal cones, but have a third with a peak sensitivity that is abnormally close to one of the other two are called anomalous trichromats (Neitz et al., 1996). These individuals have trichromatic color vision, but their ability to discriminate color differences is reduced relative to people with normal color vision. The second form of color deficiency, dichromacy, results from the absence of one class of cone opsin (Nathans et al., 1986a). The high rate of color deficiencies raises the issue of whether trichromacy is truly advantageous. Indeed, color deficient individuals are often unaware of their sensory deficiency for many years. Why then did catarrhines evolve and maintain a third type of cone? To answer this question, first we must briefly consider color discrimination and dimensionality, and the ecology of primates.

Perhaps the best place to start a discussion of color dimensionality is with the mantis shrimp. The mantis shrimp is often cited for its impressive array of spectrally tuned detectors (Marshall and Oberwinkler, 1999; Cronin and Marshall, 1989; Bok et al., 2014). Some years ago, mantis shrimp was found to have 12 spectrally distinct types of photoreceptors. The long standing assumption then was that mantis shrimp enjoys 12 dimensional color vision, vastly out doing lowly trichromatic humans. However, careful behavioral experiments in fact

revealed the mantis (Thoen et al., 2014) possesses poor color discrimination ability despite its abundance of detectors.

The mantis shrimp example leads to an important point: the number of detectors possessed by a sensory system – be it vision, olfaction, etc – is not the only relevant parameter in determining the richness or dimensionality of that system. Wavelength is a continuous variable and, therefore, theoretically an infinite number of distributions and hence colors are possible. Because humans possess only three types of cones and these cones obey the principle of univariance (Rushton, 1972; Schnapf et al., 1987), we are limited to a maximum of three dimensional color vision. In other words, many physically different distributions of light will look indistinguishable in color because the lights produce identical ratios of activation in the three classes of cones. No amount of neural processing can recover the differences in the two lights. Therefore, the number of receptors in a system places a hard limit on the number of sensations that are possible, but an appropriate nervous system is still required to realize that possibility.

In theory, the mantis shrimp could utilize all 12 of its receptors and enjoy dodecachromatic color vision (12 dimensional). But the mantis shrimp instead discriminates wavelength about 10 times worse than humans (Thoen et al., 2014). The paucity of color experience in mantis indicates that its visual system is structured very differently than primates. The mantis lacks the neural circuits required to compare the output of its 12 different photoreceptors and confer dodecachromacy. Presumably, ecological and behavioral constraints on the mantis shrimp have caused it to evolve a different strategy (Meister, 2015). Perhaps it uses its 12 detectors in a reflex-like manner to evade predators or detect prey with specific color signatures. Clearly, color vision serves a different role in the visual life of mantis shrimp. An example of this principle can also be found in the human eye. In addition to the S-, M- and L-opsins, humans also express rhodopsin in rods and melanopsin in a small population of intrinsically photosensitive ganglion cells. Rods are used for seeing at night, while melanopsin

expressing cells are thought to contribute to circadian rhythms. Neither rhodopsin (under daylight conditions) nor melanopsin contributes to the appearance of colors. Therefore, while melanopsin, M-opsin and rhodopsin all have different spectral peaks, they serve entirely distinct visual capacities and their spectral peaks are merely incidental.

What then do primates use color for and why was the addition of a third cone advantageous? An early suggestion and persistent preoccupation with those interested in this question pertains to fruit. This theory proposes that trichromacy provides an improvement in the ability to discriminate the redness or yellowness of a ripe fruit against the dappled background of green leaves (Mollon, 1989; Osorio and Vorobyev, 1996; Osorio et al., 2004; Regan et al., 2001). Individuals possessing three cones would be superior at detecting ripe fruit at a distance and thus obtaining greater nutrients. In the case when food is scarce and the pressures of evolution are highest, this advantage could be enough to select for trichromacy over dichromacy. Moreover, the consumption of colorful fruit serves to disperse the seeds from those fruits, perhaps leading to a co-evolution of colored fruit and primate vision (Regan et al., 2001). Tidy as this sounds, not everyone is convinced. Many trichromatic primates eat leaves when fruit is scarce or unavailable (Dominy and Lucas, 2001; Lucas et al., 2003). Therefore, the discrimination of color might be important for successfully identifying leaves with the highest nutritional value. Either way, observations of monkey troupes containing both trichromats and dichromats in captivity has offered some evidence for superior foraging success in trichromats (Caine and Mundy, 2000). However, long-term fitness of monkeys in the wild was not predicted by color vision dimensionality (Fedigan et al., 2014), highlighting the subtlety of teasing apart this complicated issue.

Most likely, the advantages of trichromacy are motley and manifold. In addition to identifying fruits, adding colors to the visual repertoire of an animal provides novel dimensions for identifying objects of all kinds (Wurm et al., 1993; Gegenfurtner and Rieger, 2000), may aid in the segregating of scenes (Conway, 2009; Mollon, 1989; Hansen and Gegenfurtner,

2006) and the remembrance of objects (Hansen et al., 2006; Wichmann et al., 2002). Finally, increased ability to detect changes in skin complexion may provide cues important in determining social, health and reproductive status (Mollon, 1989). Clearly, conclusively demonstrating the evolutionary advantage of color vision is challenging. Yet, the widespread adoption of trichromacy in primate lineages (Jacobs, 2008) unequivocally points to an increased level of fitness in those who possess it. Unlike Western cultures where the rate of color deficiency is high, the prevalence of dichromacy in catarrhines has been estimated at 0.002% (Jacobs, 2008). Thus, the relatively high prevalence of color deficiency in Western societies (Sharpe et al., 1999) is likely a consequence of relaxation of evolutionary pressures.

1.4 The theory of color opponency

Theoretical computations indicate that color normal humans can distinguish around 2 million shades of color (Linhares et al., 2008). Despite this large capacity for discerning color tones, when describing the appearance of an object, humans tend to break up this huge space of colors into a much smaller group of categories, such as "blue" and "green", typically numbering on the order of 8-15 (Lindsey and Brown, 2014, 2006, 2009; Webster and Kay, 2014, 2012). The categorization of color appearance leads to two observations. Firstly, discriminating one color from another is a distinctly different from describing the appearance of a color. There is no reason, as will be discussed in Chapter 2, to believe that these two tasks are carried out by the same brain circuitry. Secondly, only a small number of colors are necessary to describe and account for all of the hues we perceive in the natural world. In fact, from those we can posit that only six of them are essential: red, green, blue, yellow, black and white (Sternheim and Boynton, 1966). These colors are referred to as the unique hues and they been instrumental in the development of modern theories of color vision.

The dominant explanation of human color vision is known as the theory of color opponency. The example presented in Fig 1.1 introduced this idea. The central tenets of color

opponency have their origins in the observations of Ewald Hering (Hering, 1878, 1964) from the late 1800s. Using introspection, Hering noted two peculiar aspects of his perception of color. Firstly he observed that certain colors never appear together. Red, for instance, does not occur simultaneously with green. In fact, the addition of a small amount of green light to a red light will diminish the redness of the mixture. Secondly, Hering pointed out that a certain colors appear to be phenomenologically unmixed or pure. Orange can be satisfactorily described as a combination of red and yellow (Sternheim and Boynton, 1966). But red and yellow do not appear to be composed of any other colors. Hering called these six colors *urfarben*, or primary colors, and today they are referred to as the unique hues. The unique hues are irreducible percepts — red, green, blue, yellow, black and white cannot be described in terms of other colors. All other colors can be constructed by adding together the unique hues in differing proportions. Cerulean is a blue tinged with green, while cyan also contains blue and green, but in more equal proportions.

Earlier ideas about color vision that predominated at the time of Hering were concerned with the idea of trichromacy (Mollon, 2003). In 1801, Thomas Young (Young, 1801) had the critical insight that the optics of the eye will focus any point in space onto only a single point on the retina. Consequently, only a single receptor (he called them particles) in the retina senses any point in space. Young, therefore, reasoned that only a small number of receptors, three in fact, exist in the retina to sense color. Were the number to be any larger, humans would be blind to many colors in small regions of visual space. Young's ideas were further developed into a formal theory by Maxwell in 1855 (Maxwell, 1855) and then Helmholtz in 1866 (Helmholtz, 1924). The latter was a student of Johannes Müller, who developed the Doctrine of Specific Nerve Energies. Müller's Doctrine stated that the type of sensation – touch, vision, audition, etc – was determined by the neural fibers that carried the information. The optic nerve carries visual information and nothing else. This is why applying pressure to ones eye elicits visual phosphenes. Helmholtz took the reasoning of his mentor one step

further to relate the activity of neurons to the quality of sensation. Beginning with Young's observation that there exist three receptors in the eye – one for long, medium and short wavelengths of light – Helmholtz argued that the excitation of one of these receptors by the proper wavelength would give rise to the sensation of red, green and violet. Thus whether a light is red, green or violet is a merely consequence of the receptor that is stimulated. Each receptor, Helmholtz posited, forms a "labeled line" that carries that information down the optic nerve and into the brain (Norrsell et al., 1999).

During his lifetime Hering's observations about the nature of color perception stood in opposition to the Young-Maxwell-Helmholtz theory. By the 1950s, studies of color matching and color deficiency had solidified the existence of three cone photoreceptors and their relative sensitivity to spectral lights. But the debate over whether the three cones directly provided information to the brain about the color of objects in the world remained active until the studies of Hurvich and Jameson (1957). Building on the ideas of Hering, Hurvich and Jameson developed an experimental method, called hue cancellation, to quantify the appearance of light. In this paradigm, a volunteer was shown a mixture of two lights; for instance, a red and green appearing light. The objective of the experiment was then to change the intensity of one of the lights, say green, until the mixture appeared neither red nor green. By keeping the intensity of the red light fixed and varying the wavelength of the second light throughout the visible spectrum, Hurvich and Jameson (1957) quantified the strength of the red/green and blue/yellow systems. The remarkable and insightful aspect of these studies was that Hurvich and Jameson were able to predict, with reasonable accuracy, their hue cancellation results by adding and subtracting the cone spectral sensitivity curves.

Example hue cancellation curves are shown in Fig 1.4. These curves are theoretical but serve to demonstrate the insight revealed by these experiments. Hurvich and Jameson noticed that their blue/yellow cancellation data could be captured by taking the differences of S-cone sensitivity functions from the sum of L- and M-cones. The red/green data was

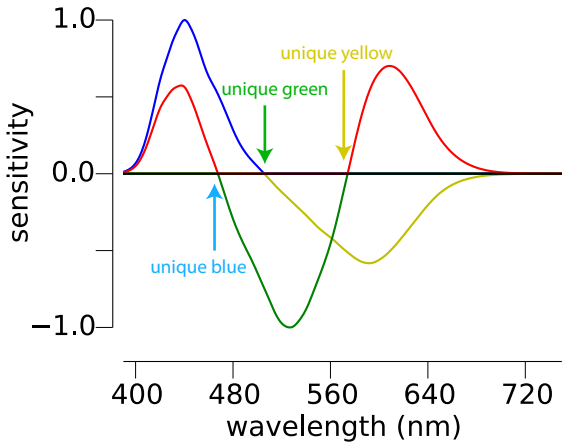

Figure 1.4: Hue cancellation curves. These theoretical curves were constructed by adding and subtracting the cone sensitivity functions shown in Fig 1.3 after correcting for lens and macular pigment filtering.

similarly well predicted by the subtraction of M-cones from the sum of S- and L-cones. Importantly, Hurvich and Jameson (1957) noted these comparisons of cone signals could be carried out in neurons early in the visual pathway. Thus, Hurvich and Jameson resolved the Hering versus Young-Maxwell-Helmholtz debate by proving both theories of color vision were partially correct. Young-Maxwell-Helmholtz were accurate in proposing that three receptors mediate color vision. And Hering was correct in supposing that two opponent mechanisms accounted for our four basic hue sensations (plus the two non-opponent sensations of black and white).

Yet the conclusions of Hurvich and Jameson were not widely adopted until the discovery of spectral opponency in the primate visual system in the mid-1960s (Jacobs, 2014). In a seminal study, De Valois, Abramov and Jacobs (De Valois et al., 1966) recorded the response of neurons in lateral geniculate nucleus (LGN) in macaque monkey. They found four groups of opponent cells that they argued corresponded to the primary hues of Hering-Hurvich-

Jameson. Physiologist and psychologist were quick to adopt the idea that the these cells were directly responsible for mediating our percepts of red, green, blue and yellow (Valberg, 2001). Returning to the idea of unique hues, their importance in understanding the neurophysiological basis of color vision now becomes clear. The unique hues occur at the locations in the spectrum (Fig 1.4) where one of the systems has a sensitivity of zero. Unique blue for example, occurs around 470 nm where the red/green system is not sensitive, thus appearing neither red nor green.

1.5 In defense of unique hues

Despite the apparent success of this line of inquiry, in recent decades, the very existence of unique hues has provoked substantial debate (Sternheim and Boynton, 1966; Vos, 1986; Logvinenko and Geithner, 2013; Logvinenko and Hutchinson, 2007; Logvinenko, 2012; Shamey et al., 2015; Bosten and Boehm, 2014; Saunders, 1997; Wool et al., 2015; Witzel and Franklin, 2014). Skeptics contend the unique hues, should they exist, must inhabit a privileged state in our perceptual world and thus in the neural code of the visual system (Stoughton and Conway, 2008). To prove this point, investigators have designed experiments seeking to reveal saliency (Wool et al., 2015; Witzel and Franklin, 2014) or reduced variability in the selection (Bosten and Lawrance-Owen, 2014) and naming of unique hues (Bosten and Boehm, 2014). Failure to find a special status of certain hues is leveraged as evidence against the existence of unique hues.

Taking a step back, it is firstly clear that caution should be exercised when interpreting these results. The usage of the word "unique" to describe the status of certain hues can be misleading. The theory of color opponency, as developed by Hurvich and Jameson, regarded the unique hues as null points of two dichromatic, opponent systems. There was no special status proposed in the representation of these hues nor have they historically been thought to represent the peak sensitivity of the red/green and blue/yellow systems that might lead

to particularly saturated or salient percepts (Hurvich and Jameson, 1957). On the contrary, they correspond to regions of middling sensitivity in the opponent systems, as is especially the case with unique blue and yellow (Fig 1.4). Instead, the introspective observation that certain hues are pure was merely a spark that led Hering to produce a hypothesis about how a nervous system, with limited hardware, could plausibly assign two million shades of color to objects in the world.

The lasting success and overwhelming simplicity of his hypothesis is a testament to its power. Objectively, there is further reason to believe Hering's proposal that certain hues are fundamentally uncontaminated. Recently, a technique called partial hue matching was developed by Logvinenko and Beattie (2011). This task requires observers to compare two colors and indicate whether color **A** and **B** share a common hue. The task requires no knowledge of color names or a man named Ewald (Hering). If there is a universal truth to the notion that certain hues are pure, the four unique hues (plus black and white) should not be matched to any other colors. Indeed, the results, with few exceptions, confirm this prediction (Logvinenko and Beattie, 2011; Logvinenko and Geithner, 2013; Shamey et al., 2015). Decades of experiments have produced results predicted from the assumption that the unique hues are a fundamental aspect of our experience of color (Stockman and Brainard, 2010). Logvinenko's studies add to this work, a direct confirmation that certain hues appear phenomenologically irreducible. The strong position taken by those arguing against the existence of pure hues is logically tenuous. *Argumentum ad ignorantiam*, or an argument appealing to ignorance, is a fallacy in logic — absence of evidence is not evidence of absence. The positive findings of Logvinenko and many others offer firm ground from which to appeal to the notion of unique hues.

Yet to be fair to other points of view, at least some of the authors mentioned above have been motivated by modern results from extrastriate visual cortex (Zaidi et al., 2014). There, neurons with sharp tunings for very specific hues have been repeatedly described

(Conway, 2013; Conway et al., 2007; Zeki, 1980). Moreover, an organized continuum of cells with preferences for each position on the color wheel was recently discovered (Li et al., 2014a). Whether or not these cells represent the neural basis of the colors we see when light impinges upon our eyes is impossible to know — for that we would require verbal reports from our monkey subjects. But in the end, the existence of these cells does not negate the fundamental truths that our perception of color is organized in an opponent fashion and that certain hues appear more simple than others. The preferences of neurons in extrastriate areas may perhaps be manifested in higher level perceptual phenomena, but remain quelled when a subject is asked to identify the wavelength of pure yellow. As mentioned earlier, the focus of the current body of work is on the early stages of color coding. So while the computations of higher centers in the brain are undeniably interesting and important, for now, I will leave unturned these tantalizing puzzles.

1.6 Normalization

One aspect of color appearance that the traditional Hering-Hurvich-Jameson model does not accurately predict are the effects of long term history. Staring at a bright long wavelength (red) light will cause the appearance of a subsequently presented object to appear less red or, in some cases, even green. The reason for this change in color is that visual neurons adapt or normalize themselves (remember the Ganzfeld) to the history of stimuli recently seen (Webster, 2011). For cases of short term exposure to a bright red light, for example, classical theories perform reasonably well at predicting subsequent perception (Hurvich and Jameson, 1957). However, the influence of history on the perceptual experience of a light extends far into the past.

The long term temporal relationship between color appearance and normalization was studied by Neitz et al. (2002), who altered the chromatic environment of subjects with colored lenses. After wearing colored lenses for 3-4 days, subjects reported the location of

pure yellow. Neitz et al. (2002) observed that the wavelength selected as pure yellow was significantly changed after about three days of lens wear. Moreover, depending upon whether the subject had been donning red or green lenses predicted the direction of the shift relative to a baseline condition. A related study on subjects before and after removal of a cataract produced similar results (Delahunt et al., 2004).

More recently, the impact of the chromatic environment on color appearance under more natural conditions was examined by Welbourne et al. (2015). The authors measured color appearance behavior in a group of volunteers during the winter and summer in England. Importantly, during the summer months changes in foliage exposed all subjects to a greener environment during their day-to-day lives. Welbourne et al. (2015) discovered a correlation between the greener environment and the location of unique yellow. The relationship they discovered was analogous to the older experimental results (Neitz et al., 2002), further highlighting the importance of the environment in normalizing color mechanisms under natural conditions.

Previously, the idea had been proposed that the environment may be the sole cause for the location and very existence of pure hues (Mollon and Jordan, 1997; Mollon, 2006; Philipona and Regan, 2006). Together, the above studies add weight to the notion that the location of unique hues are a consequence of the both the environment and neural wiring. In each case, a neural mechanism comparing the relative activity of cone signals predicted the change in color appearance after incorporating a normalization to the mean chromaticity of the environment (Neitz et al., 2002; Delahunt et al., 2004; Welbourne et al., 2015). In other words, as the mean chromaticity shifted, the neurons signaling red and green adapted to avoid signaling in response to the average distribution of wavelengths, much like the short term adaptation in a Ganzfeld situation. As a consequence of this normalization, the null point of this system, unique yellow, also shifted slightly. Thus, the environment plays an important role in setting how we see colors, but so too does the circuitry that compares the

output of cones.

1.7 The trichromatic cone mosaic

An example of a human cone mosaic imaged in a living eye with an adaptive optics scanning laser ophthalmoscope (AOSLO) (Roorda et al., 2002; Roorda, 2011; Liang et al., 1997) is shown in Fig 6.7. The fovea, the area in the human retina that gives us our highest acuity, is darker than the surrounding regions due to the small size of the cones in this region. The regularly arranged white dots in the rest of the image are cone photoreceptors. One degree rings provide a sense of how many cones sample visual space (one degree of visual angle is approximately the size of your thumb held at arms length). The white square indicates a small region of about 700 cones that have been classified as L, M or S. An enlarged image of this region is shown below, with the cone types demarcated by false colors. The classification of each cone type was obtained with a method first developed by Roorda and Williams (1999) based on the principles of densitometry (Rushton, 1972).

The capacity to routinely perform high resolution imaging of the living human eye, as shown in Fig 6.7, is a remarkable achievement of modern optics. Other sensory systems, hidden by opaque organ structures, are inaccessible in the living human. This capacity to study the cellular structure of the human retina has greatly accelerated our appreciation of normal and diseased states (Roorda, 2011; Williams, 2011). Additionally, the ability to study the cone mosaic at high resolution raises another aspect of color vision not predicted by classical models: the high degree of variability in the human cone mosaic. The opponent mechanisms as originally defined by Hurvich and Jameson (1957, 1955) added and subtracted cone signals with fixed weights (multipliers) modifying the output of each cone. The assumption around this time was that the relative number of L-, M- and S-cones would vary little in their arrangement and proportions between people with normal color vision: variability in cone weights from person to person was largely unappreciated. Yet, even around that time,

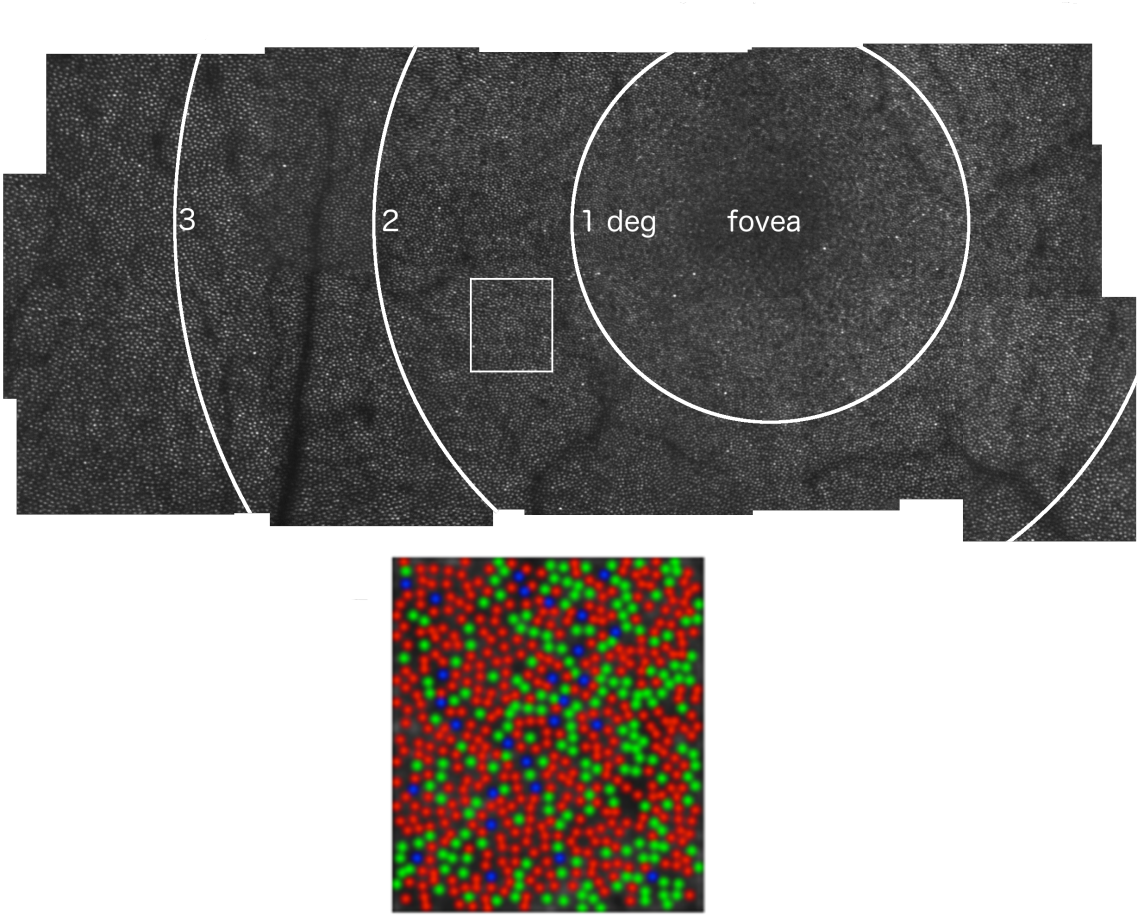

Figure 1.5: The human cone mosaic. The upper image is a high resolution image of the central retina of the authors right eye. The lower panel is a zoomed in region from the upper image with the class of each cone indicated by the color. L-cones = red, M-cones = green, S-cones = blue. See text for more details.

quantification of population wide variability in luminance sensitivity, a psychphysical measurement, led De Vries (1946) to advanced the idea that L:M-cone ratio was widely variable. However, the lack of wide ranging variability in other psychophysical measurements of spatial and color vision promoted the idea that the ratio of L:M cones was in fact largely conserved between individuals (Krauskopf, 2000).

In the absence of an anatomical or physiological method of identifying L- and M-cones in the human cone mosaic the debate over mosaic variability was not settled for another five decades. Images like the ones in Fig 6.7, first produced by Roorda and Williams (1999) and a few years later and in greater numbers by Hofer et al. (2005a), conclusively demonstrated wide variability of L:M-cone ratio in the central retina of human subjects. AO imaging and densitometry additionally validated prior estimates of the distribution of L:M ratio in the population using less direct measurements (Carroll et al., 2002; Hofer et al., 2005a). The ratio of the number of L- to M-cones is now established to vary from approximately 0.2:1 to 16:1 L:M cone ratio (Carroll et al., 2002), despite apparently normal color perception in these individuals (Neitz et al., 2002). Recent reports indicate the distribution of L:M ratio also varies between ethnic populations (Kuchenbecker et al., 2014; McMahon et al., 2008). The role, if any, of L:M ratio in color perception is unclear (Stockman and Brainard, 2010). Chapter 2 presents a hypothesis that explains why L:M ratio exerts limited impact on color appearance and makes a testable prediction about certain wavelengths of light that should be seen differently between people with different L:M ratios. Chapter 3 tests that hypothesis.

In addition to the relative number of cones in a mosaic, the spatial arrangement of those cones is also highly variable. L- and M-cones are distributed in a random spatial arrangement across the retina (Roorda and Williams, 1999; Roorda et al., 2001; Hofer et al., 2005a; Field et al., 2010; Mollon and Bowmaker, 1992). The arrangement of cones may have important implications for color vision because, as noted by Thomas Young, at each location on the retina only a single spectrally tuned detector measures light (Williams et al., 1991).

Therefore, the cone mosaic necessarily under-samples the visual world and creates a difficult challenge for the brain to solve. Consequently, the precise organization of the trichromatic cone mosaic continues to attract attention in color science (Williams et al., 1981a; Williams, 1988; Curcio et al., 1990; Mollon and Bowmaker, 1992; Roorda and Williams, 1999; Otake et al., 2000; Roorda et al., 2001; Hofer et al., 2005a; Field et al., 2010; Garrigan et al., 2010; Benson et al., 2014; Brainard, 2015). The potential influence of the spatial structure of the cone mosaic on color naming will be discussed in Chapters 3, 4 and 5

1.8 Retinal circuitry

As reviewed above, the first stage of color processing, turning radiant energy into neural activity, in the cone photoreceptors is largely settled (Neitz and Neitz, 2011; Lamb, 1995; Stockman and Brainard, 2010; Baylor, 1987). The subsequent interactions between cone signals are, however, still actively investigated. At the first synapse of the retina, signals from photoreceptors feed into about 12 different bipolar cells (Wässle, 2004). Detailed physiological characterization has revealed the exquisite tuning of these early visual neurons for distinct properties of the visual scene, presumably a result of evolutionary specializations designed to enhance specific forms of information (Masland, 2012). The ever growing catalog of cell types and circuits amassed for the mammalian retina has been reviewed extensively elsewhere (Masland, 2011; Field and Chichilnisky, 2007; Dacey et al., 2003; Sanes and Masland, 2015; Hoon et al., 2014). Here, I will present a brief high level description of the areas of retinal circuitry relevant to color processing (Fig. 1.6). Subsequent chapters will further detail each of these components.

1.8.1 The receptive field

The concept of receptive field has already been inherent in the discussions above, but I will briefly define its meaning before moving on to a discussion of retinal neurons. A receptive

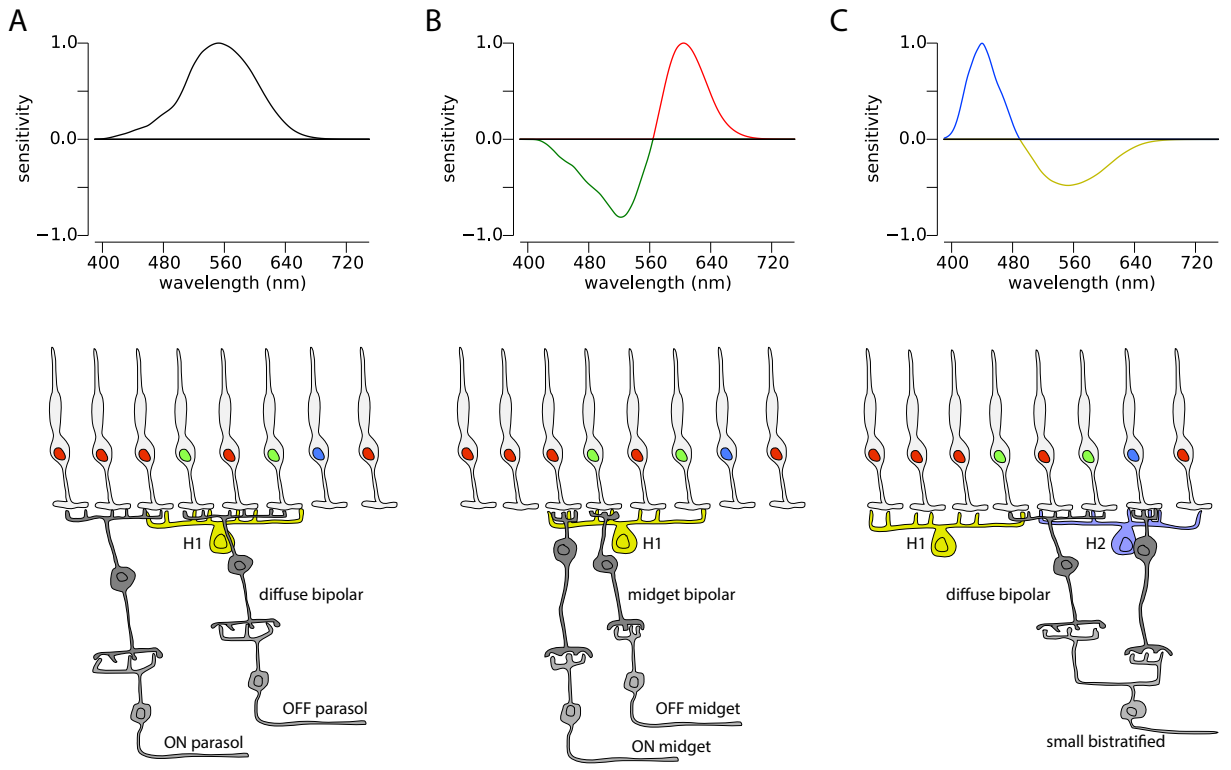

Figure 1.6: Circuit diagrams of the most common ganglion cells in the primate retina and their associated spectral sensitivity. A. ON- and OFF- parasol ganglion cells. This circuit (bottom) adds L- and M-cone inputs and creates a cell that responds in a manner similar to human black/white perception (top). B. ON- and OFF-midget ganglion cell circuits. Near the fovea midget ganglion cells take the difference between a single L- and M-cone and its neighboring cones, producing many cells that antagonistically compare L- and M-cones. Many midget ganglion cells are inhibited (excited) by shorter, greenish-blue wavelengths and excited (inhibited) by longer, reddish wavelengths. However, the null point of this theoretical cell is about 560 nm, which does not correspond to any of the unique hues (Compare to Fig 1.4). C. The small bistratified ganglion cell circuit differences S-cones from the summed activity of L- and M-cones. Often cited as the basis of blue/yellow color vision, this cell has a null point typically around 480 nm, which is about 30-40 nm shorter than the average wavelength identified by humans as purely green (Kuehni, 2004).

field refers to stimuli in the world that cause a neuron to alter the rate at which it fires action potentials. In the case of visual neurons that stimulus is light. The visual receptive field can be described by the location in visual space that the neuron samples, the wavelengths of light it is sensitive to, the spatial structure (lines, dots, faces, etc) of light it responds to and the list goes on. Early in the visual pathway, in the retina, the receptive field of neurons are typically described by a combination of spatial extent and location, spatial frequency (think acuity), wavelength and temporal duration of light. Even, the cones themselves have receptive fields and the wavelength dimension of their receptive fields are shown in Fig 1.3. Below is a brief discussion of the receptive field properties and computations that occur in the retinal neurons that process the signals from cones.

1.8.2 Horizontal cells

The first stage of comparison between nearby cone signals occurs in the lateral interactions imposed by horizontal cells (Thoreson and Mangel, 2012; Hirasawa et al., 2012; Jadzinsky and Baccus, 2013). A single horizontal cell integrates signals from cones within its receptive field and antagonistically relays that signal back to those cones; in a sense subtracting the signals of nearby cones. More accurately, the antagonism of horizontal cells introduces a divisive signal. The photoreceptors themselves encode fluctuations in intensity in a roughly logarithmic manner: a light that increases in intensity by a hundred times, will produce an approximate doubling of photoreceptor activation. A subtraction of two signals that have been logarithmically transformed is equivalent to dividing, or taking the ratio, of the original signals.

To understand the dynamics of horizontal cells, consider a single cone positioned within a larger mosaic, patiently waiting for photons to arrive from a dark world. In the absence of light, all of these cones will be depolarized and releasing the neurotransmitter, glutamate, on downstream neurons (Baylor, 1987; Rushton, 1972). Should light fall on our single cone

it will be hyperpolarized (activated) and decrease its rate of glutamate release. Should light begin to fall on its neighbors, however, the rate of glutamate release – a proxy for its activity – will again increase (i.e. decreased activity). This relationship was discovered in the cones of turtle by Baylor et al. (1971), and has now been documented in many species (Thoreson and Mangel, 2012), including primate (Verweij et al., 2003). The reason why our single cone has a decrease in activity despite seeing the same amount of light in its tiny piece of visual space is because horizontal cells sum the activity of all of its neighbors and subtract that signal.

The horizontal cells, therefore, act to compute roughly a ratio (the exact computation will depend upon the adaptation state of the cones) between the intensity of light falling on a cone and its neighbors. By taking the ratio between these signals, horizontal cells introduce the first computation towards differentiating intensity from wavelength. If an L-cone, for instance, is positioned close by to an S-cone, horizontal cells will subtract the output from these two cones and produce a spectrally opponent signal. The possible importance of horizontal cells in color vision was not lost on the physiologists who first studied their function in fish (Svaetichin and MaCnichol, 1959). However, the initial excitement over the potential role of these cells in color vision diminished shortly after their first characterization. Because horizontal cells difference cones at different locations in the retina, they do not completely eliminate the problem of distinguishing fluctuations in intensity from wavelength. Consider again a single cone in a mosaic. As a dark and light edge passes over it, there will be a moment where the border of the light falls exactly over the cone. The light will excite this cone and half of its neighbors, but the other half of its neighbors will still be in the dark. The strength of the surrounding cones, exerted via horizontal cells, will only be at 1/2 maximum. The cone will, therefore, produce a response to this edge regardless of whether the light is composed of a single wavelength or a broad distribution of many. Thus, the problem of differentiating fluctuations in intensity from wavelength has not been solved by horizontal

cell feedback alone.

Yet, the notion that horizontal cells may play a critical role in color vision has not diminished. Modern theories of color processing maintain that the initial differencing of cone signals in horizontal cells does play a major role in establishing color opponency. However, most modern accounts then solve the problem of differentiating a white edge from a green spot in the cortex (De Valois and De Valois, 1993). But there is some evidence that the complicated process of disentangling intensity and wavelength might occur in the horizontal cells of the retina. Poppel (1986) reported normal color induction (an illusion used to study spatial color comparisons) in an individual who suffered an injury to part of the pathway connecting the LGN to primary visual cortex. The injury left the subject blind in part of his visual field, but when part of the stimulus was placed in the scotoma, the appearance of the illusory colors were unaltered. Because cortex was no longer receiving the input from LGN necessary to generate the illusion, these findings argue in favor of a retinal origin of color induction.

Another line of reasoning supporting the idea that the horizontal cells may be more important in the computations of color comes from comparative physiology. Color opponency, of the type necessary to account for color perception, has been reported in horizontal cells of fish (Kamermans et al., 1998; Van Leeuwen et al., 2007; Joselevitch and Kamermans, 2009; Daw, 1967; Svaetichin and MaCnichol, 1959; Sabbah et al., 2013). In fact, it has been hypothesized that the first vestiges of color vision were been borne out of a necessity to overcome the flicker of light refracted through the rippling surface of shallow Cambrian waters 500 million years ago (Maximov, 2000; Marshall et al., 2015). Returning to the point, the fact that primates do not exhibit the same form of spectral opponency in their horizontal cells is often leveraged as a species difference and evidence for more specialized circuitry downstream of the cone-horizontal cell synapse. However, evolution tends to modify the old, rather than invent the new; presenting an equally plausible possibility that horizontal

cell mediated color vision might not be such a bad idea after all (Van Leeuwen et al., 2007; Joselevitch and Kamermans, 2009).

The theoretical work presented in Chapter 2 reinvigorates the idea that horizontal cells in primates indeed plays, not only a critical, but the *central* role in the computations of color vision. A recent anatomical discovery points an additional signaling mechanism in the horizontal cells that may be of critical importance to primate color vision (Puller et al., 2014a,b). The fact that cone terminals themselves are spectrally opponent yields the solution — the network of horizontal cells imposes surround inhibition directly onto the terminal of each cone in its receptive field cones, while the newly discovered pathway operates to induce a second site of opponency in the dendrites of bipolar cells.

1.8.3 Bipolar cells

The visual responses generated by cones and shaped by horizontal cells is next projected into the bipolar cell layer (Fig. 1.6) (see Euler et al. (2014) for recent review). Grossly, bipolar cells come in two varieties, those that respond to increments of light (ON) and those that respond to decrements of light (OFF). Roughly 12-15 subtypes of bipolar exist in the mammalian retina (Euler et al., 2014) each painting their own unique picture of the incoming light patterns. The details of those subtypes are not important for the current discussion. What is important, is that bipolar cells make synaptic contacts with cone terminals. Therefore, bipolars receive an input that can be though of as the activity of a cone(s) minus the activity of horizontal cells.

It is worth noting, direct evidence that bipolar cells in primates receive a signal of this kind has been sparse. Recording electrical potentials in primate bipolar cells has been famously challenging. Located in the middle of the retinal column, the cell bodies of bipolars are nearly inaccessible to the electrode of physiologists. Thus, most evidence of bipolar physiology is from non-primate species (Boycott and Wässle, 1999), inferred from anatomical studies

(Boycott and Wässle, 1999; Grünert et al., 1994; Kolb and Marshak, 2003) or from recordings of retinal ganglion cells in which horizontal cell contribution to the cone/bipolar computation can be pharmacologically extinguished (McMahon et al., 2004). The only direct recordings of primate bipolar cell receptive fields come from Dacey et al. (2000a), who managed to collect quality recordings from 12 bipolars. Importantly, the authors learned that the center and surround – the excitatory (+) signal from cones and inhibitory surround (–) from horizontal cells – was roughly balanced in their recordings. In other words, the subtraction that takes place between a cone and its neighbors is balanced, at least at the level of bipolar cells. In response to a diffuse light, the activity in the center and surround would chancel each other. A balance between the center and surround is assumption made in future chapters.

There are three additional distinctions between subclasses of bipolar cells that are relevant for color vision. In primate retina, a specialized group of bipolar cells, known as midget bipolars (Fig. 1.6B), make synaptic contacts with only a single cone in the central retina (Dowling and Boycott, 1966; Boycott et al., 1969; Kolb et al., 1992; Kolb and Marshak, 2003; Boycott and Wässle, 1991; Hendrickson, 2005). Because they contact only a single cone, these cells inherit spectral opponency from the cone-horizontal cell subtraction discussed above, making them a central player in constructing color opponency. Diffuse bipolar cells make synaptic contacts with the terminals of multiple cones (Fig. 1.6A) (Boycott et al., 1969; Boycott and Wässle, 1991). This amounts to an addition of cone signals, for example L+M. Finally, S-cones have their own unique bipolar circuitry (Fig. 1.6C). The S-cone bipolar cell makes selective contact with 1-3 S-cones and is an ON type (Mariani, 1984). S-cones are additionally contacted by diffuse OFF bipolars, but whether or not S-cones are contacted by OFF midget bipolars is a source of considerable contention (Klug et al., 2003; Neitz and Neitz, 2011). Chapter 2 discusses the role these three cell classes play in color vision in considerably more detail.

1.8.4 Ganglion cells

Finally – after traversing through the cones, horizontal cells, bipolar cells and amacrine cells (a second layer of lateral inhibition that will not be discussed here) – visually evoked signals reach the retinal ganglion cell layer. Here the visual information is combined in still new ways and sent to the LGN, the way-station to the cortex. Again, there are many more types of ganglion cells than I will discuss here (Masland, 2012) and I will only briefly describe three.

Analogous to the midget bipolar cells, primates have developed a specialized ganglion cell type called the midget ganglion (Fig. 1.6B). In the central few degrees of vision, they make up around 90% of this layer (Dacey and Lee, 1994) and draw input exclusively from one midget bipolar (Dacey and Petersen, 1992; Kolb and Marshak, 2003). Therefore, the midget bipolar-ganglion pathway forms a one-to-one connection with cones, providing high resolution information to the brain. As a consequence of sampling from individual cones, midget ganglion cells also carry significant spectral opponency (Crook et al., 2011) and have become the textbook explanation of red/green opponency. The midget ganglion cells also form a high resolution system that serves as the major input to cortical areas concerned with the construction of form and, ultimately, the recognition of objects (Livingstone and Hubel, 1988; Ungerleider and Mishkin, 1982; Merigan and Maunsell, 1993). Human visual acuity and contrast sensitivity are known to be greater for achromatic patterns of light (Mullen, 1985; Sekiguchi et al., 1993b,a). In fact, outside of the very central retina, visual resolution reflects the sampling limit of the midget ganglion cells (Rossi and Roorda, 2010). Therefore, it has been suggested that midget ganglion cells may contribute to black/white vision as well (Wiesel and Hubel, 1966).

In most existing models, blue/yellow color vision is thought to be mediated by the small bistratified cells that receive excitatory S-cone input from the ON-type S-cone bipolar cell and also from diffuse OFF-type bipolar cells with L+M signals (Fig. 1.6C) (Dacey and Lee, 1994;

Lee et al., 2010). Thus, the small bistratified ganglion carries S - (L+M) spectral opponency and is excited by blueish light and inhibited by yellowish light (Crook et al., 2009; Field et al., 2007). In Chapter 2, I will point out numerous problems with this interpretation, including the exact wavelengths that this cell prefers relative to the colors reported by humans, and motivate an alternative retinal substrate. Chapters 3 and 5 offer evidence, albeit indirect, that is consistent with this alternative pathway for blue/yellow color vision.

Lastly, the parasol ganglion cell draws samples of the visual world down from the diffuse bipolar cells (Fig. 1.6A). These cells have larger receptive fields (Croner and Kaplan, 1995) than the midgets or small bistratified and are highly sensitive to contrast (Kaplan and Shapley, 1986). Because they sample diffuse bipolars, parasols have receptive fields that are non-opponent (L+M). As a result, some have suggested that the parasols represent the black/white pathway in primate vision (Lee, 2004). While ruling out a contribution from parasols to achromatic vision would be unwise, Chapters 2 and 4 will make the case that they are not the only mediators of our high resolution black/white vision.

Conclusion

I have offered a summary of the history and current landscape of color vision research. Along the way I highlighted the tremendous success of modern theories and pointed out places where theory does not align with observation. Over the course of the next five chapters I will motivate and test a theory of color vision that solves some of these conundrums and leaves others to be yet re-imagined.

Chapter 2 describes a circuit in the outer retina capable of constructing the early stages of color representation and makes numerous predictions about the character of color sensation. In Chapter 3 I test a few of those predictions and compare the results against other existing models. Chapters 4 and 5 approach these questions of neural circuitry by probing the sensations associated with individual cones in living humans. The work in Chapter 4

specifically confronts the hypothesis that midget ganglion cells participate in red/green perception in addition to achromatic high resolution vision. Chapter 5 develops an account of how the brain interprets signals from single cones and provides definitive evidence that M-cones participate in the sensation of blue. Finally, Chapter 6 explicitly models the networks of horizontal cells in the outer retina. This work focuses on the propagation of S-cone signals through non-classical pathways in the retina, provide an explanation for why S-cone signals have not been routinely measured in midget ganglion cells and highlight some remaining enigmas of horizontal cells.

Chapter 2

NEUROBIOLOGICAL HYPOTHESIS OF COLOR APPEARANCE AND HUE PERCEPTION

2.1 Abstract

De Valois and De Valois (1993) showed that to explain hue appearance, S-cone signals have to be combined with M vs. L opponent signals in two different ways to produce red-green and yellow-blue axes respectively. Recently, it has been shown that color appearance is normal for individuals with genetic mutations that block S-cone input to blue-on ganglion cells. This is inconsistent with the DeValois hypothesis in which S-opponent konio-geniculate signals are combined with L-M signals at a 3rd processing stage in cortex. Instead, here we show that color appearance, including individual differences never explained before, are predicted by a model in which S-cone signals are combined with L vs. M signals in the outer retina.

2.2 Introduction

The theory of color opponency maintains that primate trichromacy arises through the comparison of two dichromatic systems, red vs. green (RG) and blue vs. yellow (BY) (Hurvich and Jameson, 1957; Stockman and Brainard, 2010). The existence of four unique hues, red, green, blue and yellow, occurring at the spectral neutral points of these two systems is a corollary prediction of opponency; consequently, determining the spectral positions of unique hues has received considerable attention in color science.

Across populations of color normal individuals the spectral position of uncontaminated hues exhibit substantial inter-subject variability (for review see Kuehni (2004)). The most notable variation occurs with unique green, which can deviate as much as 65 nm between

individuals (Kuehni, 2004; Jordan and Mollon, 1995; Abramov et al., 1991; Abramov and Gordon, 2005; Gordon and Abramov, 1977). A complete neurobiological explanation of color appearance must, therefore, specify the neurons and pathways responsible for hue perception, accurately predict the wavelength of each unique hue, while simultaneously explaining the variability between observers. Such an account has never been developed (Valberg, 2001; Kuehni, 2004).

Hering (1878) originally proposed opposing pairs of BY and RG processes as an alternative to trichromatic theory. Later, von Kries (1905) proposed the possible resolution that trichromacy could be valid at the receptor level, while opponent processing might apply to a higher level of neural processing. Zone theories with multiple processes at higher stages were developed and elaborated by several people including Schrödinger (1925), Muller (1930), and Judd (1966). Hurvich and Jameson (1957) successfully formulated theoretical equations to describe the relationship between the cone inputs and opponent processes that could reasonably fit measures of chromatic-opponent response functions from a hue cancellation task, thus providing quantitative empirical support for multi-process theories. The questions that have remained concern the underlying physiological processes responsible for opponent hue perception. Addressed here are the neurobiological post-receptoral mechanisms underlying specifically hue perception, the aspect of color in which stimuli are classified as red, blue, green, or yellow.

The current ideas of the neurobiological basis for hue perception have focused on the small bistratified ganglion cells that receive S-(M+L) cone input as the retinal origin of the BY channel, while midget ganglion cells with opponent interaction between L-M cones are believed to be the retinal origin of the RG channel. If hue perception is based on retinal small bistratified S-(L+M) cells and L-M and M-L midget ganglion cells, then our perceptions should be predictable from the responses of those cells. However, in fact, there are conspicuous differences between human hue perception and what is predicted from the

responses of S vs. (L+M) and L vs. M cells.

The standard model in which midget L vs. M and small bistratified ganglion cells are assumed to form the physiological basis of hue perception grew out of a proposal by De Valois et al. (1966) that spectrally opponent neurons in the LGN could account for human hue perception. Nonetheless, later, De Valois and De Valois (1993) wrote that from early on they were aware of a large contradiction at shorter wavelengths between human hue appearance and LGN cell responses, which the group made note of in their 1966 paper. The problem is that M-L midget ganglion cells, which have been hypothesized to be the substrate for perception of green, fire vigorously to wavelengths below 475 nm. For example, for a 470 nm light, the putative "green-ON" ganglion cells typically have response amplitudes (in spikes/sec) of about 80% of peak. Yet, normal human observers do not perceive any greenness in 470 nm lights. A similarly glaring problem exists for the sensation of red. "Red-ON" L-M cells, which are putatively responsible for the sensation of redness, increase firing for wavelengths longer than about 580 nm. This predicts that long wavelengths should be the only spectral region where redness is perceived; however, this is not the case. Red sensations "reemerge" at short wavelengths below about 470-480 nm and wavelengths below about 440 nm evoke nearly equal red and blue sensations; however, the "red-ON" L-M midget ganglion cells of the standard model do not respond to short wavelengths.

De Valois and De Valois (1993) point out how the standard model disagrees with experiment in terms of the appearance of hue in color space. The angular direction of the L vs. M chromatic axis is not along either the red-green or the blue-yellow unique hue axis, but is roughly in-between them, along an orange-cyan chromatic axis. They had the profound insight that color experience can only be explained by opponent mechanisms in which S-cone signals modulate the L vs. M opponent interactions in two different ways. First, adding S signals to the L-cone side of an L vs. M opponent process produces (S+L) vs. M opponency rotating the axis so it corresponds with the RG direction in color space. Second, adding

S-cone signals to the M-cone side of an L vs. M opponent process produces (S+M) vs. L opponency rotating the axis so it corresponds with the BY direction in color space. Thus, M vs. L opponency is not just the main contributor to the RG system, but to both the RG and the YB systems. So ultimately, for example, the M not the S, cones provide the primary contribution to the blue signal (especially for wavelengths above 460 nm). The discrepancy in the sign of the M contribution to blueness has become well recognized in the psychophysical literature (Drum, 1989; Webster et al., 2000a; Valberg, 2001; Neitz and Neitz, 2008; Guth, 1991; Mollon, 2003), however, the problem is often ignored in accounts of the neurobiological basis of hue perception that have emphasized the S-(M+L) small bistratified ganglion cells as the basis for hue perception.

The persistence of the standard model in spite of being inconsistent with the experimental facts of human hue perception is probably partially because the sensation of yellow based on the summed activity of M+L cones is more intuitive then yellow perceptions based on L-cones opposed to S+M. Moreover, the small bistratified ganglion cell with S-(L+M) cone inputs matches the configuration of cone inputs in models proposed by Muller (1930), Judd (1966), and Hurvich and Jameson (1957). Perhaps even more importantly, the classical study defining the cardinal directions of color space (Krauskopf et al., 1982) found that psychophysical detection of thresholds using an adaptation paradigm matched ganglion cell physiology not only for the L vs. M opponent mechanism but for detection involving an S-(L+M) opponent system. Vision scientists have had much more confidence in measurements of detection threshold as representing a physiological reality than measures of hue appearance which are more subjective. Nonetheless, the analysis presented here is based on the premise that the question of whether or not hue perception, and specifically, the spectral locations of unique hues have neurobiological basis can be addressed scientifically by experiment. We argue that if a neurobiological hypothesis explains and accurately predicts what hues are seen, including biological correlates of individual differences, it can be taken as evidence that

hue perception has a legitimate biological basis.

The standard model in which L vs. M midget and small bistratified ganglion cells are the direct physiological substrates for the RG and BY hue channels neither explains or predicts peoples hue experience. As Richard Feynman famously said in his lecture on the scientific method at Cornell University in 1964, if a model "disagrees with experiment, its wrong. In that simple statement is the key to science". Thus, the standard model is wrong with respect to explaining hue experience. However, rather than coming up with an entirely new model when a compelling theory has become widely accepted but proven wrong by experiment, it is natural to try to modify the model in an attempt to rescue it. The De Valois and De Valois (1993) insight that the L vs. M axis can be rotated appropriately to form the RG and BY axes by the addition of S-cone signals to L- or M-center opponent signals respectively, offered a logical revision to the standard model. The revision required only additional stages localized in the cortex in which S-ON signals originating in the small bistratified ganglion cells of the retina are combined with M vs. L signals of the midget ganglion cells. However, ad hoc revisions often add complexity and are susceptible to the addition of unknown and therefore untestable entities. The weakness in the serial model proposed by De Valois is that the transformations theorized to occur in the cortex are not based on any known circuitry. Cortical cells with input from all three cone types arranged as required to account for hue perception have been demonstrated (Conway, 2001; Conway and Livingstone, 2006) but the locus where they are combined is not known and the relative weights of the three cone inputs cannot be predicted from the theory.

The De Valois and De Valois (1993) theory holds that S-cone signals to the small bistratified ganglion cells are required to rotate the L-M axis to the RG and BY axes. That prediction can be evaluated by examining hue appearance in individuals that have mutations in genes encoding the glutamate receptor, mGluR6, responsible for signaling between the S-cones and the blue cone bipolar cells (Mariani, 1984). Glutamate released by cones produces

a hyperpolarizing synaptic potential in on-bipolar cells by binding to the metabotropic glutamate receptor mGluR6 (Vardi et al., 2000). In people who have inactivating mutations in the GRM6 gene there is no direct feedforward communication between S-cones and S-cone bipolar cells. This, in turn, interrupts feedforward of S-cone signals to the small bistratified cells. Thus, the DeValois and DeValois theory predicts that individuals who lack S-cone inputs to small bistratified cells should base their hue perceptions on a single, unrotated, L vs. M axis. In individuals with gene mutations that render mGluR6 nonfunctional, the loss of direct feed-forward photoreceptor-to-on-bipolar signaling can be clearly demonstrated by the absence of the ERG b-wave (Dryja et al., 2005; O'Connor et al., 2006). Individuals with these mutations also manifest complete autosomal recessive congenital stationary night blindness (ARCSNB) resulting from the loss of synaptic transmission between rods and rod on-bipolar cells. However, despite the synaptic defect, the best visual acuities are nearly normal (20/15 20/40) and people with this from of complete CSNB have normal hue perception for central vision (Dryja et al., 2005; Terasaki et al., 1999; Bijveld et al., 2013b). DeValois and DeValois postulated that S-cone signals via the small bistratified cells are required for both normal BY and RG hue perception, but neither are disturbed when S-cone transmission to the small bistratified cell is blocked. The hypothesis of a cortical locus of S-cone signals from small bistratified cells being combined with L vs. M opponent signals to produce the RG and BY hue axes does not appear to be borne out by experiment.

In summary, predictions of both the standard model in which hue perception is based on L vs. M midget and small bistratified ganglion cells or a revision of it where S-cone signals from small bistratified cells are combined with L vs. M signals in the cortex are not consistent with experimental findings. Here, we examine an alternative to the standard hypothesis that is compatible with the finding of unaltered hue perception in individuals with mGluR6 mutations. S-, M- and L-cone signals are known to be combined in the H2 horizontal cells of the outer retina. Earlier, it was proposed that H2 horizontal cells could

be the basis for a subset of midget ganglion cells having (S+L) vs. M and (S+M) vs. L inputs required to explain hue perception. We have proposed that S-cone feedback to a subset of L and M cones would rotate the color axes of a small subset of L vs. M midget ganglion cells as required by DeValois and DeValois (Mancuso et al., 2010; Neitz and Neitz, 2011). According to this hypothesis, neurons with the combinations of cone inputs required for hue perception arise in the retina, not in the cortex. H2 horizontal cells may also employ a signaling pathway, originally described in rodents (Varela et al., 2005; Duebel et al., 2006), using GABA (gamma-Aminobutyric acid) to send feed-forward signals directly to bipolar cells (Puller et al., 2012, 2014b,a). In macaque retina, the molecular components of this putative feed-forward pathway are highly enriched beneath S-cones and they co-localize with a marker for H2 horizontal cells. The enrichment at S-cones was not observed in either mouse or ground squirrel indicating this specialization may have evolved in the primate lineage specifically for hue perception. This feedforward pathway is an even more likely candidate than horizontal cell feedback because it provides a mechanism whereby S-ON and S-OFF signals could be injected directly into midget bipolar cells carrying L vs. M opponent signals. The midget system is a primate innovation that predominately projects to the ventral visual stream. The elaboration of this feedforward system may have been an important step in the evolution of color processing associated with the ventral occipitotemporal cortex which is related to the conscious perception of hue and not well developed in other mammals. These GABA mediated signals bypass the cone-to-bipolar glutamatergic synapse so S-cone signals in this putative pathway would be unaffected in people with mGluR6 mutations, explaining their normal hue perception.

It is clear that the majority of M vs. L ganglion cells do not receive any significant amount of S-cone input (e.g. Sun et al. (2006)). However, the theory requires only a small subset of midget ganglion cells to carry S-cone signals to account for hue perception. Recordings from large samples of cells in LGN have identified a group of cells, about equal in number

to S-(M+L) cells, that have input from M-cones with the same sign as S-cones, i.e., they are (S+M)-L cells as required by the proposed retinal locus for hue perception (Tailby et al., 2008b). Because the only cells in the retina known to carry opponent signals from M vs. L cones are midget ganglion cells, this second class of blue sensitive cells appears to reflect the existence of a small subclass of midget ganglion cells that could be the substrate for the blue side of the perceptual BY hue opponent system. Tailby et al. (2008b) found the chromatic properties of S-OFF cells in the LGN to be heterogeneous, and one population had L-(S+M) inputs as required for the yellow side of BY hue opponency and predicted by the hypothesis that S-OFF signals may be injected directly into midget bipolar cells by GABA mediated feedforward. Cells with the required cone inputs were also reported in the retina in the classical studies of de Monasterio and Gouras (de Monasterio, 1978; de Monasterio et al., 1975). Although, in their studies, beta-band absorption of L-cones was found to mimic S-cone input (de Monasterio and Gouras, 1977), chromatic adaptation could be used to distinguish responses mediated by S-cones from those mediated by beta-band absorption of L-cones, revealing a small subset of ganglion cell receiving (S+L) vs. M and (S+M) vs. L inputs.

The theory that the opponent interactions in the arrangement proposed by DeValois occur within the retina greatly simplifies the mechanisms of color appearance. The current work develops this theory and tests its predictions against established observations of hue experience. We focus, in particular, on unique green because it has proven particularly challenging to explain with previous neurobiological or perceptual models.

2.3 Methods

2.3.1 Constructing a color space

Color spaces, such as the CIE *rgb* space, derived from color matching functions are, by design, organized such that the percepts associated with monochromatic lights fall on the perimeter

of the space. All points within the space are, therefore, associated with colors elicited by all spectra other than monochromatic stimuli. This mathematical formalism offers a precise and economical way of representing color in a three dimensional coordinate system.

A trichromatic color space was derived from a set of known spectral sensitivity functions (Carroll et al., 2000), with peak sensitivities of 559, 530 and 419 nm for L, M and S pigments, respectively. Correction for photoreceptor optical density and lens and macular filtering were introduced according to (Stockman and Sharpe, 2000), creating $l(\lambda), m(\lambda), s(\lambda)$ fundamentals. Color matching functions, $R(\lambda), G(\lambda), B(\lambda)$, were then derived through Grassman's law,

$$\begin{bmatrix} l_r & l_g & l_b \\ m_r & m_g & m_b \\ s_r & s_g & s_b \end{bmatrix}^{-1} \begin{bmatrix} l(\lambda) \\ m(\lambda) \\ s(\lambda) \end{bmatrix} = \begin{bmatrix} R(\lambda) \\ G(\lambda) \\ B(\lambda) \end{bmatrix} \tag{2.1}$$

where l_r... represent the sensitivity of the corrected photopigments to each of the lights that define the color space, here 650, 530 and 460 nm. To ensure that equal energy white falls at (1/3, 1/3, 1/3) in the space, the color matching functions were normalized to integrate to 1 across the visible spectrum. Finally, $R(\lambda), G(\lambda), B(\lambda)$ were transformed into *rgb* space with the usual equations (Brainard and Stockman, 2010):

$$r = \frac{R}{R+G+B}, g = \frac{G}{R+G+B}, b = \frac{B}{R+G+B} \tag{2.2}$$

The Cartesian location of the copunctual point, $\mathbf{b}$, of any dichromatic system within the *rgb* space can be found through matrix multiplication:

$$A\mathbf{x} = \mathbf{b} \tag{2.3}$$

where A is the system matrix from Eq. (2.1) (left most matrix), and $\mathbf{x}$ is a 3x1 vector indicating the absent dimension. For example, the tritan copunctual point can be found with

Eq. (2.3) when $\mathbf{x} = \begin{pmatrix} 0 & 0 & 1 \end{pmatrix}^T$. The location of a more complex dichromatic system, such as S - (L+M), can be obtained if the same principle is applied with the weights of the L and M inputs after they have been normalized to sum to 1, $\mathbf{x} = \begin{pmatrix} 0.75 & -0.25 & 0 \end{pmatrix}^T$. Note, the weight of the M-cones must be made negative.

2.3.2 The model

Phototransduction

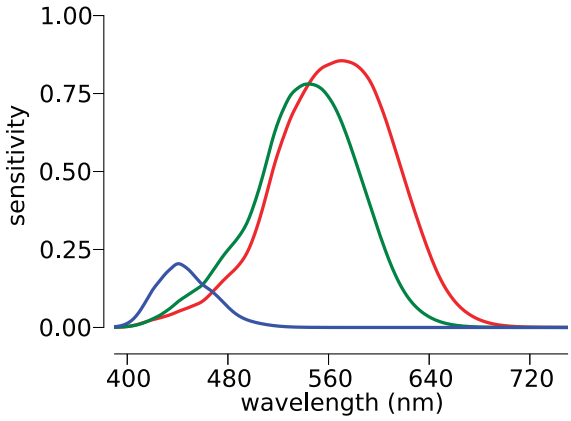

Figure 2.1: The cone fundamentals. Spectral sensitivity functions with peaks of 559, 529 and 519 nm were corrected for lens and macular filtering to produce the curves shown here.

The sensors responsible for the absorption of photons are known to be the three classes of cone photoreceptors. Since the cone opsin sequences were first reported by Nathans (Nathans et al., 1986b), a class of L and M opsins, differing each by as few as a single nucleotide, have been identified with distinct peak sensitivities (Neitz et al., 1991) (see (Neitz and Neitz, 2011) for review). To incorporate these normal shifts in peak absorption, we used sensitivity functions that include a parameter for peak sensitivity (Carroll et al., 2000), allowing us

to assess the impact of this variability on hue perception. To complete the first step in hue processing (Fig. 2.1), the spectral sensitivity functions are corrected for optical filtering (Stockman and Sharpe, 2000). Inter-subject variability in lens and macula filtering are not considered here, but are expected to play a role. In particular, the lens is known to increase in optical filtering as a function of age (Pokorny et al., 1987). Photopigment optical densities were assumed to be 0.4, 0.38 and 0.33 for LMS cones. Variability in optical density has been observed to modulate color appearance (Neitz et al., 1999), the impact of this variability on the model is considered in the *Discussion* section.

Cone opponency

After phototransduction, the second step in processing (Fig. 2.2), is hypothesized to take place in the midget system. Here feedforward input from cones is expected to be combined with input from horizontal cells, creating cone opponent signals aligned with the unique hue axes. This transformation of information differs most significantly from the DeValois model, in which the final combination of cone signals required to explain hue perception was assumed to occur at a higher level (De Valois and De Valois, 1993). Instead, we propose that hue perception is mediated exclusively by a small subset of midget ganglion cells in which central L- or M-cones are adjacent to S-cones and there is sufficient interconnection via H2 horizontal cells to introduce significant S-cone input. In this scenario S signals feed through H2 horizontal cells, producing L vs. (S+M) and M vs. (S+L) interactions at the level of the bipolar cells. Support for opponency in the outer retina has been observed experimentally in recordings from S-cones (Packer et al., 2010) and H2 horizontal cells (Dacey et al., 1996), which carry S, M and L signals.

In the central retina there are four types of midget bipolar cell/cone combinations. The cones are either L or M and the bipolar cells are either ON or OFF cells. In each case, the S-cone inputs are sign reversed compared to the direct feedforward from cone to bipolar cell.

In other words, OFF bipolar cells receive S-ON input and ON bipolar cells receive S-OFF input via the H2 horizontal cells. Thus, we propose S-cone input transforms the analogous four types of midget ganglion cells into four lines transmitting the four hue sensations, yellow, blue, green and red, respectively. A significant difference between this model and all other previous models is that hue mechanisms are specifically associated with ON vs. OFF bipolar cells, with yellow and green associated with ON bipolar cells and red and blue hue sensations associated with OFF bipolar cells as shown in Table 2.1.

Table 2.1: Proposed mechanisms.

L-(S+M)	yellow	ON-bipolar
(S+M)-L	blue	OFF-bipolar
M-(S+L)	green	ON-bipolar
(S+L)-M	red	OFF-bipolar

For simplicity, here the pair of mechanisms, blue and yellow, are taken to be the inverse of each other, so mathematically the BY system is treated as a single entity. The same is true of the RG system. However, physiologically we propose discrete mechanisms for each of the four hues as given above. We presume that each of the four is rectified at some stage, as in the DeValois and DeValois model.

In our model, for each hue mechanism, one side of the opponency is derived from summed horizontal cell input that combines S-, L- and M-cone responses. Because of this arrangement, the character of opponent interactions responsible for hue perception will vary based on the ratio of L- and M-cones in the mosaic surrounding a given cone. In the case of the central retina where midget ganglion cells receive excitatory input from only a single L- or M-cone (Dowling and Boycott, 1966), this produces a ganglion cell with the spectral sensitivity, $g(\lambda)$

described by,

$$g(\lambda) = \delta(\lambda) - \omega\Big(\rho S(\lambda) + (1-l)M(\lambda) + lL(\lambda)\Big) \tag{2.4}$$

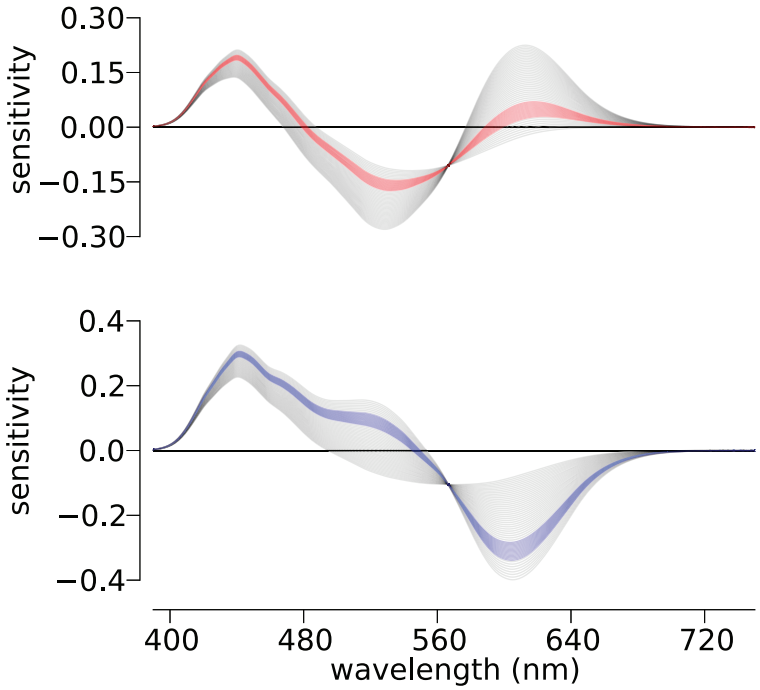

Figure 2.2: The family of sensitivity curves produced by the RG and BY mechanisms. Each curve represents a different value for l in Eq. (2.4). Highlighted in red and blue are the most probable curves in a retina with an L:(L+M) cone ratio of 0.75. The upper plot are the predicted sensitivity curves for the RG mechanism and the lower for BY.

where $\delta(\lambda)$ is taken to represent the direct pathway of the cone-to-bipolar circuit that involves a single synapse from a cone onto an ON midget bipolar cell. An OFF midget is created by $-1 * g(\lambda)$. In the case of the BY system $\delta = L(\lambda)$, while $\delta = M(\lambda)$ in the RG system. l is the proportion of L to (L+M) in the indirect pathway, signaling through

horizontal cells that contact L, M and S-cones (Dacey et al., 1996). Lower thermal noise of the S-cones (Aho et al., 1988) was assumed to amplify the S signal, ρ, into the indirect pathway by 1.3, or the ratio between M+L and S thermal noise (544.5/417). Our only assumption is that at this ganglion cell level, responses of chromatically opponent cells null to equal energy white, requiring that ω in Eq. (2.4) is adjusted such that:

$$0 = \int_{\lambda=390}^{750} g(\lambda)\, d\lambda \tag{2.5}$$

This assumption is supported by our earlier demonstration that changes in an observers chromatic environment modulate the appearance of unique yellow (Neitz et al., 2002). It was observed that the wavelength of a subjects unique yellow shifted after exposure to long periods of chromatic alteration. Afterward, when subjects were exposed to the everyday environment, unique yellow shifted back to baseline. A simple normalization mechanism based on a resetting to an equal energy spectrum after exposure to altered chromatic experience well described the data. That mechanism is formalized here. The model presented predicts precisely how differences in chromatic environment will change the unique hues. The earlier results suggest that the majority of individuals are exposed to environments that average overtime to a close match to equal energy white. For simplicity, we assume here that everyone is adapted to an equal energy spectrum though variability in white settings has been noted (Werner and Schefrin, 1993) (see below).

Frequency summation

Eq. (2.4) produces physiologically based spectral sensitivity functions for midget ganglion cells that closely match hue appearance data. However, the scaling constant associated with the L and M input, l, must be specified. The final component of this model (Fig. 2.3) assumes a random wiring hypothesis (Paulus and Kröger-Paulus, 1983) and uses the L:M cone ratio to specify the input of L and M into the surround of an average ganglion cell in the observers

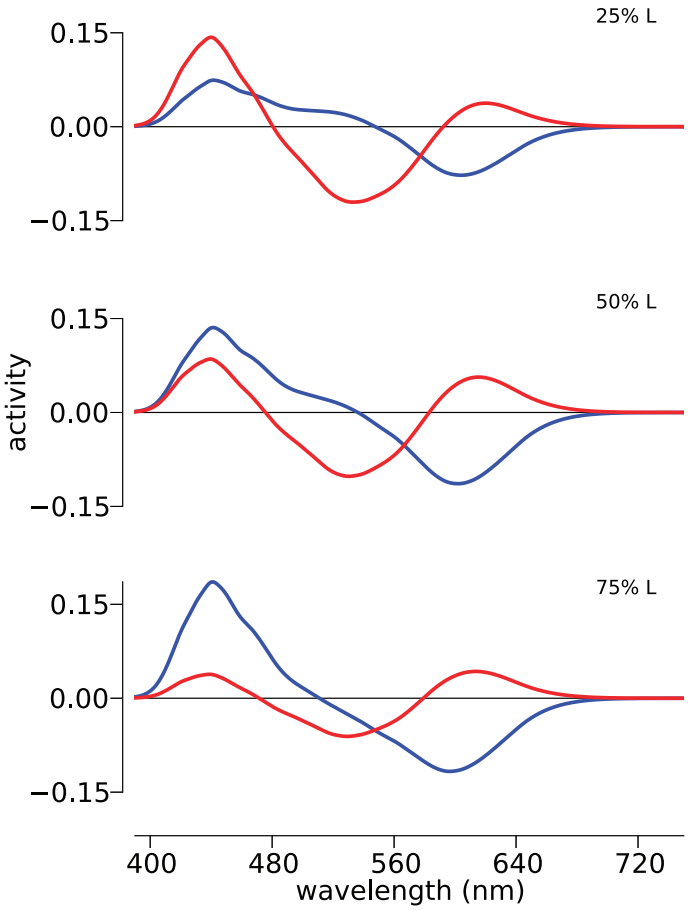

Figure 2.3: The sensitivity of the chromatic mechanisms. By changing the %L (L/(L+M) x 100) cones in the observer's retina, a family of valence curves is produced for the RG (red lines) and BY (blue lines) mechanisms. Note the null point of the BY curves shifts considerably between the three conditions plotted.

retina. We accomplish this mathematically by first iteratively computing all possible curves (Eq. (2.2)), which amounts to changing the proportion of L to (L+M) in Eq. (2.4). The generated units are then weighted based on the probability of occurrence and summed:

$$\alpha(\lambda) = \sum_{r=0}^{n} g_r(\lambda)\, P(S|r) \tag{2.6}$$

with l in Eq. (2.4) equal to r/n and $n = 100$. The weights for each unit are computed with a binomial distribution parameterized by P_L, or the L:M ratio across the entire retina:

$$P(S|r) = \binom{n}{r} P_L^r (1 - P_L)^{n-r} \tag{2.7}$$

The above model can be extended to cases where more than one cone contacts a single bipolar cell, as is the case in the periphery (Dacey et al., 2000a). In this scenario, both L and M signals are assumed to contact midget bipolar cells through the direct pathway, $\delta = L(\lambda) + M(\lambda)$. These signals are then weighted by a binomial distribution parameterized by the L:M ratio, as in Eq. (2.7). This scenario produces exponentially more combinations of direct and indirect cone arrangements. However, as previously noted (De Valois and De Valois, 1993), increasing the number of cones contributing to the direct pathway decreases the number of strongly opponent cells. The implications of this change on color appearance are considered below.

All of the equations above were implemented in the open source programming language Python (http://www.python.org/). Source code can be freely obtained from https://github.com/bps10/color/tree/JOSA.

2.4 Results

2.4.1 Color space and unique green

We used a custom physiologically based color space and the concept of confusion lines to determine the basis for published individual differences in unique green (Ayama et al., 1987). A dichromatic system represented in a trichromatic space necessarily contains directions along which the relative activation of its two receptors do not change. This is often shown as confusion lines emanating from a copunctual point. An example of this is drawn in Fig. 2.4A for a tritan observer in chromaticity space. Extending this logic, the confusion lines of any dichromatic system based on the same three cone photopigments, including those based on constant weighted sums of two of the photopigments opposed to the third with a single null point, can also be represented in color space.

In the case of the BY system, there is a confusion line that nulls the system and corresponds to a line along which lights will be identified by a trichromatic viewer as uniquely green. This implies that for a linear model of hue perception to be accurate, a line from the systems copunctual point to the wavelength identified as uncontaminated green must be possible.

Unique green data, reprinted from (Ayama et al., 1987), for two observers at 10 trolands illumination is plotted in Fig. 2.4B after transformation into *rgb* space derived from the Neitz spectral sensitivity functions (Carroll et al., 2000) as described in *Creating a Color Space*. The points do not transform exactly into the current space due to the non-linear differences between Judd-Vos fundamentals that the data are reported in and the fundamentals employed here. These differences results in two points falling outside of the color space. However, this irregularity does not impact the current analysis.

At 100% purity, the two observers identify 498 and 522 nm light as uniquely green, respectively. These observers both fall well within the range of normal observers (Valberg,

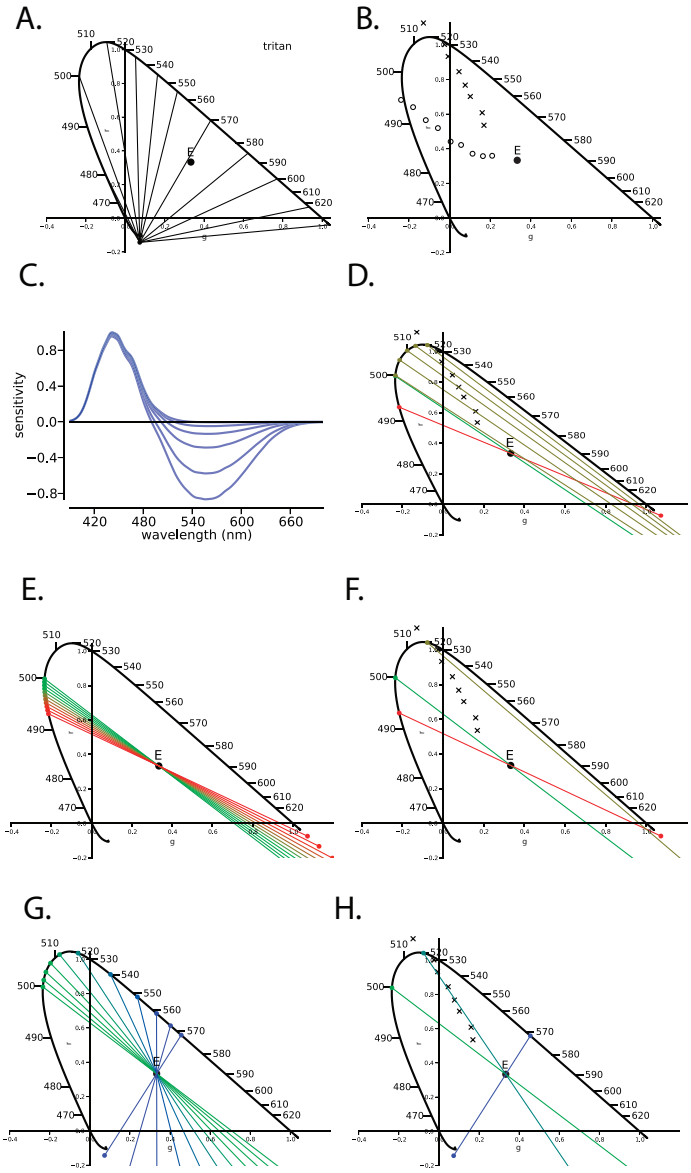

Figure 2.4: Comparison of the standard model with the BY midget ganglion cell theory proposed here. A *rgb* color space (**A**) was constructed from the Neitz fundamentals (Carroll et al., 2000) and data from (Ayama et al., 1987) was best fit to the space in a least squares sense (**B**). **C** demonstrates the effect of varying k in $S - k(L + M)$. This scenario is not capable of matching the 522 nm unique green of observer 2 and simultaneously passing through equal energy white (**D**). **E** simulates changing k in $S - (kL + (1 - k)M)$, again failing to fit the data from observer 2 (**F**). Finally, varying k in $L - (kS + (1 - k)M)$ results in a good fit with the data (**G** and **H**).

2001; Kuehni, 2004), demonstrating the wide variability in the perception of unique green. For both observers, as the purity of the match light is decreased the identified light approaches equal energy white at the (x, y) coordinate of (1/3, 1/3), as expected.

To account for the variability in unique green, a BY system based on comparing S vs. (L+M) signals has two means of shifting the spectral location of green. The first, demonstrated in Fig. 2.4C, involves modulating the contribution of S into the BY sensitivity function. This leads to a situation where the confusion line does not pass through equal energy white (Fig. 2.4D). The second possibility for modulating the null point of an S-(L+M) system is to vary the contribution of L and M (Fig. 2.4E). The range of values possible for unique green under this manipulation, however, only varies from roughly 490 to 500 nm, or the spectral neutral points for a protan and deutan observer. This again results in a situation where the confusion line of the system cannot be drawn through equal energy white (Fig. 2.4F). These results demonstrate that a BY system based on the output of S vs. (L+M) neurons is not able to account for either the location or axis along which the BY system nulls for the vast majority of individuals or the known variability in unique green.

In contrast, for a BY system derived from the comparison between L and (M+S) signals, there is a considerable spectrum of values possible for unique green. As the ratio of S to M goes from a pure L vs. S opponency (protan confusion line, red line in (Fig. 2.4H)) to a pure L vs.M opponency (deutan confusion line, green line in (Fig. 2.4H)), the range of values exceeds 60 nm (Fig. 2.4F). Consequently, we were able to produce a good fit to the data for observer 2 that passes through equal energy white. This demonstrates conclusively that S-cones contribute to BY hue appearance by summing with M-cones. In the case of this observer, the expected contribution of S is about 0.48 and 0.52 for M.

One caveat to our analysis is that we assumed all observers see an equal energy stimulus as their white point. A large population study of achromatic points indicates that this simplification is a reasonable assumption (Werner and Schefrin, 1993). The mean location

of white was approximately equal energy (x,y=0.31,0.31) with relatively little variability, particularly within an age group. Observer 2 falls close to the population mean for the percept of unique green and the extrapolation of a white point near equal energy is consistent with population measures.

2.4.2 Spectral location of unique hues

On the basis of the findings above, we developed a color model that includes S-cone contribution to both BY and RG hue perception (see *Methods*). The spectral sensitivities of the BY and RG systems (Fig. 2.3) under the BY midget ganglion cell theory, are parameterized most significantly by the ratio of the L- to M-cones in the retina. To further appreciate the extent to which color appearance is expected to change as a function of L:M ratio, we iteratively changed the L:M ratio in our model. The expected null points of the BY and RG systems were found for each cone ratio producing the relationship between L:M cone ratio and unique hues plotted Fig. 2.5.

Most notably the model produces a range of 495 to 555 nm for unique green, with the greatest action occurring between L:M cone ratios of 0.4-0.8. Importantly, this is the range of ratios in which most individuals are known to fall (Carroll et al., 2002). In comparison, yellow and blue are expected to produces considerably smaller spectral ranges. Fig. 2.5 also demonstrates the effect of L-cone peak sensitivity on unique hue perception. The effect is largest in the case of unique green, though the general relationship between hue and L:M ratio is unchanged. Effects of a similar magnitude are found when varying the peak sensitivity of M- and S-cones.

2.4.3 Agreement with observed data

Wide variability in L:M cone ratios between normal observers has been established in the literature (Roorda and Williams, 1999; Carroll et al., 2000, 2002; Neitz et al., 2002; Hofer

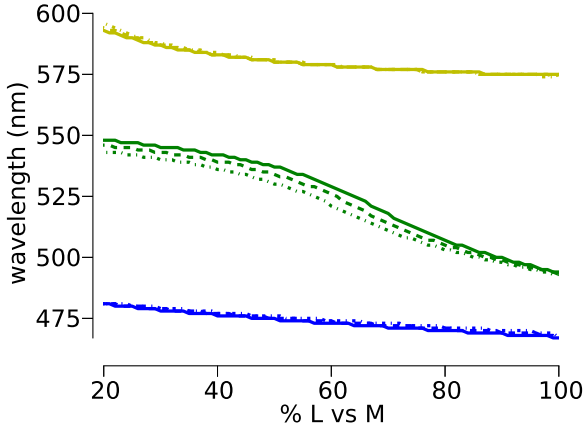

Figure 2.5: Spectral locations of unique hues as a function of L:M cone ratio. The color of the line represents the unique hue and style of the line indicates the peak sensitivity of the L photopigment: solid = 559 nm, dashed = 557 nm, dashed dotted = 555 nm

et al., 2005a). We used the L:M ratio and peak L-cone sensitivity of each observer reported in Table 1 of (Carroll et al., 2002) to find the expected wavelengths identified as uniquely blue, green and yellow.

For this analysis we assumed peak sensitivities of 529 and 417 nm for the M and S-cones. The results produced a distribution of unique green that closely matches that observed by (Volbrecht et al., 1997) (Fig. 2.6). Similarly, RG hue perception based on M vs. (S+L) inputs accurately predicts the narrow distributions for unique blue and yellow as observed experimentally. Table 2.2 displays the mean and standard deviation (StDv) expected for these three hues.

2.4.4 Variation with eccentricity

Finally, the number of cones directly synapsing on each midget ganglion cell is known to increase with eccentricity. To account for these changes, we introduce multiple cones to the

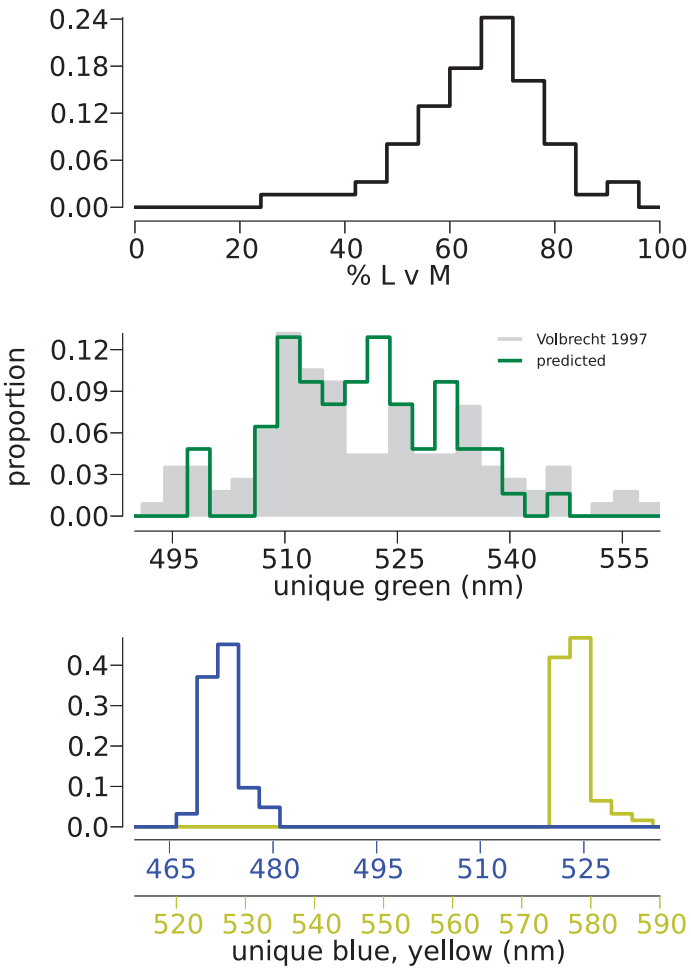

Figure 2.6: BY ganglion cell theory predicts unique hue variability. A distribution of L:M cone ratios is plotted in the top figure. Using this data, a predicted distribution of unique green was produced (green trace) and overlaid over an observed plot from (Volbrecht et al., 1997) (gray area). The bottom plot displays predicted distributions for unique blue and yellow.

Table 2.2: Predicted values of unique hues.

hue	mean (nm)	StDv (nm)	N
green	520.6	10.8	62
yellow	577.2	2.3	62
blue	471.9	2.3	62

direct pathway, δ in Eq. (2.4). This greatly increases the possible combinations of L- and M-cones in both the direct and indirect pathways. Accounting for all possible arrangements leads to a large shift in unique green towards shorter wavelengths similar in direction and magnitude to reports in the literature (Nerger et al., 1995; Volbrecht and Nerger, 2012) (Fig. 2.7). This analysis also predicts a desaturating effect of increasing eccentricity (De Valois and De Valois, 1993), which as been observed psychophysically (Gordon and Abramov, 1977; Nerger et al., 1995; Volbrecht and Nerger, 2012).

2.5 Discussion

The BY midget ganglion cell model presented here has both explanatory and predictive power. First, it meets the criteria of a good scientific hypothesis that its predictions are falsifiable by experiment. Second, the model provides an explanation of why hue perception is not disturbed in individuals with GRM6 mutations that have no S-cone input to small bistratified ganglion cells. In the model proposed here, S-cone contributions to hue perception arise from horizontal cell input that bypasses the defective synapses in mGluR6 patients. Third, the model explains why there is such large range of individual differences in unique green but little variability in unique yellow. S vs. M cone weights to the percept of blueness that occur with variation in L:M cone ratio produce large shifts in unique green but similar variation in S vs. L weights to the precept of redness produce little change in

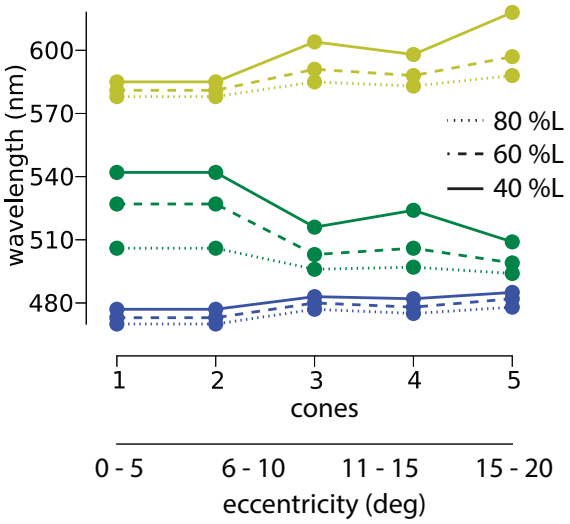

Figure 2.7: Change in unique hues with eccentricity. Hue is expected to vary with eccentricity due to the increasing number of cones with direct input to midget ganglion cells at more eccentric locations. The eccentricity indicated here is approximate.

unique yellow. Fourth, it can explain the hue shifts in unique green that are observed for peripheral vs. central vision. Fifth, the model explains why we have unique hues at all - they are the null points of opponent dichromatic subsystems that have their origins in a subset of retinal ganglion cells. This is in contrast to alternative accounts that have been offered over the years involving cultural or linguistic arguments, the nature of real-world stimuli (Mollon and Jordan, 1997) or interactions between the three cone types and exposure to natural illuminants and surfaces (Philipona and Regan, 2006). Finally, the model predicts the spectral locations of the unique hues without the addition of any post-hoc assumptions. A model capable of accurately capturing both the mean and spectral location of these three hues, as well as the variation between observers is unprecedented as far as we are aware. Moreover, it can predict how unique hues will vary as a function of spectral environment, lens and macular pigment density, cone photopigment spectral sensitivity, and cone ratio, each of which can be addressed by experiment.

2.5.1 Hue appearance

A recent review by Kuehni (2004) reported the mean and standard deviations of the unique hues across a series of studies using a variety of experimental paradigms. We have aggregated the reported values, weighted the mean and standard deviation based on the number of subjects, and produced a population estimate for green, yellow and blue.

Table 2.3: Observed values of unique hues.

hue	mean (nm)	StDv (nm)	N
green	527.2	14.8	648
yellow	577.8	2.9	411
blue	476.8	5.3	411

These results, shown in Table 2.3, demonstrate very similar characteristics to the ones we predict (Table 2.2) for a smaller population of observers. Both the mean and standard deviation of our simulations closely resemble the meta analysis findings. The deviation between the predicted and observed distribution (Table 2.3 vs. Table 2.2 and Fig. 2.6) may be due at least in part to the fact that the population of L:M cone ratios included only men, while observed data plotted in Fig. 2.6 (gray histogram) and the aggregate data in Table 2.3 assessed color appearance in both men and women. Female subjects introduce the possibility of multiple opsin genes with both a 555.5 and 559 nm L peak expressed. Indeed, Volbrecht, Nerger and Harlow found significant differences in the performance between males and females on unique green, with females tending towards shorter wavelength and greater variability (Volbrecht et al., 1997). Both of these trends are predicted by the current model.

Shifts in optical filtering are also expected to introduce between-subject variability. For example, a change of L and M optical densities from 0.5 to 0.3 shifts the expected mean unique yellow for our population of observers from 579 nm to 575 nm, while blue and yellow shift only about 1 nm. Variation in optical density together with the introduction of females to the population of observers is expected to increase the standard deviation associated with each of the three hues. Together these factors may account for the systematic underestimation of variability in the model (Table 2.2) relative to the meta analysis above (Table 2.3). The L:M ratio of an observer is predicted to have a substantial impact on color appearance under the current theory. In particular, the location of uncontaminated green is expected to vary widely, shortening as the proportion of L increases, as shown Fig. 2.6. The small spectral shifts in peak sensitivity resulting from single nucleotide polymorphisms in the opsin sequence give rise to a family of L and M pigment sensitivity curves. While most observers have am M peak of 530 nm and a peak L of either 555.5 or 559 nm (or both) (Carroll et al., 2002), the model can be adjusted to predict color appearance for observers with more rarely observed sequences. The effects of these shifts on hue perception are expected to be smaller

in magnitude than the impact of L:M ratio (Fig. 2.5). The change in uncontaminated blue and yellow are negligible for all observers. Interestingly, the common 3.5 nm variation in L peak is expected to shorten unique green by almost 10 nm for an observer with a 0.5 L:M ratio.

We have also explored the effect of increasing the number of cones with direct input to midget ganglion cells, as occurs in the periphery (Boycott and Wässle, 1999). Increasing the number of direct contacts will produce many more combinations of opponent cells than appear in the fovea. The consequence of such an arrangement is that fewer cells will have a single cone type with direct input to the midget ganglion cell. This decrease in strongly opponent cells will serve to desaturate color appearance (De Valois and De Valois, 1993), consistent with observations reported in the literature (Gordon and Abramov, 1977). Moreover, as demonstrated in Fig. 2.7, this model predicts a shortening of unique green with increasing eccentricity. This relationship has been noted by Nerger, Volbrecht and Ayde (Nerger et al., 1995). It is also worth noting that we have not accounted for the change in expression of L- and M-cones at increasing eccentricities (Neitz and Neitz, 2011). These changes will impact hue perception in the very far periphery and can be introduced by simply changing the assumed L:M cone ratio.

2.5.2 Physiology

The BY midget ganglion cell theory requires the existence of midget cells that carry L vs. (M+S) opponency. The existence of these cells is consistent with recordings in LGN (Tailby et al., 2008b) and were previously reported in ganglion cell recordings (de Monasterio, 1978; de Monasterio et al., 1975). A schematic representation of proposed BY ganglion cell model is shown in Fig. 6.1. The BY circuit is built by summing the input from L, M and S-cones and then differencing this signal from an L-cone directly contacting a bipolar cell. In the case of the ON pathway, this will produce a yellow signal, while the OFF pathway will result

in blue. For the RG system an M-cone is differenced from neighboring cones to produce red (OFF pathway) or green (ON pathway).

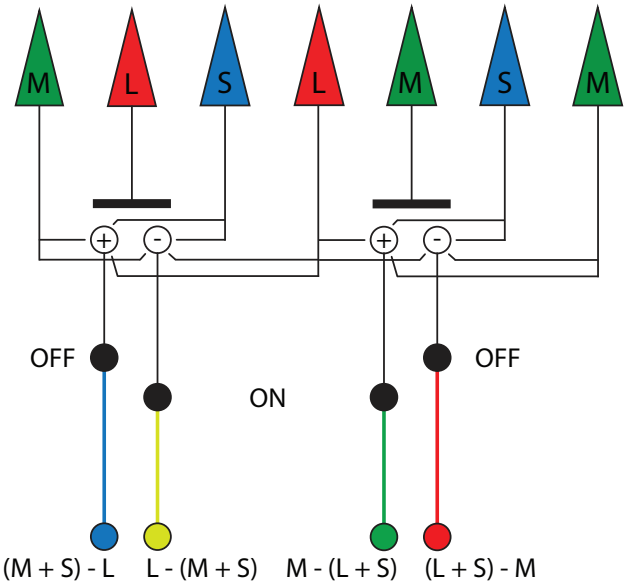

Figure 2.8: Schematic representation of the BY midget ganglion cell theory. A BY system is built by summing the input from L-, M- and S-cones and then differencing this signal from an L-cone directly contacting a bipolar cell. In the case of the ON pathway, this will produce a yellow signal, while the OFF pathway will result in blue. In the case of the RG system an M-cone is differenced from neighboring cones to produce red (OFF pathway) or green (ON pathway).

These circuits could be built via inhibitory horizontal cell input from neighboring cones through a feedback pathway, but we think it is more likely based on a newly described feedforward pathway. Either way, H2 horizontal cells receiving S, M and L signals and H1 cells with input from L- and M-cones, are opposed to inputs from a central cone. Recent anatomical experiments from our laboratory provide evidence for the existence of the feed-forward pathway (Puller et al., 2012, 2014b,a). Such a mechanism would differ substantially

from classical horizontal cell feedback. In this scenario, signals from nearby cones would be integrated in the horizontal cells and fed forward directly into the bipolar cells, creating a bipolar cell with input in which the single center cone opposes a sum of surrounding cones. In addition to this central opponency, there would be the color opponent horizontal feedback onto cones from a larger surround, thus, the proposed arrangement would produce a "double opponent" character. For example, S-cones contributing an ON signal to OFF bipolar cells via H2 horizontal cell feedforward would receive inhibitory S-cone feedback from surrounding S-cones. This could contribute to color constancy of conscious hue perception. Also, it is possible that if the spatial aspects of the double-opponent-like behavior of the cells are configured appropriately, the subset of midgets carrying hue information would not respond to white-dark edges. This would make their response properties quite distinct from conventional L vs. M midget ganglion cells that respond well to white-dark boundaries.

2.5.3 Parallel vs. Serial models

Classically, detection thresholds have been considered to be mediated by S vs. L+M and L vs. M neural channels that correspond to the cardinal directions in color space. Serial models are the favored explanation for why unique hues lie along lines that are rotated relative to the cardinal directions. In these models (De Valois and De Valois, 1993; Stockman and Brainard, 2010) an early stage of color processing is accomplished by L vs. M midget and small bistratified ganglion cells and the outputs of the pre-cortical neurons are recombined at a later stage to produce color opponent channels responsible for hue perception. However, parallel models have been considered. Danilova and Mollon (Danilova and Mollon, 2012b) recently demonstrated a region of enhanced discrimination in color space that corresponds to the subjective category boundary between reddish and greenish hues and suggest that the discrimination is based on a "non-cardinal" opponent neural channel in equilibrium. They offered a parallel model as one possible explanation of why the performance of certain tasks

is based on cardinal opponent neural channels while the performance of other perceptual tasks is based on "non-cardinal" channels. They point out that the absolute number of a given cell type may not be so important and that "central decisions in a particular task may well be based on the signals of a minority type of cell."

The possibility of a parallel model was also considered in the classical study defining the "cardinal directions of color space "(Krauskopf et al., 1982). It was noted that results of one observer suggested a residual selective habituation effect of stimuli at 45° relative to the cardinal axes. In addition to offering a serial model that has become the most conventional explanation, saying there may be "yet another set of adaptable mechanisms at a third level in the visual system", they also suggest the possibility of a parallel model in which there could be "two populations of mechanisms with their maximum sensitivities distributed about the cardinal axes".

Our results are consistent with these earlier proposals of a parallel model. Here we demonstrate the explanatory and predictive power of a parallel model in which a small subset of midget ganglion cells mediate conscious hue perception. At the same time, the large majority of midget ganglion cells that have L vs. M opponency may mediate performance on detection tasks. Similarly, the small bistratified ganglion cells could be important for certain kinds of detection tasks while the (S+M) vs. L midget ganglion cells proposed here mediate conscious hue perception. This could explain the finding that color vision was normal in CSNB1 patients assessed with the FM 100-hue test (Terasaki et al., 1999). However, B-Y perimetry demonstrated detection of S-cone isolating flashes was reduced significantly at 15°-to-30° compared to 0°-to-15° in CSNB1 compared control subjects.

2.5.4 Alternative models

The model proposed here offers an explanation of why hue perception is undisturbed in people with mutations that interrupt S-cone signals to small bistratified cells. Earlier, it

occurred to us that a parallel model might explain how gene therapy was capable of conferring trichromatic color vision in adult monkeys (Mancuso et al., 2009, 2010); however, it was the observation of preserved hue perception in individuals with mGluR6 mutations that further inspired the work presented here. Thus, it is worth considering the possibility of other explanations for the preserved color vision in individuals with mGluR6 mutations.

S-OFF signals have been observed in primate LGN (Derrington et al., 1984; Tailby et al., 2008b). As introduced earlier, a subset of S-OFF LGN cells have L-(S+M) inputs as expected from the GABA mediated feedforward hypothesis presented here. However, a population of S-OFF LGN cells with (L+M)-S inputs is also observed, suggesting the possibility of a different S-OFF pathway carrying S-cone signals out of the retina that could provide an alternative explanation for the preserved color vision in mGluR6 mutants. Though the retinal basis of the (L+M)-S cells is unknown there are a few potential sources of their S-OFF signals. In primates, besides the small-bistratified ganglion cell, the only anatomically distinct and physiologically characterized ganglion cell type that has S-cone specific input is the "giant" melanopsin containing ganglion cell. These cells are S-OFF/(L+M)-ON and project to LGN in addition to other targets (Dacey et al., 2005). Remarkably, application of the ON-pathway agonist, 2-amino-4-phosphonobutyric acid (L-AP4), completely blocks the S-OFF light response in the primate melanopsin ganglion cells (Dacey et al., 2002), indicating S-OFF signals are transmitted to the inner retina via the ON S-cone bipolar cell which does not communicate with S-cones in mGluR6 mutant individuals. The arrangement in melanopsin ganglion cells is similar to S-OFF ganglion cells recently discovered in ground squirrel (Chen and Li, 2012; Sher and DeVries, 2012) in which S-OFF responses arise from S-ON bipolar cells and are sign reversed by an S-cone selective amacrine cell. Like macaque melanopsin ganglion cells, the S-OFF responses are blocked by application of L-AP4. Whether an analogous cell type exists in the primate retina is unknown, but if they do exist and contribute to the population of (L+M)-S LGN cells, along with the melanopsin

ganglion cells, S-cone inputs to them would be blocked in mGluR6 mutant individuals. The same would also be true of the large bistratified type of retinal ganglion cell, which draws excitatory inputs from S-cones via ON-bipolar cells (Dacey and Packer, 2003).

Another potential source of S-cone signals is the occasional S-cone input to the centers of OFF midget bipolar cells observed in the far periphery by Field et al. (Field et al., 2010). These inputs would be intact in mGluR6 mutant individuals but they are sparse and are only known to occur in peripheral midget ganglion cells that draw from around a dozen cones. If these do provide a significant S-cone signal it might be expected to be most prominent in the periphery. Instead, the opposite is true for individuals with CSNB who show deficits in S-cone mediated detection specifically in the periphery (Terasaki et al., 1999). Finally, one anatomical study by Klug et al. (2003) has reported the existence of S-cone OFF midget ganglion cells in the central retina of macaques. However, the existence of an S-cone OFF midget bipolar cell is uncertain. The putative S-cones were not identified by any kind of functional marker in the Klug experiment, and it is possible that "S-cone" terminals they reconstructed belonged to L- or M-cones that happened to be missing an ON midget bipolar cells. Additionally, it is possible that the S-cone ON bipolar cells connecting to the misidentified cones were not S-cone ON-bipolar cells but the recently described "giant bipolar cell" (Joo et al., 2011). Regardless, they propose the existence of an S-cone OFF midget ganglion cell for every S-cone in the central retina, yet to date no S-cone midget ganglion cells have been identified physiologically in the central retina. If S-OFF midget ganglion cells do exist or if the peripheral S-cone inputs described by Field et al. are important for color vision, a model would have to be developed to explain how cells with a (L+M)-S configuration could be responsible for all the aspects of normal hue perception explained here.

2.5.5 Future work

The model elaborated here is dependent upon H2 horizontal cells generating opponency at the level of the midget bipolar cells. H2 horizontal cells are known to carry sign reversed S+M+L potentials (Dacey et al., 1996), and they have been shown to generate an L+M surround in S-cone terminals (Packer et al., 2010). Anatomical evidence has demonstrated sites of synaptic contact between H2 horizontals and L- and M-cone pedicles (Dacey et al., 1996), however, there is no published evidence for feedback from H2 horizontal cells onto other types of cones. Our model predicts an S-cone component to the H2 mediated surround in a small subset of L- and M-cones neighboring S-cones. It has been possible to visualize S-cone terminals morphologically (Packer et al., 2010). Thus, in future work it should be possible to test this prediction of the model by recording responses to S-cone isolating stimuli from L- and M-cone terminals adjacent to S-cones in an in vitro, whole-mount preparation of macaque retina. The model also predicts a GABA mediated feedforward pathway from H2 horizontal cells onto bipolar cells which will be manifest in S-cone responses detectable in a subset of midget ganglion cells that can be suppressed by application of GABA antagonists. In the future, this prediction could be tested by recording midget ganglion cell responses to S-cone isolating stimuli with and without application of GABA antagonists.

Another area of future work will be to directly explore the non-linear behavior of hue perception that has been noted throughout the literature. One example is the non-linear interaction between hue and saturation, known as the Abney effect (Abney, 1909; O'Neil et al., 2012). As a spectral hue is desaturated, the location of the unique hues are known to deviate from an expected linear trajectory towards equal energy white. In the future, a further elaboration of our model could be tested by evaluating its ability to account for these non-linearities. Desaturating a spectral light will change the weights on the RG and BY mechanisms, due to differential adaptation of the S vs. L/M cones, introducing non-linear behavior. The most extreme case will occur with the percept of unique red. A

monochromatic long wavelength light will drive L and M cones in almost equal proportion, but produce virtually no excitation of S cones. As more white is added to the red light, more S contribution will be added to the percept, causing a re-weighting of the (S+L) and (S+M) side of the RG and BY mechanisms, thereby non-linearly changing the position of red as a function of saturation. This could explain the non-complementary nature of the red and green unique hues.

Chapter 3

CIRCUITRY TO EXPLAIN HOW THE RELATIVE NUMBER OF L AND M CONES SHAPES COLOR EXPERIENCE

3.1 Abstract

The wavelength of light that appears unique yellow is surprising consistent across people even though the ratio of middle (M) to long (L) wavelength sensitive cones is strikingly variable. This observation has been explained by normalization to the mean spectral distribution of our shared environment. Our purpose was to reconcile the nearly perfect alignment of everyones unique yellow through a normalization process with the striking variability in unique green, which varies by as much as 60 nm between individuals. The spectral location of unique green was measured in a group of volunteers whose cone ratios were estimated with a technique that combined genetics and flicker photometric electroretinograms. In contrast to unique yellow, unique green was highly dependent upon relative cone numerosity. We hypothesized that the difference in neural architecture of the blue-yellow and red-green opponent systems in the presence of a normalization process creates the surprising dependence of unique green on cone ratio. The experiments described here were done to test different theories of color vision processing that incorporate L and M cone ratio and a normalization process. The most successful model was one that relies on recently discovered circuitry that is capable of combining short (S) wavelength sensitive cone signals with the output of L/M opponent pathways in the outer retina.

3.2 Introduction

Remarkably, while people agree about some colors, there is surprising disagreement across people about others. For example, the wavelength of unique green varies so widely (from 490-555 nm) that pure green to one person can look pure blue to another. This striking fact of human color vision has never had an adequate biological explanation. M:L cone ratio is also strikingly variable, but, until recently, it has seemed highly unlikely to be the cause of individual differences in unique green which is the neutral point of the blue-yellow (BY) opponent system. This is because there is evidence that unique yellow, the neutral point of the red-green (RG) system, is set by normalizing of cone signals through experience (Neitz et al., 2002). The process results in remarkable consistency across people exposed to environments with similar chromatic content compensating for differences in cone ratio (Neitz et al., 2002; Brainard et al., 2000).

Long unanswered questions together with recent discoveries of the genetics of human color vision (Neitz and Neitz, 2011) and the circuitry of the primate retina (Puller et al., 2014b,a) have prompted us to consider alternative theories of the circuitry responsible for hue perception (Schmidt et al., 2014). The relationship between cone ratio and unique green has not been as well investigated and our recent theoretical work indicates that the degree to which cone ratio might be predicted to influence unique green in the presence of a chromatic normalization process depends on the underlying circuitry.

Color appearance cannot be directly related to cone signals; instead, the outputs of the three cones must be combined to account for each of the four hue sensations (Hurvich and Jameson, 1957). The small bistratified ganglion cell with its S-ON/(L+M)-OFF spectral opponency (Crook et al., 2009; Dacey and Lee, 1994) is typically regarded as the retinal basis of blue-yellow (BY) color signals (Mollon, 1999). The simplest hypothesis about the neural substrate for color appearance asserts that small bistratified cells are directly responsible for our perceptions of blue and yellow. Therefore, the neutral point of these cells would be

expected to correspond to the sensation of pure green, i.e., a color in the middle-wavelength region of the spectrum, which is neither bluish nor yellowish. However, the observation that an S versus L+M mechanism, like the small bistratified cells, cannot directly account for human BY color appearance has often been noted. Numerous groups have demonstrated that blue-yellow color vision can only be explained by opponent circuitry in which M cones act synergistically with S cones to signal blueness (De Valois et al., 1997; De Valois and De Valois, 1993; Drum, 1989; Hofer et al., 2005b; Webster et al., 2000b; Schmidt et al., 2014).

Building upon these results, we recently demonstrated that a theoretical BY mechanism, separate from the small bistratified cells, which combines S+M cone signals versus L could capture the known variability in unique green (Schmidt et al., 2014). Assuming the same environmental normalization process that accounts for the very limited variability in unique yellow (Neitz et al., 2002), our theoretical circuit in which S and M signals are summed in the retina predicts large changes in unique green with cone ratio. The theory proposes that human hue sensations are mediated by four different subclasses of midget ganglion cells which receive S-cone input via a newly discovered feed-forward pathway from S-cones via HII horizontal cells directly to midget bipolar cells (Puller et al., 2014a,b). Specifically, we propose that OFF-midget ganglion cells with S-cone ON feed-forward (Puller, Haverkamp, et al., 2014) input and L-cone centers serve the sensations of blue while those with M-centers serve sensations of red. ON-midgets with S-cone OFF feed-forward input and L-cones centers serve yellow while those with M-centers are responsible for green sensations. The proposed retinal origin for neurons that serve BY color vision and have S+M inputs differenced from L cone signals is consistent with recordings from cells early in the visual pathway that would have inherited this input arrangement. For example, cells with S+M inputs have been found in the lateral geniculate nucleus (LGN) (Derrington et al., 1984; Tailby et al., 2008b) and primary visual cortex (Conway, 2001; Horwitz et al., 2007; Horwitz and Hass, 2012). According to our theory, the majority of midget ganglion cells (>90%) that do not receive

S-cone input do not mediate hue sensations, rather they are only involved in producing conscious achromatic luminance sensations in spite of their L/M opponency.

Here, we further test the predictions of our theory compared to the standard LGN theory in which small bistratified ganglion cells are responsible for blue-yellow color vision and two versions of the De Valois and De Valois (1993) multistage model in which outputs of the small-bistratified and midget ganglion cells are proposed to be recombined in cortex. Unique hues were measured in volunteers for whom M/L cone ratios were estimated. Our proposed retinal circuit made more accurate predictions compared to the other theories across a wide range of observations.

3.3 Methods

Participants

14 (8 male, 6 female) color normal subjects (assessed with a Nagel anomaloscope) were recruited from the University of Washington community. They ranged in age from 22 to 60 years with a mean of 37 (σ=14.04) years. Three of these participants also enrolled in a study of hue cancellation, including one of the authors (BPS, S2). One individual (male, 33 years) with incomplete Congenital Stationary Night Blindness (CSNB1) participated in a separate study. Research on human subjects followed the tenets of the Declaration of Helsinki and was approved by the Human Research IRB at the University of Washington.

Measurement of M:L cone ratio

We measured M:L cone ratio with an established technique that combines genetic and electrophysiological analysis (Carroll et al., 2000, 2002; Hofer et al., 2005a; McMahon et al., 2008). For all statistical analysis %M was used (M / (L+M) x 100). %M was used here rather than %L for clarity, since the arguments presented are centered on the contribution of M cones to the BY system.

Light source

Monochromatic stimuli were produced with a Gooch and Housego OL 490 controllable light source (Crognale et al., 2009). Light output was controlled with custom software written in C# (Microsoft Inc.) or MATLAB programming languages. For all experiments, spectra had a full bandwidth at half maximum of 10 nm. Output from the OL 490 was directed with a liquid light guide to either an integrating sphere or a Maxwellian view system. The light source was calibrated with a SpectroCal (Cambridge Research Systems) spectroradiometer and an optometer (Gamma Scientific, flexOptometer).

Unique hue procedure

Unique yellow and green were determined with a randomly interleaved forced choice double staircase procedure (Neitz et al., 2002). All experiments were carried out in the dark. Participants were positioned on a chin rest and freely viewed the circular 1.5 degree integrating sphere. The mean luminance was 34 cd m^{-2}. Each light remained on until a selection was made; a one second pause separated each light. The program terminated after ten reversals. The step size was adaptive, decreasing to one nm after the third reversal. The final five reversals were averaged for each staircase. Each hue was tested three times per session. Therefore a total of six staircases were averaged for each hue. Subjects completed at least two sessions. The first session was discarded for practice. The order of unique hue measurements was randomized for each session.

Macular pigment optical density

Macular pigment optical density was measured with an established psychophysical technique (Wooten et al., 1999). The OL 490 produced a square wave 50% duty cycle alternation (at 14 Hz) between a 462 nm test light and a 575 nm reference. The integrating sphere subtended 1.5 degrees and its output was superimposed on a blue adapting background (471

nm dominant wavelength) from an organic light emitting diode monitor with a beam-splitter. The luminance of the background adapting light and the reference were kept at 3.31 cd m^{-2} and 1.78 cd m^{-2}, respectively. Participants controlled the intensity of the test light. Subjects viewed the test region with their right eye and were permitted to change the intensity of the test light for as long as needed. The starting intensity was randomly selected. Each measurement was an average of 5 trials. Each subject completed two sessions of the foveal and parafoveal (6 degrees) condition. The first session for each condition was discarded as practice. Optical density was taken as the ratio of the intensity of the test light in the foveal condition to the intensity in the parafoveal condition (Wooten et al., 1999).

Iris Lightness

Iris lightness was measured as following Welbourne et al. (2013) A 14.2 megapixel Sony NEX-5 with an Advanced Photo System type-C (APS-C) sensor and an HVL-F7S flash (Sony) was used. The camera settings were: 1/160 shutter speed, F5.6 aperture and ISO800 sensitivity. The lens zoom was set to 35 mm, which is roughly equivalent to an 85 mm lens on a standard digital single lens reflex (SLR) camera.

Hue cancellation

Hue cancellation (Hurvich and Jameson, 1957) was performed with a single channel Maxwellian view optical system and the OL 490 light source, which simultaneously delivered test and cancellation stimuli. Test lights ranged from 484 to 582 nm in 7 nm steps with the order of presentation randomized. Cancellation lights consisted of the subjects unique blue or unique yellow (Werner and Wooten, 1979), as determined with the procedure outlined above. Retinal illuminance of each test light was set to 2.3 log trolands, assuming the luminous efficiency function of Sharpe et al. (2005). The circular field subtended 3.4 degrees on the retina and was presented to the right eye. Stimuli were presented for 1 s with a minimum of 3 s between

presentations. Experiments were carried out in a dark room with no background adaptation. Two practice sessions were provided prior to data collection. Subjects were instructed to use a hand held controller to adjust the intensity of the cancellation light until the mixture appeared neither blue nor yellow. Subjects were allowed as many presentations as necessary within each trial. Sessions lasted between 10 and 20 minutes and no more than 3 sessions were completed in a single sitting. Each subject completed 5 sessions. The average relative radiance necessary to cancel each test stimulus was corrected for differences in lens filtering due to aging relative to a 20 year old standard lens (Pokorny et al., 1987).

The measured hue cancellation values were then arbitrarily scaled to minimize the least squares difference to the four models described below (Model. For each subject, the L cone photopigments were set to peak at the genetically determined maximum sensitivities. The S cone peak was assumed to be 421 nm for all subjects. The relative weightings of the L and M cones were allowed to vary in determining the best fits to the hue cancellation results. The best fitting relative M/L contributions were then compared to the M/L cone ratios determined experimentally.

Control analysis

To assess the potentially confounding effect of age in our analysis (Schefrin and Werner, 1990), we ran a multiple regression that included %M and age as factors. Age did not significantly add to the predictive power of either of the unique hues (data not shown). Therefore, we did not consider age as a factor in subsequent analyses.

Statistics

All statistical models were implemented in the open source programming language, Python, with the NumPy, SciPy and StatsModels statistical computing extensions. Error bars are represented as ± standard error of the mean.

3.4 Models

As explained in the introduction, we contrasted how well four biologically motivated models of color appearance predict the large population variability in unique green. Each model was based on a plausible neural circuitry underlying primate color appearance. The purpose of these experiments was to study how the neurobiology would be expected to shape the character of color experience were it the basis of human color vision. All models were constructed with the spectral sensitivity functions from (Carroll et al., 2000) and lens and macula density filters from (Stockman and Sharpe, 2000).

LGN model

The LGN model (Fig. 5.1A) implements a classical S(L+M) BY channel and a RG mechanism that differences L and M cone signals. These opponent interactions are based on the commonly observed opponency in primate LGN (Derrington et al., 1984; Reid and Shapley, 2002; Tailby et al., 2008b) that have their retinal origins in the small bistratified (Dacey and Lee, 1994) and midget ganglion cells (Benardete and Kaplan, 1999; Calkins and Sterling, 1996), respectively. Each channel incorporated a normalization process to the mean environmental spectrum (equal energy white) to account for the known plasticity in hue perception after changes in spectral environment (Belmore and Shevell, 2008; Delahunt et al., 2004; Neitz et al., 2002). The normalization process consisted of a single multiplier applied to one side of the opponent equation that was adjusted until the theoretical opponent response integrated to zero (no response) when exposed to the mean spectrum. The environmental mean spectrum was assumed to be equal energy for simplicity. L and M cone inputs were summed to unity, with the contribution from L and M representing their relative numerosity.

Fig. 5.1A shows how the S(L+M) cone opponent signals of small bistratified cells are expected to change as %M is varied over the range most commonly found in the population (Carroll et al., 2002). Though this mechanism predicts a small change in unique green, it

could account for only a very small fraction of the wide range of wavelengths selected as unique green by color normal observers (Kuehni, 2004). The spectral location of unique yellow is also expected to be largely stationary.

De Valois model

The De Valois model (Fig. 5.1B) is an implementation of the model described by De Valois and De Valois (1993). The motivation for this model was to explain the transformation in opponent responses between LGN and cortex necessary to account for human hue perception. The model begins by taking the cone fundamentals (first stage) and opposes them (second stage) in a manner reflective of typical retinal/LGN neurons. In the third stage of the model, cortical cells are built by linearly combining second stage neurons from both the parvocellular and koniocellular pathways. The proportion of M to L cones influence both the second and third stages of this model, but the M:L ratio was assumed in the original publication to be 1:2. Here we permitted M:L cone ratio to vary in order to study the impact of that variable on the expected perception of color in individuals with differing M:L ratios. The model was otherwise constructed as described in the original publication and did not contain a normalization process.

The predictions of this model are shown in Fig. 5.1B. Unique yellow is expected to vary little across a large range of %M values, reaching very long wavelengths in subjects with highly skewed cone ratios. Unique green is predicted to follow an inverted U-shaped function (Fig. 5.1B right column). At low %M, unique green approaches that of a deutan viewer (0%M), while with increasing %M unique green shifts to longer wavelengths, before plateauing at 518 nm between 55-65%M and finally sloping back down towards the protan (100%M) spectral neutral point (about 490 nm) at still greater %M values.

Hybrid model

Our theory differs from the DeValois Model in two ways. The circuity is different and the De Valois model does not include normalization to the environmental mean. In order to separate possible differences in the accuracy of the predictions that are attributable to differences between the circuit models from those that are related to the normalization, we introduced a normalization procedure to the second stage of the De Valois model, such that their S-opponent, M-opponent and L-opponent cells (De Valois and De Valois, 1993) were normalized to integrate to zero through the same scalar multiplier described in *LGN model*. The third stage of the model was otherwise unaffected. We refer to this as a "hybrid" model (Figure 1C). The predictions of this model are similar to the De Valois model with more exaggerated unique yellow values at the extremes of the %M range, a broader plateau and longer unique green values at all locations.

Midget ganglion model

Finally, we compared the predictions of a model of color appearance that we recently proposed based upon a newly discovered feedforward pathway from H2 horizontal cells directly onto cone bipolar cells (Schmidt et al., 2014). Like the De Valois model, our theory results in a BY system with S+M versus L opponency and a RG system that opposes (L+S) and M signals. However, there are for major differences between our theory and theories that propose an added cortical stage to reconcile the physiological properties of midget and small bistratified cells with hue perception. According to our theory, 1) small bistratified cells do not contribute to conscious hue perception. 2) The majority ($> 90\%$) of midget ganglion cells do not contribute to conscious hue perception. 3) Green and yellow hues are specifically relayed through ON pathways, while red and blue sensations are carried by off pathways. 4) Color and achromatic luminance are separated in the outer retina. Previously, we have shown that our proposed midget ganglion cell circuit predicts the mean spectral locations

and variances of the unique hues reported in the prior literature (Schmidt et al., 2014). The midget ganglion model was constructed as described previously, with the exception that the S cone gain used here was slightly different then reported earlier (Schmidt et al., 2014) in which an equal quantum spectrum was employed (however, an equal energy spectrum was reported in error in the description). Changing from a quantal to energy spectrum does not change the prior or current results in a meaningful way except that the S cone weight is now set to one.

Under our proposed neural architecture, unique yellow is largely unchanged across a wide range of M:L ratios (Figure 5.1D). Unique green, on the other hand, is predicted to shift from 504 nm to 541 nm for retinas with 15 %M to retinas with 55 %M. The large shifts in unique green that are predicted to accompany changes in %M are the result of the characteristics of an opponent site in outer retina for the BY system and the large separation (of about 110 nm) in spectral peak of the S and M cones. According to this theory, +S-cone input is added to the center of a small subset of OFF-midget bipolar cells that have direct input from L cones. This produces a +S-L center. The excitatory input from M cones in the surround is the origin of the M cone input to blueness and this predicts a large effect of M:L ratio on unique green. For example, in retinas with a high proportion of L cones, many midget ganglion cells with L cone centers will have all L cone surrounds; those with S-cone feed-forward input are BY cells with +S-L opponency. The null point of +S-L cells is short-shifted and the more cells like this a person has, the shorter his unique green. In contrast, in more M-cone dominated retinas, many midget ganglion cells with L cone centers will have pure M cone surrounds producing more M biased (S+M)-L opponency contributing to longer shifted unique green.

3.5 Results

Hurvich and Jameson (1957) famously formulated theoretical equations assuming S versus

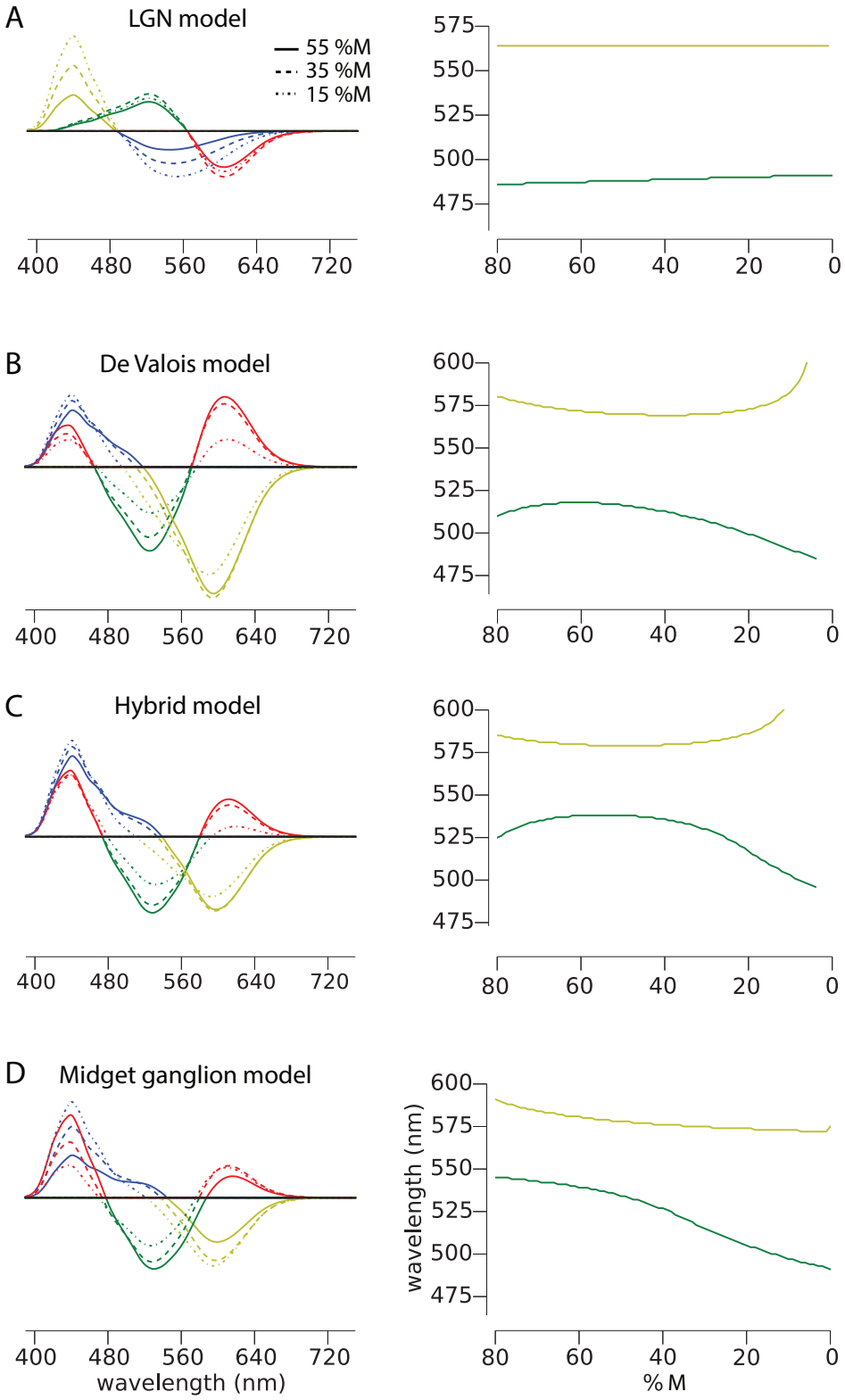
A
LGN model
55 %M
35 %M
15 %M
400 480 560 640 720
575 550 525 500 475
80 60 40 20 0
B
De Valois model
400 480 560 640 720
600 575 550 525 500 475
80 60 40 20 0
C
Hybrid model
400 480 560 640 720
600 575 550 525 500 475
80 60 40 20 0
D
Midget ganglion model
400 480 560 640 720
wavelength (nm)
600 575 550 525 500 475
wavelength (nm)
80 60 40 20 0
% M

Figure 3.1: Predicted relationship between L:M cone ratio and unique hues depends on the underlying circuitry. The predicted influence of a normalization process in the presence of varying %M is shown for the spectral sensitivity of RG and BY chromatic mechanisms under different assumptions about the underlying circuitry. A. A RG and BY system (left column) incorporating the predominant spectral opponency of LGN does not predict large variation in unique hues with %M (right column). B. The cortical model proposed by De Valois and De Valois anticipates substantial variation in unique green and yellow. C. A hybrid model that is built through normalizing the retinal component of the De Valois model (B) also demonstrates a substantial dependence upon cone numerosity. D. Finally, a theoretical BY system comparing S+M against L signals predicts large changes in unique green with changes in %M.

L+M inputs to opponent processes that could reasonably fit measures of chromatic-opponent response functions from a hue cancellation task. Their work provided quantitative empirical support for multi-process theories over the Helmholtzian view that separate neural pathways carrying signals from three cone types could directly account for color experience. Here we tested the hypothesis that variation in unique green is the result of variation in cone ratio and that differences in the underlying circuitry for BY and RG color vision are responsible for the differences in the variability of unique green and unique yellow. Since wide variability in unique green with cone ratio is predicted for opponent models that difference S+M versus L (Fig. 5.1B-D) but not the S versus (M+L) originally assumed by Hurvich and Jameson (Fig. 5.1A), we first reexamined how well each model could account for chromatic response functions using modern measurements of the cone spectra derived from physiological measurements that were individualized for each volunteer from genetic data.

M cones contribute to blueness

We studied the appearance of monochromatic test lights in the middle wavelength portion of the visible spectrum in three subjects using a hue cancellation procedure (Hurvich & Jameson, 1957; Werner & Wooten, 1979). The participants were instructed to change the intensity of a canceling light until the appearance of blue and yellow was extinguished from the mixture. The intensity required to cancel the test light is plotted in Fig. 5.2. In this portion of the spectrum the data behave monotonically, with decreasing blueness as the wavelength of the test light increases until reaching a null point after which yellow is increasingly sensed.

In order to measure the contribution of each cone type to these appearance measurements, we fit four models. The black dotted lines in Fig. 5.2 represent the LGN model (S(L+M)), which reflects cone inputs to small bistratified cells and the original mechanism proposed by Hurvich and Jameson (Fig. 5.1A). In all three subjects, this model was unable to satisfactorily describe the data, corroborating prior findings under similar experimental conditions (Werner

& Wooten, 1979). In comparison, the three channels carrying S+M signals opposed to L were more successful in capturing the features of our data. The De Valois model (dashed dotted line) was least successful of the three S+M versus L models. The inability of this function to fit the data comes about from the lack of a normalization process. In the absence of a normalizing mechanism, the De Valois model does not integrate to zero, leaving the yellow side of their function with substantially more weight than the blue side, thus producing a poor fit to the blue data. The hybrid and midget ganglion cell models (blue and yellow lines) produce identical fits to the data and were the most successful at describing our findings. The root mean squared errors (RMS) for each model are recorded in Table 3.1.

Table 3.1: Model fits to hue cancellation data for three subjects. Each value is the RMS error of the model to the hue cancellation data.

model	S1	S2	S3
midget ganglion	0.03	0.04	0.08
hybrid	0.03	0.03	0.08
De Valois	0.08	0.06	0.12
LGN model	0.18	0.16	0.17

The relative number of M cones and unique green

A second interesting feature of our cancellation data is the prediction produced by each model for the relative number of M cones in each volunteers retina. In the four models compared here, the relative strength of L and M cones to the opponent mechanisms is set by the ratio of M:L cones in the subjects retina (see MODELS section). As shown in Fig. 5.1A, the LGN model predicts that increasing the relative number of M cones should produce a stronger M cone contribution to yellowness (Fig. 5.1A: left column), and consequently shorter unique

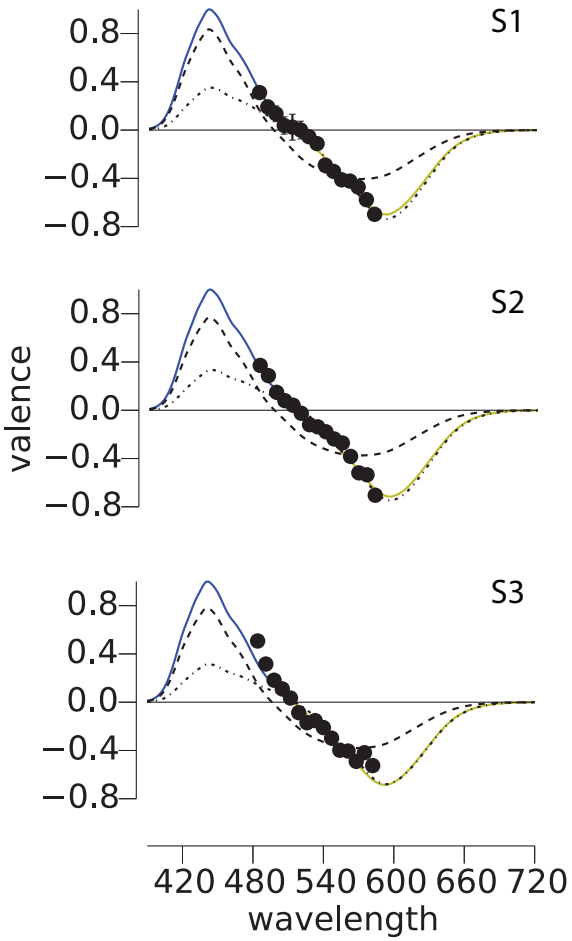

Figure 3.2: Three subjects made hue cancellation settings for wavelengths between 484 and 582 nm at a luminance of 200 Td. The relative intensity of the cancellation necessary to eliminate the sensation of blue and yellow is plotted for each subject. Two models of BY opponency were fit to each subjects data. The dotted lines demonstrate the best fit LGN, S(L+M) system. Dashed-dotted lines represent the De Valois (S+M)L mechanism, while the colored lines are an (S+M)L model with a normalization (hybrid and midget models produce identical fits). In each case, the BY system is best fit with a system summing S and M cones and incorporating a normalization mechanism to the mean environmental distribution.

greens (Fig. 5.1A: right column). As a result, to fit our hue cancellation data, this model minimizes M cone contribution in each fit (Table 3.2), resulting in a prediction of 0% M cones in each subjects retina (compare to the objectively measured ERG %M).

In contrast, over the normal range of %M values (15-55 %M), the three S+M versus L systems described here predict increasing M contributions to blueness with increasing M:L ratio and hence longer unique greens. However, the specifics of the relationship between the BY function and %M differ between these three models. Both of the cortical models are influenced by M:L cone ratio at both the second stage, where opponency is introduced, and the third stage, where opponent neurons from LGN are summed together based on their relative numerosity - a visual system with more M than L cones will consequently have more M cone center midgets. Hence, at the extreme M:L values, the asymmetries in the M:L ratio begin to cancel and produce BY functions with null points that naturally return back to the dichromatic null points (Fig. 5.1B&C). In the three subjects studied here, the midget ganglion cell model predicted values of %M closer to the values measured with our ERG and genetic technique than the two cortical models (Table 3.2).

Table 3.2: Estimated %M from ERG versus fitted models.

model	S1	S2	S3
ERG %M	40	44	27
midget ganglion	37	35	33
hybrid	21	20	19
De Valois	61	61	55
LGN model	0	0	0

The relative number of M cones is correlated with unique green

The observation that M:L ratio estimated from fitting theoretical models roughly follows the objectively measured values of M:L ratio motivated us to further test whether the strength of M cone input to blue might be correlated with the relative number of M cones in a larger sample. Due to the difficulty in obtaining hue cancellation data in a large number of subjects, we measured only unique green and yellow in the larger sample.

The spectral locations of unique green and yellow in our subjects have been plotted as a function of the subjects relative number of M cones in Fig. 5.3. These are remarkably well fit by our previously published predictions (solid lines) that are based upon an S+M versus L mechanism that incorporates cone ratio and an environmental normalization process (Schmidt et al., 2014). The position of unique green (the null points in Fig. 5.1C) provides a measure of the strength of M cone input to blue: longer unique greens suggest a stronger input from M cones (Fig. 5.1C). By the same logic, the spectral location of unique yellow provides an assessment of the strength of M cones to the sensation of green. As observed earlier (Neitz et al., 2002), unique yellow (μ=574.7, σ=3.7 nm), a spectral neutral point of the RG system, was not significantly correlated (r^2=0.156, p=0.162) with the relative number of M and L cones. In striking contrast, the neutral point of the BY system, green (μ=525.7, σ=11.5 nm), was significantly correlated with %M (r^2=0.51, p=0.004). S

The search for biological correlates to explain hue perception has a long history (Kuehni, 2004) and individual differences in iris lightness, and macular pigment optical density (MPOD) have been weakly correlated with unique green (Jordan and Mollon, 1995; Welbourne et al., 2013). To assess the potentially confounding impact of these factors on our analysis, we also measured MPOD and iris lightness in our subjects. We found lighter irises had shorter values for unique green, similar to the previous studies. A linear regression indicated that this relationship was statistically significant for unique green (r^2=0.319, p=0.035), but not for unique yellow (r^2=0.071, p=0.358). Next we measured MPOD in our subjects and found

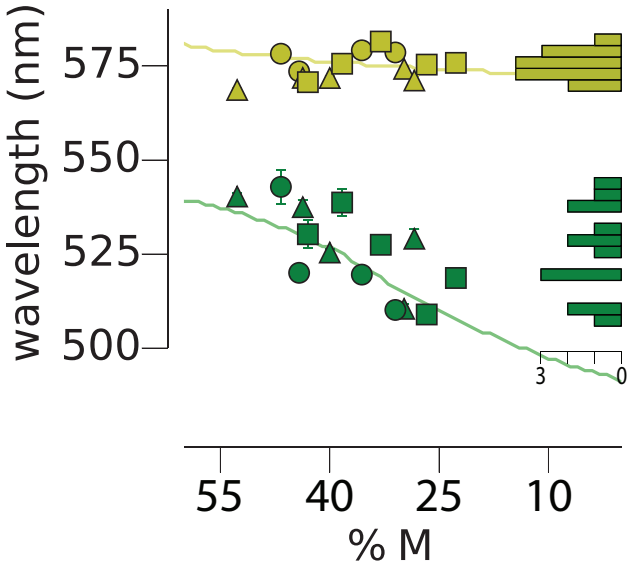

Figure 3.3: M cone input to blue is correlated with cone ratio. The spectral position of unique yellow and green were determined for fourteen subjects. The abscissa denotes %M (M/(L+M) x 100). Symbols represent peak L-cone sensitivity: circles=559 nm, squares=557.25 nm and triangles=555.5 nm. Green and yellow symbols show determinations of unique green and unique yellow for each subject. Continuous lines are the predictions of the model that most accurately predicted our subjects unique hue results, the midget ganglion model (Fig. 5.1D). The histograms on the right show the distribution of unique hue settings. Scale bar denotes number of subjects.

qualitatively similar results to those of Welbourne et al. (2013). A multiple regression with MPOD, iris lightness and %M produced a significant prediction of unique green ($F_{3,10}$=4.735, p=0.026), capturing 58.7% of the variance. However, after controlling for all other predictors, %M was the only factor that contributed significantly to this prediction (t=-2.357, p=0.04). In comparison to the results for green, the same regression against unique yellow captured only 19.5% of the variance and was not a significant predictor ($F_{3,10}$= 0.807, p= 0.518) of spectral location. Together these results support the hypothesis that M cones act synergistically with S cones to produce blue and that the magnitude of L and M cone signals in opponent circuitry is set by their relative numerosity.

Predictions for each subject were generated for the four models of color appearance studied. As expected (compare Fig. 5.1A and Fig. 5.3), the LGN model did not produce accurate predictions for any of our subjects and was out of further analysis. The RMS error for the three remaining models is shown in Table 3.3. For both unique yellow and green, the midget ganglion model produced the most accurate predictions for our 14 subjects. Pair-wise T-tests revealed that the midget ganglion model significantly out performed the De Valois model, but the performance of the midget ganglion model did not reach significance against the hybrid model (Table 3.3).

The neural locus of opponency

While the above findings lean in favor of the midget ganglion model over the two cortical hypotheses, they do not conclusively resolve the neural locus at which S cones are injected into L M opponent circuits. To further examine this question we studied an individual with a genetic lesion rendering silent the transmission between cones and ON-bipolar cells. Individuals with complete Congenital Stationary Nightblindness (CSNB1) are identified clinically by difficulty seeing at night and an absent b-wave, corresponding to ON-bipolar cell excitation, in ERG recordings (Dryja et al., 2005). Previous studies have reported normal

Table 3.3: Model fits to unique hue data. Mean and standard deviation (std) in nm.

model	Green	Yellow
	mean (std)	mean (std)
De Valois	15.3 (8.7)	5.2 (3.2)
hybrid	8.9 (7.0)	5.8 (3.4)
midget ganglion	7.1 (4.5)	3.7 (2.7)
	t-test, p	t-test, p
De Valois vs midget	-3.67, 0.002	-9.06, <0.001
hybrid vs midget	-0.66, 0.52	-2.05, 0.06

color discrimination in patients with CSNB1 (Bijveld et al., 2013a; Dryja et al., 2005). Here we extend these findings and confirm normal color appearance behavior in a CSNB1 patient. The subject reported no difficulty completing the task. Comparison of his unique yellow and green to color normal subjects demonstrated the spectral lights chosen by our CSNB1 subject are indistinguishable from color normal subjects. His unique blue (488.1 nm) is also well within the range of normal subjects (461-495 nm) (Kuehni, 2004), falling 1.5 standard deviation from the population mean (477.9 nm, 6.8 nm). These results confirm the persistence of undisrupted hue perception in CSNB1 individuals despite the absence of S-cone input to their small bistratified cells, consistent with the hypothesis that ganglion cells, other than small bistratified cells, are responsible for BY hue perception.

3.6 Discussion

Our findings reveal a significant correlation between the relative number of L and M cones in a subjects retina and the character of sensations associated with middle wavelength lights. This solves a long-standing mystery of the physiological basis of the huge variability in color

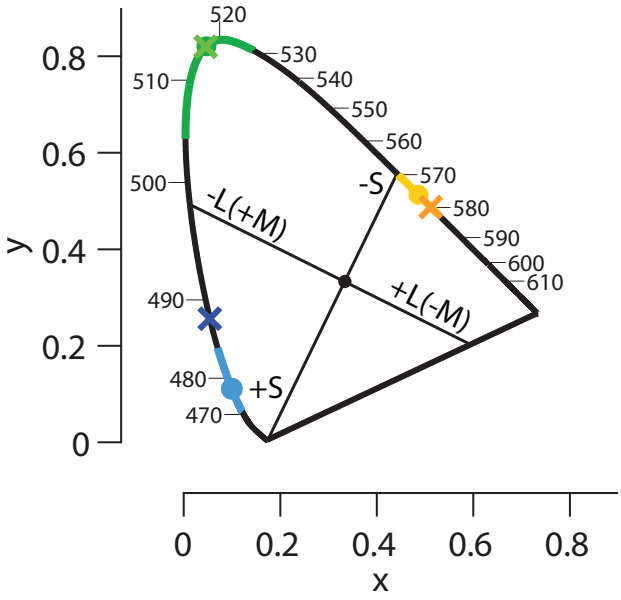

Figure 3.4: Absence of ON bipolar signal does not disrupt color appearance. Unique hue results from a subject with CSNB1 (crosses) are plotted against mean values for normal subjects in the CIE diagram (circles represent mean, solid colored lines denote 1 standard deviation) (Kuehni, 2004). Cardinal axes are drawn following the conventions of Derrington et al. (Derrington et al., 1984). Note the unique hues do not align with the cardinal axes.

vision in the middle-wavelength part of the spectrum. A greater percentage of M cones bias the sensation of the purest green towards longer wavelengths. To account for these results we compared the predictions of four potential neural circuits through a mathematical modeling exercise. For all of our results, the character of human hue sensation was best captured by a circuit based in a small subset of midget ganglion cells that receive S cone input (Schmidt et al., 2014).

Two conclusions that are most clear from these experiments are 1) human blue/yellow hue perception is based on neural circuits in which S+M cone inputs are differenced from L. The three models that incorporated an S+M versus L circuit made significantly more accurate predictions than hue perception based directly on an S (M+L) circuitry. 2) Normalization to the mean spectral environment is required to explain hue perception. This seems to be an important general principal of opponent systems. Such systems operate efficiency when the relative weighting of the opposing inputs are adjusted to null to the average stimulus. Thus, only deviations away from the mean are transmitted, no energy is wasted in signaling the mean and the operating range of the detector is perfectly aligned with the relevant distribution of energies in the environment.

The remaining issue investigated here is the underlying biological substrate for the S+M versus L circuity required to explain BY color vision. Below we further consider the results presented here as well as additional results from the literature and suggest further tests to distinguish the possible underlying neural mechanisms.

Hue cancellation

Based on recent evidence that S and M cones sum to produce the sensation of blue (for review see Stockman and Brainard (2010)), we were motivated to reexamine classical hue cancellation curves first measured by Hurvich and Jameson (Hurvich and Jameson, 1957). Under the conditions employed here, we found an S (M+L) mechanism, as originally pro-

posed, was not able to account for our results (Fig. 5.2). This observation has been noted before (Stockman and Brainard, 2010; Werner and Wooten, 1979) and is extended here in volunteers with known photopigment genetics and M:L cone ratios. In the three models that summed signals from S and M cones to produce blue, we found substantially improved fits to our data. We further noted that the cortical model of color processing proposed by De Valois and De Valois produced a less satisfactory fit to the blue side of the three measured BY functions (Fig. 5.2). The De Valois model was not designed to null to a white stimulus and thus predicts a stronger yellow mechanism relative to blue. In comparison, the hybrid and midget ganglion models, which incorporate a normalization mechanism to the mean environmental spectrum, did produce close fits to our data.

The blue/yellow system and M:L ratio

In addition to measuring the psychophysical strength the BY system, we also measured the %M cones in our three subjects using flicker ERG and genetics. This allowed us to compare the best fit M and L cone weights for each of the model systems to the relative number of M and L cones measured in each subjects retina (Table 3.2). In our three subjects, the best-fit midget ganglion model assumed M and L cone weights closest to those measured with ERG. This finding reflects the idea that retinal ganglion cells sample the cone mosaic randomly and that cone weights tend to be set by the relative numerosity of cone types (Buzás et al., 2006; Deeb et al., 2000; Field et al., 2010; Lennie et al., 1991; Paulus and Kröger-Paulus, 1983). One caveat to this analysis is that both of the cortical models examined are U shaped functions with two M:L ratios that produce identical BY functions. However, because %M values greater than 70% are extremely rare in populations of Caucasian with normal color vision (Carroll et al., 2002; McMahon et al., 2008), we did not permit the fitting procedure to move above 70%M. Adding this constraint does not reduce the quality of fit, but it does ensure the best fit solution will always fall between 0-70%M.

Encouraged by the hue cancelation results, we explored the relationship between %M and hue sensation in greater detail with unique hue measurements. The unique hues are thought to represent the null points of the two dichromatic color systems (Hurvich and Jameson, 1957) and thus serve as an abbreviated method of comparing color appearance mechanisms between individuals. The most surprising result from this series of experiments was the correlation observed between unique green and M:L cone ratio (Fig. 5.3). After correcting for other factors known to influence the perception of unique green, iris lightness and macular pigment optical density, we found that M:L cone ratio was still statistically predictive of the wavelength selected as purely green. In the same group of subjects, unique yellow was not dependent upon cone ratio, confirming previous findings (Jordan and Mollon, 1997; Neitz et al., 2002).

To account for these results, we examined the predictions for each of our subjects made by four neurobiologically motivated theories of color appearance that incorporate M:L cone ratio into their cone weights. All three models that opposed S+M against L signals captured the general trends in our data. Over the range of %M values in our volunteers (23 53 %M), all of the models predicted relatively unchanging wavelengths of unique yellow and a steady decline in the wavelength of unique green with decreasing %M values. When the predictions of each model were directly compared, the midget ganglion model outperformed the two cortical models in both unique yellow and green predictions (Table 3.3). The midget ganglion model forms a BY circuit through an OFF midget pathway. In the central retina where midget centers draw excitatory input from a single cone, the BY circuit would contain a pure L cone center differenced from a surround of S, M and L cones. Adding additional M cones lengthens the wavelength of unique green. However, in the cortical models, the third stage of processing, which sums L/M opponent cells with S (L+M) cells, the effect of adding more M cones is partially canceled out. Therefore, both cortical models, especially the original De Valois model, underestimate the effect of %M we observed in our subjects.

Similarly, in the case of unique yellow, decreasing the strength of M cones below 25% leads to rapidly increasing unique yellow settings in the two cortical models (Fig. 5.1B&C). In comparison, the midget ganglion theory, due largely to its retinal normalization mechanism, predicts largely unchanged values for unique yellow in this low %M region. Together these differences between the midget ganglion and cortical models led to better predictions from the midget model and lends further support to the interpretation that the unique hues are formed in a small subset of midget ganglion cells.

Environmental normalization

The experiments carried out here were additionally motivated by the evidence that hue sensations are subjected to a normalization mechanism (Belmore and Shevell, 2008; Delahunt et al., 2004; Miyahara et al., 1998; Neitz et al., 2002; Pokorny and Smith, 1987; Walraven and Werner, 1991; Werner, 1996). The sensations of white and yellow vary little between subjects despite large differences in M:L cone ratio (Jordan and Mollon, 1997; Miyahara et al., 1998; Neitz et al., 2002; Pokorny and Smith, 1987) and pre-retinal optical filtering (Delahunt et al., 2004; Walraven and Werner, 1991). Moreover, sudden shifts in spectral environment lead to predictable changes in hue appearance that are accounted for by a gain scaling mechanism (Delahunt et al., 2004; Neitz et al., 2002; Werner, 1996), though see (Belmore and Shevell, 2008).

The necessity of the hypothesized normalization mechanism is most clearly demonstrated in the performance of the De Valois model versus the hybrid model. The only difference between these two theories is the incorporation of a normalization process to the environmental mean spectrum, such that the second stage (retina/LGN) mechanisms in the original De Valois model were made to integrate to zero. The addition of this normalization produces a null response to a white stimulus (assumed to be equal energy white for simplicity). The hybrid model produced a superior fit to both our hue cancelation data (Figure 5.2) and unique hue

data (Figure 5.3).

ON pathway defects

Most modern theories of color vision circuitry propose that the S cone signals contained in the output of the small bistratified ganglion cell are the retinal basis for BY color vision. This includes the two cortical hypotheses discussed presently, which postulate a cortical stage combining the S cone rich small bistratified with L/M parvocellular neurons. Therefore, complete absence of S cone inputs to the small bistratified cells, as happens in people with mutations that interrupt signaling between S-cones and S-ON bipolar cells should have a profound effect upon on BY color vision. Contrary to this standard view, the midget ganglion model hypothesizes that blue hue perception is mediated by OFF midget bipolar cells with the +M component coming from the surround and the +S component coming from GABA mediated feedforward input and is unaffected by cone to ON bipolar signaling that is disabled in people with mGluR6 defects (Dryja et al., 2005; **?**; Schmidt et al., 2014). Previous reports have indicated that mGluR6 mutations are not associated with abnormalities in color vision as assessed with standard clinical tests (Bijveld et al., 2013a; Dryja et al., 2005). Here we extend these findings and confirm normal color appearance in a subject with complete congenital stationary night blindness. The preservation of normal unique hue settings presents a challenge to cortical models.

Color appearance in individuals with skewed M:L cone ratios

A challenging result for all models of color appearance to account for are the known values of unique hues in observers with highly skewed M:L ratios. On one extreme are heterozygous female carriers of protan dichromacy. These women necessarily have very high percentages of M cones, typically around 75%M for Caucasian women (Neitz and Neitz, 2011). In two small studies of such women, color appearance was indistinguishable from controls (Jordan

and Mollon, 1997; Miyahara et al., 1998). Across both studies, however, 5 out of 6 and 2 out of 2 subjects, respectively, had unique greens shorter than 510 nm. It is therefore reasonable to hypothesize that a larger group of individuals with unusually high %M cones might reveal a statistical trend towards shorter than average unique greens. This prediction is captured in the De Valois and hybrid model, but not the midget ganglion model (Fig. 5.1B&C versus Fig. 5.1D). On the other extreme, subjects with very low percentages of M cones are also known to have unique hues similar to controls (Jordan and Mollon, 1997; Neitz et al., 2002). While all three models with S+M input to the blue side of the opponent mechanism predict a return to shorter unique green values in people with low %M, only the midget ganglion model accurately predicts the wavelength of unique yellow in these subjects, which do not differ significantly from the population mean around 578 nm (Jordan and Mollon, 1997; Neitz et al., 2002).

Evolution of color vision

The theories elaborated here provide different explanations for how color vision evolved in primates and how gene therapy "cures" color blindness in adult squirrel monkeys (Mancuso et al., 2009; Neitz and Neitz, 2014). A highly influential hypothesis about the evolution of trichromatic color vision in primates proposes that the BY system, differencing S and M cones, is a phylogenetically ancient circuitry, while the RG system is a relatively recent subsystem comparing L and M cone signals (Mollon, 1989, 1999). The signals of these two pathways are carried in distinct anatomical pathways (Chatterjee and Callaway, 2003) and only later recombined to form the perceptual hue axes, presumably requiring some rewiring in cortex during evolution to bring the two subsystems together. Thus, if color blindness was treated in adulthood, in the absence of a period of neural plasticity with all three cone types present, the brain might not be able to sort out color signals from achromatic contrast and the treated individual could experience achromatic textures rather than have a true color

experience (Makous, 2007).

In the midget ganglion theory, achromatic and chromatic sensations are separated in the retina and the circuitry required for hue perception arises immediately upon the addition of a third cone type. This circuit does not require neural plasticity or an additional developmental process. After the addition of a third cone through evolution or viral vector, the midget ganglion cells that served achromatic spatial contrast before treatment continue to serve their same role. They would become L/M opponent but still serve as labeled lines for achromatic contrast. A benefit of the therapy would be improved detection of equiluminant red-green boundaries but the associated sensations would still be black and white. Before treatment, a subset of midget ganglion cells receiving S cone feed-forward input would have served BY color vision, OFF midgets for blue and ON midgets for yellow. After treatment, the OFF midget serving blue sensations with be split into two classes, one with L cone centers and one with M cone centers. The ON midgets would be similarly divided. The new spectral sensitivities would permit RG and BY color discrimination. The final requirement is that the organism be able to learn that the labeled line formally signaling blue has been split into two lines signaling red and blue and the former yellow line is split into yellow and green.

Achromatic sensations

The separation of achromatic and chromatic sensations is a major challenge for the visual system. In the retina, the majority of midget ganglion cells carry both RG chromatic and achromatic spatial information. The prevailing theory of color vision proposes that the midget system, with its intermingled chromatic and achromatic signals, performs "double duty", serving both high-resolution spatial vision and chromatic vision. These theories then presume that the two channels are de-multiplexed in cortex through presently poorly defined circuitry (Boycott and Wässle, 1999; De Valois and De Valois, 1993; Ingling Jr. and Martinez, 1983; Lee et al., 2010; Shapley and Hawken, 2011; Shapley and Hugh Perry, 1986).

The midget ganglion theory posits L/M opponent midget ganglion cells mediate achromatic sensations, black and white. The origins of this idea go back to Wiesel and Hubel (Wiesel & Hubel, 1966) who argued that the center-surround L/M spectrally-opponent cells in the LGN are as good a candidate as the magnocellular cells for the mediation of black-white contrast mechanisms. Although, the idea that L/M opponent cells do double-duty has often been proposed, it has also been argued previously that they only mediate achromatic sensations (Calkins and Sterling, 1999; Rodieck, 1991). Thus, the midget ganglion theory argues that the vast majority of midget cells, probably $> 90\%$, only serve achromatic sensations. Together these are the basis for high acuity achromatic vision. A smaller subset of midget ganglion cells with feedforward mediated S-cone input mediate chromatic sensations.

Future predictions

It is now technically feasible, using adaptive optics, to confine a targeted spot of light to an individual cone (Harmening et al., 2014) and this can be done in retinas in which cones have been classified as L, M and S. Contrary to double-duty models, the midget ganglion model predicts that a majority of L and M cones even those surrounded by cones of the opposite type will give rise to sensations of white, not color. Moreover, there should be clusters of cones that are nearly always associated with strong chromatic percepts. Finally, according to the theory, M cones in the surrounds of midgets with L cone centers serve blueness and M cones centers serve green sensations. Thus, it should be possible to illicit blue sensations or green sensations from a single cone depending on the background conditions.

3.7 Conclusion

Many aspects of human color vision cannot be explained by standard theories. These include a huge variability in unique green compared to unique yellow. Here we show that the majority of the variability in unique green is caused by individual differences in cone ratio and that

this observation and many others can be explained by a theory in which separate subtypes of midget ganglion cells mediate the sensations of black, white, blue, yellow, red and green respectively.

Chapter 4

REPRESENTATION OF COLOR AND ACHROMATIC PERCEPTS IN THE HUMAN CONE MOSAIC

4.1 Abstract

Color vision depends upon comparisons of signals from photoreceptors sensitive to different wavelengths of light. The neural implementation of these comparisons remains unsettled. Parvocellular neurons, often cited as the basis for red-green color vision (Solomon and Lennie, 2007; Lee et al., 2010), are excited by both black and white edges and spots of red or green light (Wiesel and Hubel, 1966), thus mixing achromatic and chromatic signals. One possible resolution to this problem, known as the "double duty" hypothesis, is that the cortex de-multiplexes signals from parvocellular neurons (Derrington et al., 1984; Boycott and Wässle, 1999; De Valois and De Valois, 1993). A second hypothesis, originating from Weisel and Hubel (Wiesel and Hubel, 1966), maintains that the parvocellular stream delivers high resolution achromatic information to the brain, in parallel to a separate class of color dedicated visual neurons (Livingstone and Hubel, 1988; Calkins and Sterling, 1999; Schmidt et al., 2014; Rodieck, 1991b; Danilova and Mollon, 2012a). We addressed this debate by studying color perception on a single cone scale in human subjects. Using adaptive optics imaging (Liang et al., 1997; Roorda et al., 2002) and densitometry we classified each cone in a patch of retina as long (L), medium (M) or short (S) wavelength sensitive (Roorda and Williams, 1999). We then delivered small spots of light (0.5 arcmin) to single cones (Harmening et al., 2014). We found individual cones tended to elicit only a single color sensation and cones driving the same color sensation were often spatially clustered. Moreover, the cones predicted by the "double duty" hypothesis to carry the strongest color signals were

more likely to signal white. Together, our evidence adds weight to the long-standing notion that chromatic and achromatic information are separated in the retina and carried to the brain in parallel neural pathways.

4.2 Results and Discussion

Two male subjects participated in the study. Single cones were stimulated with an adaptive optics scanning laser ophthalmoscope (AOSLO) coupled with high resolution eye tracking (Arathorn et al., 2007) and correction for chromatic aberration (Harmening et al., 2012). Subjects reported the color of each flash. The correction of optical aberrations with adaptive optics has been used previously to deliver cone sized spots of light to human subjects in a similar color naming paradigm (Hofer et al., 2005b). However, stimulation of individual cones was not possible. Our system permitted repeated stimulation of cones of interest within and across experimental sessions (Harmening et al., 2014). Cone targeted spots were generated with a 543 nm monochromatic channel, though the exact wavelength had a minimal influence upon color responses (Extended Data Fig. 4.5).

Cone targeted flashes of light (500 ms) were presented on a dim background that was adjusted by the subject to appear white at the start of each experiment. The exact conditions varied slightly from day to day, but these fluctuations did not substantially impact our findings (Extended Data Fig. 4.6). In the case of a large stimulus, chromatic contrast from a white background that modulates only L-cones produces a red sensation, while light exclusively exciting M-cones appears green or greenish-blue (Extended Data Fig. 4.7). The extent to which these large field predictions will generalize to single cone stimulation is unknown.

Under our experimental conditions, the percepts reported by subjects were reliable. Stimulation of the same cone in different sessions, sometimes many months apart, produced highly correlated responses (Extended Data Fig. 4.8). The average error in stimulus targeting (see methods) was 0.22 and 0.15 arcmin for S10001 and S20076, respectively, less than a quarter

the size of a single cone at this eccentricity. Furthermore, targeting errors were not predictive of color name responses (Extended Data Fig. 4.9). The reliability of percepts generated in this unnatural experimental paradigm validates the precision of our light delivery system and demonstrates the ability of the nervous system to interpret signals generated by single cones in a repeatable manner.

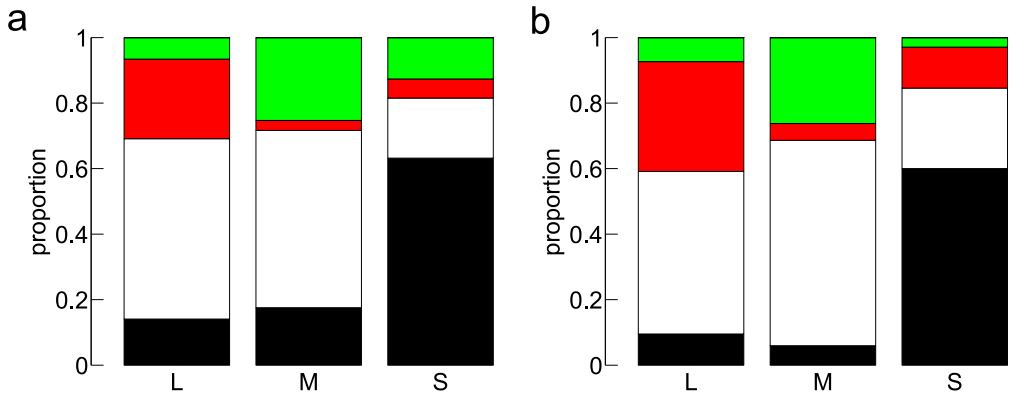

Figure 4.1: Distribution of responses across the three cone types. a. Color naming behavior from S10001 across 78 L cones, 53 M cones and 6 S cones. b. Color naming behavior from S20076 across 99 L cones, 49 M cones and 6 S cones.

Across both subjects a total of 300 cones were targeted for color naming. The distribution of responses elicited from both subjects is plotted as a function of stimulated cone type in Fig. 4.1. These results demonstrate very similar trends between both subjects. Chi-square tests on these categorical data indicate that the naming behavior of both subjects differs significantly from a random distribution across the three cone types (X^2 (6, N=3905) = 750.2, $p < 0.001$ for S10001, X^2 (6, N=4045) = 1031.3, $p < 0.001$ for S20076).

The targeting of S-cones with a 543 nm light serves as a control under these conditions, as S-cones are insensitive to this wavelength (Stockman et al., 1999). As expected, when light was confined to S-cones, both subjects were unable to see the flash on >60% of the

trials. Moreover, since subjects were permitted to repeat trials this number likely represents an underestimate of the true number of trials that would have gone undetected. This finding, together with our measurements of targeting error, is consistent with a large majority of the light from each flash falling on the targeted cone with the surrounding cones capturing only a small fraction of the photons – reaching threshold on <40% of trials in the case of the S-cone trials. Subsequent analysis focused on L- and M-cone stimulation.

Two-tailed t-tests on the color naming behavior associated with L- and M-cone stimulation revealed that red responses were more likely to be driven by L-cones (t_{129}=5.13, $p < 0.001$ for S10001, t_{144}=5.24, $p < 0.001$ for S20076), while green was more likely to come from the excitation of M-cones (t_{129}=-5.62, $p < 0.001$ for S10001, t_{144}=-4.95, $p < 0.001$ for S20076). Due to the close similarity in color naming behavior between our two subjects, we grouped cells across subjects in subsequent analyses.

Across both subjects, the majority (54.5%) of reports were white. Therefore, we sought to distinguish two possible scenarios that could have generated this behavior. One possibility is that all cones signal white on a majority of trials, but stochastically signal a hue on a small number of trials: predominantly red in the case of an L-cone and green in the case of an M-cones. Alternatively, the behavior summarized in Fig. 4.1 could have been achieved if the majority of L- and M-cones purely signal white while a small handful of cells purely signal red or green percepts. The former would be more suggestive of a multiplexed representation of hue and achromatic signals, while the latter would be expected for a parallel representation of color sensation.

To address this question, we developed a metric called response purity (number of responses in max category / number of trials). The results of this analysis for all L- and M-cones are shown in Fig. 4.2. The mean response purity of our two subjects was 0.78, while a random Monte Carlo resampling of all of the responses predicted a mean response purity of 0.61 (Fig. 4.2b) with the probability of our results occurring by chance much less than

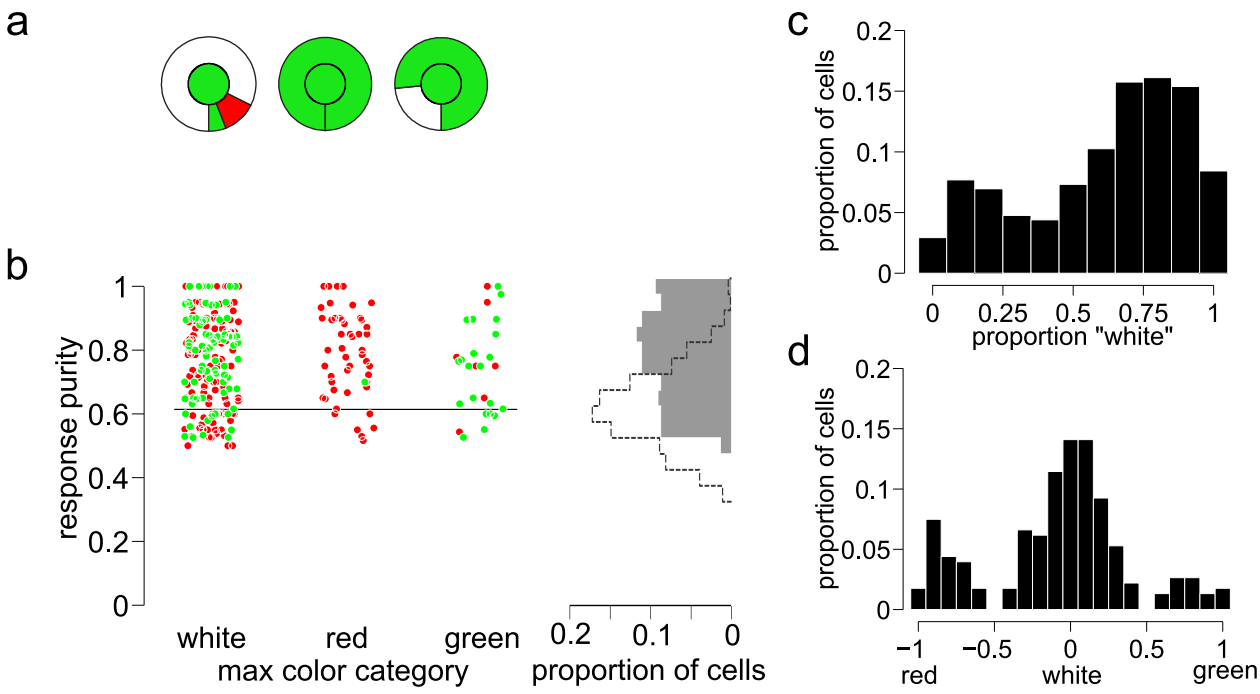

Figure 4.2: Color sensations from individual cones. a. Three examples of M cones from our dataset. The inner circle denotes the cone type (green = M cone). The outer circle is a histogram representing the color sensations elicited from those cones. b. The response purity of response for L (red dots) or M (green dots) cones plotted as a function of the dominant response from that cone. The histogram to the right displays the distribution of response purity in our data (solid gray) and a Monte Carlo resampling of our data (dotted gray line). c. Normalized histogram of the proportion of white responses across all L and M cones. d. Distribution of RG metric in L and M cones in high purity cones. Cones with response purities below the Monte Carlo mean of 0.61 were excluded from this analysis (18% of L/M cones).

10^{-6}. This analysis supports the interpretation of a parallel representation in which most L/M-cones reliably signal white, while a small fraction predominantly drives red or green responses. Further supporting this interpretation, the proportion of white responses elicited by each cell exhibited a bimodal distribution (Fig. 4.2c). Most cones signaled white on a majority of trials, while a small group had a low proportion of white responses and were dominated by red or green. To quantify the strength and distribution of color responses, we defined a red-green metric (Gordon et al., 1994) (RG) as $(g-r)/T$, where r was the number of times red was reported, g was the number of green reports and T was the number of trials. A similar result was found when we scored the responses of each cell according to the RG metric and eliminated the low purity cones (Fig. 4.2d).

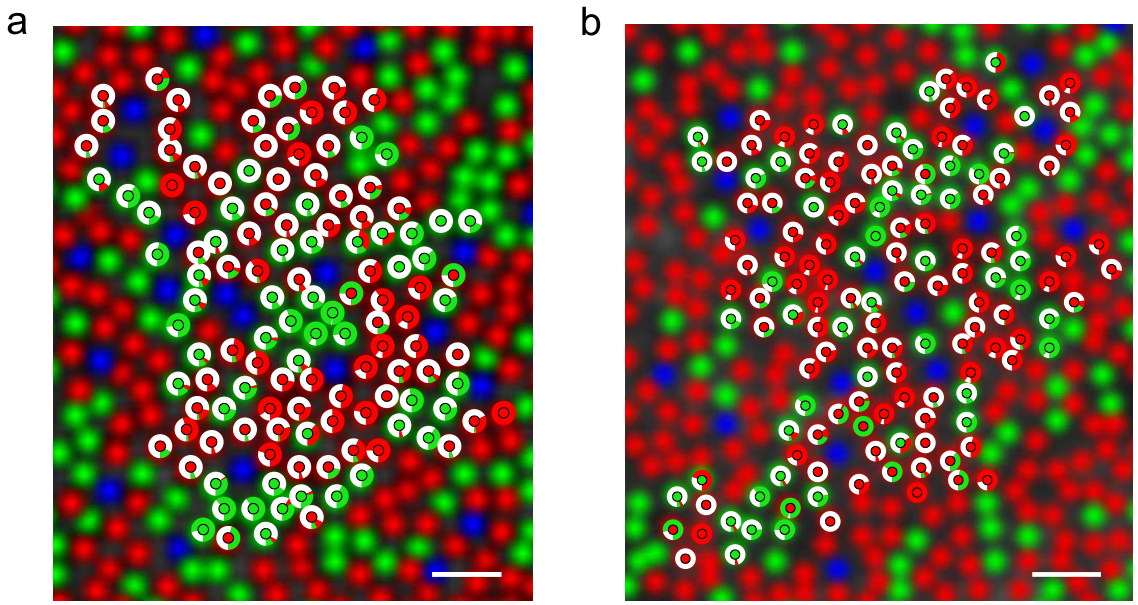

Figure 4.3: Color sensations in a trichromatic cone mosaic. Color responses from individual cells are plotted over the classified cone mosaic in two subjects. a. S10001. b. S20076. Scale bar = 2.5 arcmin.

A response histogram for each L/M-cone from S10001 and S20076 overlaid on his classified

mosaic is shown in Fig. 4.3. In both subjects, we observed substantial structure to the spatial organization of color sensation at the level of the cone mosaic. Most striking is the tendency for cells that elicit a color to cluster near each other (Extended Data Fig. 4.11). In both subjects, we found patches of 2-5 cones signaling green or red surrounded by larger groups of L- and M-cones predominantly signaling white. The apparent segregation of color categories into distinct populations of cells (Fig. 4.2, 4.3) and clustering of cones signaling the same color (Fig. 4.3, Extended Data Fig. 4.11) are indicative of a parallel coding strategy of early color representation. In contrast, a "double duty" representation of color would predict a more equal distribution of color responses throughout the L/M-cone mosaic.

At the center of the debate between "double duty" and parallel representation is the role of parvocellular neurons in color perception(Calkins and Sterling, 1999; Schmidt et al., 2014; Rodieck, 1991b). At the eccentricity studied here, neurons in the parvocellular visual pathway make up more than 90% of the ganglion cells sampling the cone mosaic (Dacey, 1994), receive excitatory input from only a single cone and indiscriminant surround input from neighboring cones (Lee et al., 2010; Dacey and Packer, 2003). This arrangement confers L/M spectral opponency in a majority of these cells (Lee et al., 2010; Dacey and Packer, 2003), leading to the speculation that the parvocellular pathway may underlie our sensations of red and green (Dacey and Packer, 2003; Mollon, 1999). Our results stand at odds with these predictions: the cones most likely to generate spectral opponency in a parvocellular neuron, those surrounded by cones of opposing type, were not more likely to generate red or green percepts (Fig. 4.4 and Extended Data Fig. 4.11). In fact, all 10 examples in our dataset drove white percepts on greater than 50% of trials.

Our findings support the interpretation of parvocellular (Type 1) neurons put forth by Wiesel and Hubel, who argued that because these cells confound spatial and chromatic information they are ill-suited to distinguish red/green from black/white (Wiesel and Hubel, 1966). Instead, Wiesel and Hubel proposed, as we observed here (Fig. 4.4), parvocellular

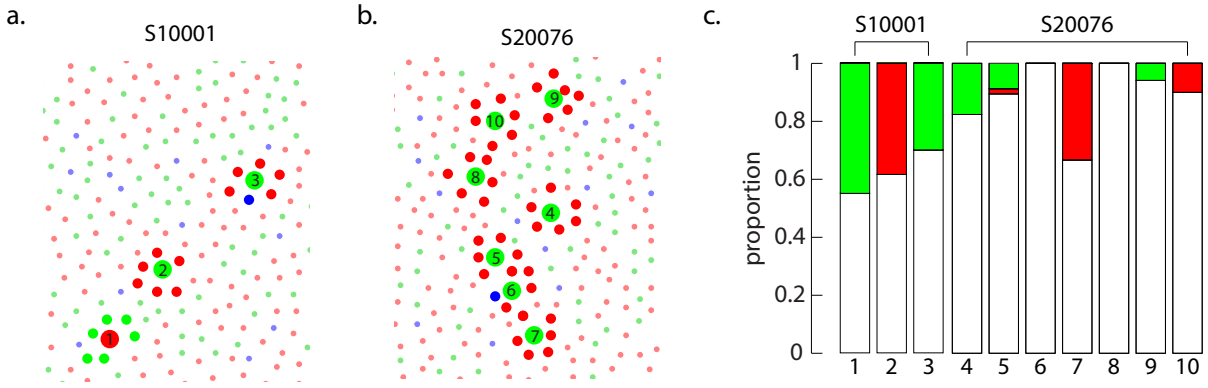

Figure 4.4: Opponent neighborhoods produce white sensations. Cones surrounded by neighbors of differing type are highlighted. Large circles represent the targeted cone; smaller circles highlight the six nearest neighbors. a. S10001. b. S20076. c. Color responses from the 11 cones with pure opponent arrangements.

neurons are well positioned to signal black and white at high resolution (e.g. reading black and white letters). Furthermore, we found small clusters of cones strongly signaling color sprinkled amongst a sea of white signaling cones. These groups of color signaling cones are reminiscent of the larger, less numerous, type II cells described by Wiesel and Hubel (Wiesel and Hubel, 1966), which are ideally suited to signal color to the brain (Wiesel and Hubel, 1966; Rodieck, 1991b). The relative preponderance of white signaling cones in our data set is also in qualitative agreement with the lower spatial acuity of the red-green compared to black-white system (Mullen, 1985).

Single cone stimulation has been used to study cone contributions to visual receptive fields in lateral geniculate nucleus (Sincich et al., 2009) and excised monkey retina (Li et al., 2014b). Here we used single cone stimulation to reveal the spatial structure of color percepts at the level of the human cone mosaic. Together these experimental paradigms offer an unprecedented opportunity to link cellular physiology, anatomy and visual perception in

humans and primates.

4.3 Methods

4.3.1 Subjects

The two subjects (BPS and WST) were both adult male Caucasians and had normal color vision (Hardy-Rand-Rittler plates and anomaloscope). Prior to experiments, drops of 1% tropicamide and 2.5% phenylephrine were administered to dilate the pupil and paralyze accommodation. Custom bite bars were used to stabilize the subject. Informed consent was obtained from each subject and all experimental procedures adhered to the tenets of the Declaration of Helsinki.

4.3.2 AOSLO imaging and stimulation

A previously described multi-wavelength AOSLO (Roorda et al., 2002; Harmening et al., 2014) was used for imaging and delivery of stimuli. Briefly, a 842 nm infrared (IR) channel was used for imaging and wavefront sensing and a 543 nm channel was used for stimulation. Optical aberrations were corrected with a deformable mirror, which achieved near diffraction-limited imaging and stimulus delivery (Roorda et al., 2002). IR images were used to perform real-time, high-resolution eye tracking with a mean error of 0.15 arcmin (Arathorn et al., 2007). Longitudinal chromatic aberration (LCA) and transverse chromatic aberration (TCA) between the IR and stimulus channel were measured and corrected following published procedures (Harmening et al., 2012). TCA was measured before and after each session. Data were discarded if TCA was found to differ by more than 0.45 arcmin between the start and end of the session. Stimulus flashes were 3 pixels (roughly 0.45 arcmin) in diameter, which is less than half the size of a cone inner segment at the retinal eccentricity studied (1.5 degrees), and 500 ms in duration.

4.3.3 Cone classification

Before beginning single cone experiments, of a small patch (about 0.5 degrees of visual angle) of the cone mosaic was classified at a location of 1.5 degrees from the fovea. The procedure for obtaining reliable classification of each cone was a modification of the earlier methods (Roorda and Williams, 1999) and has been published elsewhere (Sabesan et al., 2015a). Mosaics of 800 and 631 cones were obtained for S10001 and S20076, respectively. The percentage of L-cones (L / (L+M)) in subject S10001 was 66.2 %L and 66.7 %L in S20076.

4.3.4 Psychophysics

The infrared (IR) wavefront sensing beacon (840 nm) produced a 1.2 degree square that was dimly reddish purple in appearance. A background leak from the stimulus channel (543 nm) produced a slightly brighter greenish appearing square. In order to extinguish the color sensations produced by these conditions, a DLP projector was brought into focus on the subjects retina in Maxwellian view (Extended Data Figure 3). At the beginning of each session the subject was set the background to be as dim and white as possible. The chromaticity and luminance of the background was measured with a matching technique. A patch the same size as and adjacent to the background was generated with the external projector. One subject was then given control over the chromaticity and luminance of the adjacent patch and asked to achieve a match in chromaticity and luminance to the background. This procedure was carried out two times. The patch was then measured with a PR650 spectroradiometer (Photo Research). The chromaticity of the background was 0.32, 0.30 in CIE 1931 xy space and the luminance was 46 cd m^{-2}, though both varied slightly between sessions and subjects. Slight variability in luminance and chromaticity of our background did not confound our results as repeatability was high across days and with lower intensity spots (Extended Data Fig. 4.6& 4.8).

Each cone of interest in our dataset was targeted 20 times during each experimental session. Within a session, between 6 and 10 cones were tested (120 200 trials), with presentation randomly interleaved amongst the cones to prevent subject bias. L- and M-cones that were seen on fewer than 9 trials were excluded from analysis. Responses were encoded with a tablet device. Subjects selected from 6 possible choices: red, green, blue, yellow, white and not seen. Subjects were permitted to repeat trials as needed.

4.3.5 Delivery error calculations

The location of the stimulus was recorded on each frame of each trial. The 500 ms stimulus extended over 15 frames of the scanning source. A video was recorded during each trial and saved for analysis off-line. The location that the stimulus was actually delivered was computed for each frame relative to the center of each targeted cone. The mean absolute distance between the actual delivery and the intended location was computed for each trial.

4.3.6 Identification of high probability S-cones

We limited our analysis of S-cone frequency of seeing to S-cones that were most confidently classified. S-cones are insensitive to the imaging wavelength used in our densitometry technique (543 nm). Therefore, they absorb a low fraction of photons and appear bright regardless of adaptation state. Cones that classified as high confidence S-cones exhibited low absorbtance across all three adaptation states used in the classification studies and had low variability between trials. Less confidently classified S-cones were more variable in their absorbtance properties across adaptation states and trials.

4.4 Supplementary Information

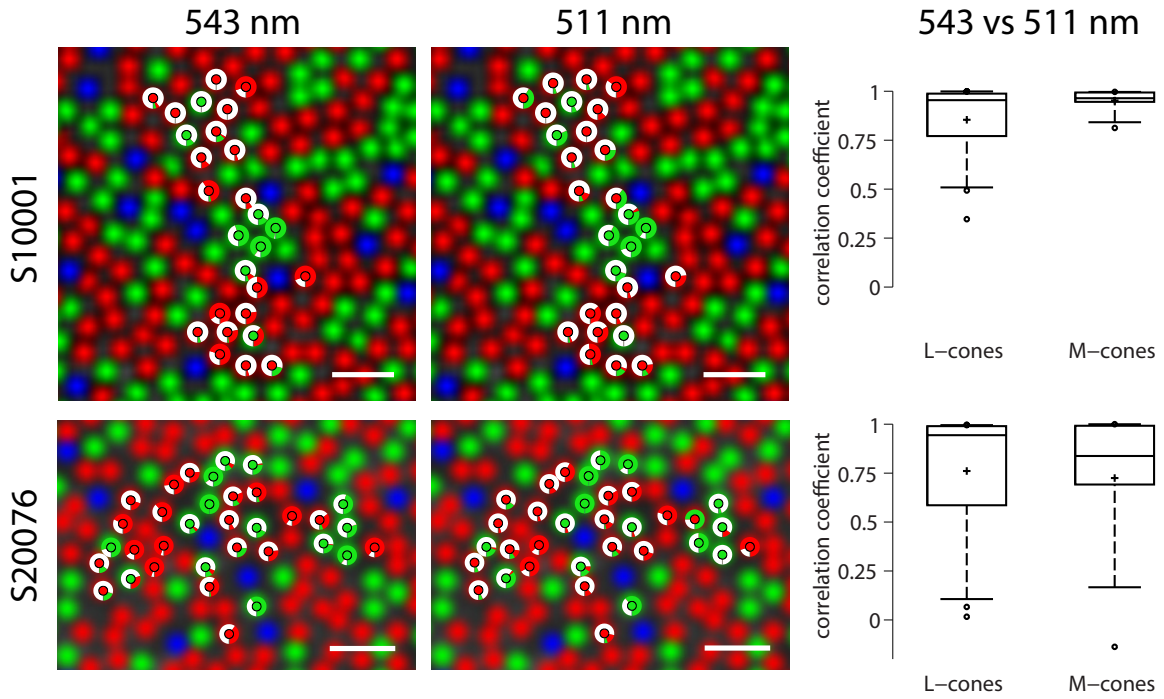

Figure 4.5: Wavelength invariance of color signals. Subsets of cones in both subjects were retested using a 511 nm stimulating light. On a cone by cone basis, the responses to a 511 nm stimulus were highly correlated with the responses obtained with a 543 nm light. The top row represents data collected from S10001 using a 543 nm (left column) versus a 511 nm channel (middle column). The bottom row is data from S20076. The box plots in the right column represent the distribution of correlation coefficients across L and M cones. Plus marks indicate the mean; the solid line denotes the median.

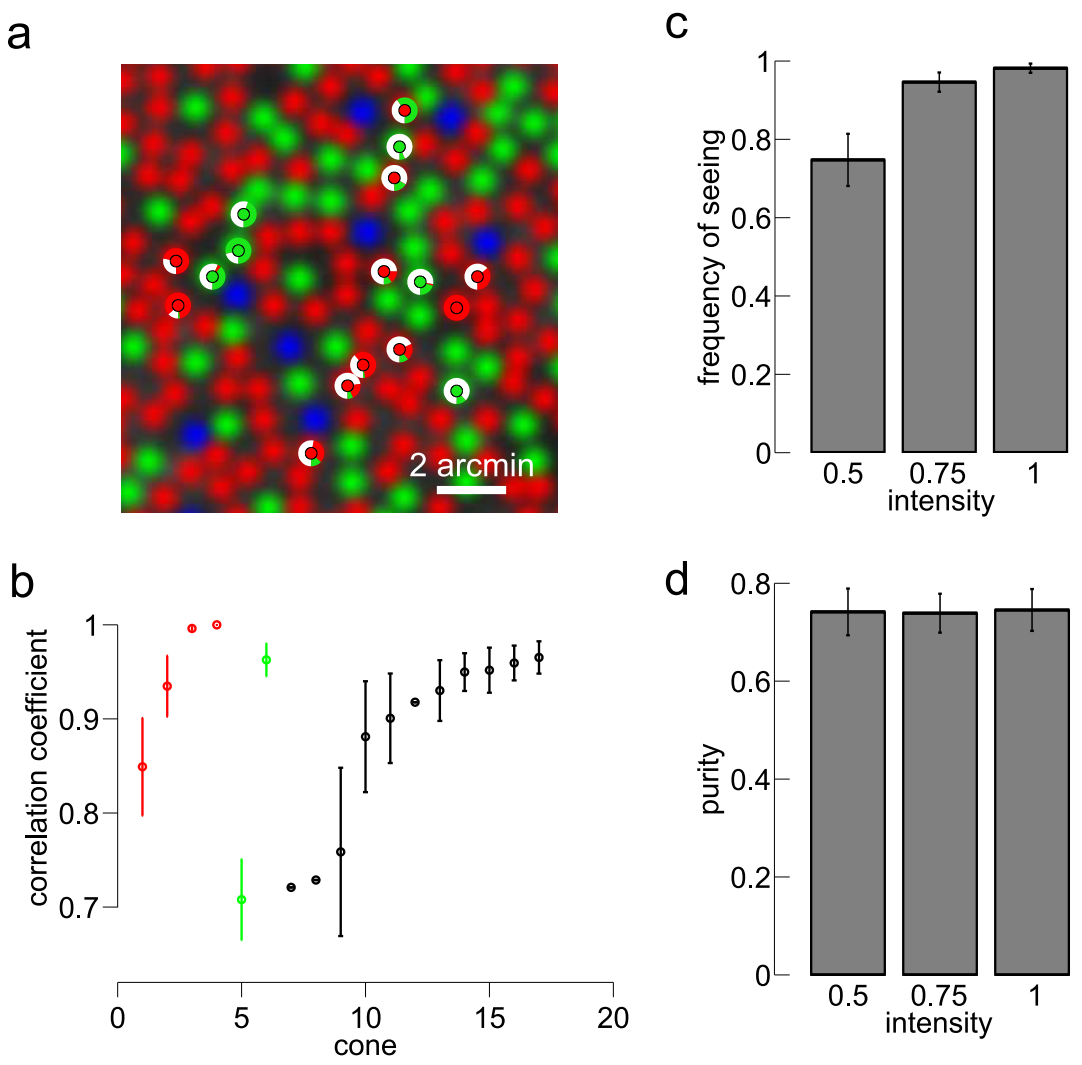

Figure 4.6: Intensity invariance of color signals. a. Response histograms for 18 cones that were targeted in one subject (S20076). 3 cones were selected during each trial and stimulated with 3 different intensities (0.5, 0.75 and 1 a.u.). b. R2 values between the three conditions are shown for each of the 18 cones tested. Color of the points corresponds to the dominant color category elicited by each cone. Error bars are SEM, some points do not have error bars because the frequency of seeing was too low in the 0.5 intensity condition to compute correlation coefficients. The mean correlation coefficient across all cones was 0.87. c. Frequency of seeing decreased with decreasing intensity. d. Response purity did not change as a function of intensity.

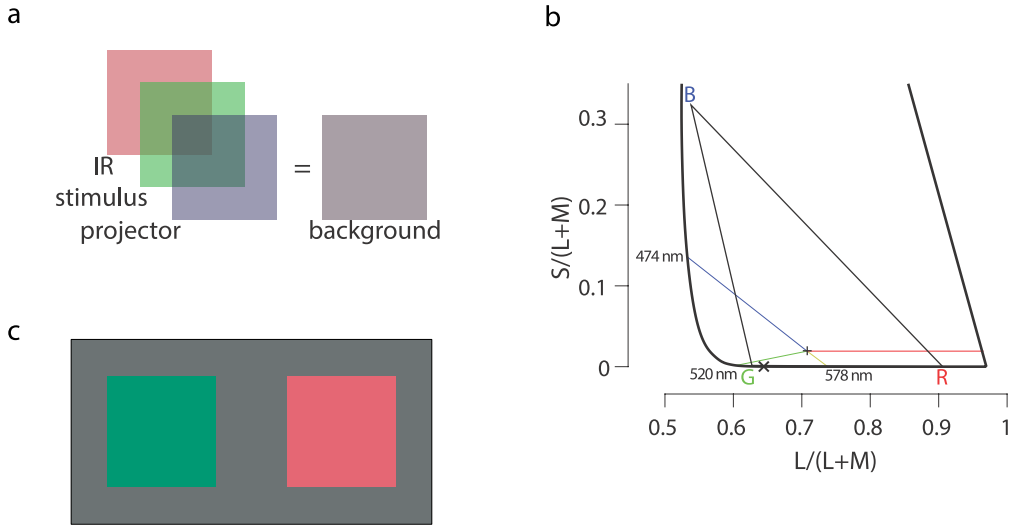

Figure 4.7: Psychophysical conditions and predictions from large field stimuli. a. The background of these experiments was a combination of a dimly visible infrared (IR) wavefront sensing beacon, a leak from the stimulus channel (543 nm) that appeared green and an external projector. At the beginning of each session the subject adjusted the luminance and chromaticity of the projector until a dim achromatic background was achieved. b. The R, G and B primaries of the external projector are displayed in Macleod-Boynton chromaticity space 1. The x mark on the spectrum locus represents the 543 nm green stimulation channel. The infrared channel is not plotted here. The red, green, blue and yellow lines are population means for the unique hues. A plus sign represents the location of an equal energy white, for illustrative purposes. Under large field conditions, stimulation of only L cones from a white background (rightward direction from the cross) will drive red responses, while stimulation of M cones (leftward direction) will produce a green or greenish-blue color. c. Examples of cone isolating stimuli from a gray background. These conditions produce a greenish percept when only the activity of M cones are increased relative to the background or a reddish percept when only L cones are modulated.

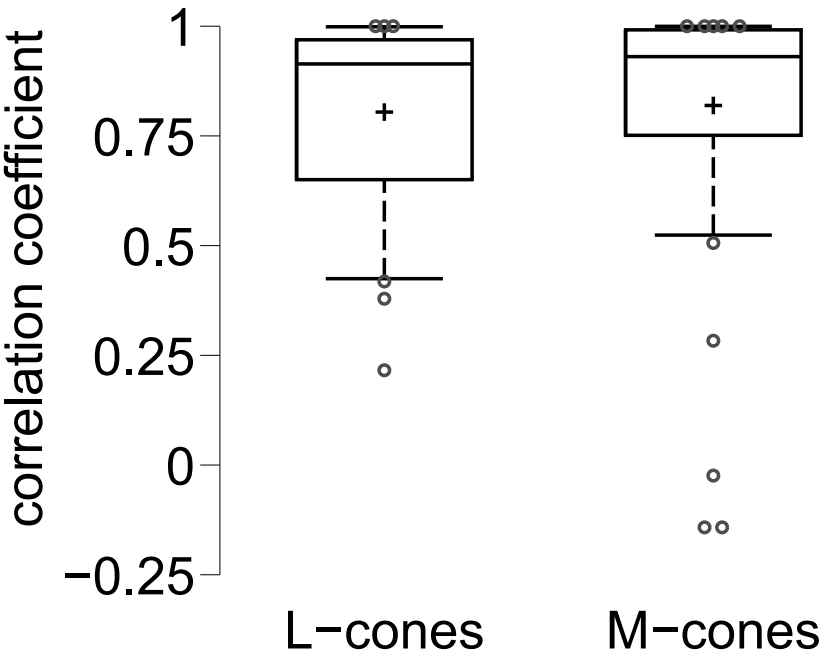

Figure 4.8: Color percepts are repeatable. Distribution of correlation coefficients in L and M cones pooled from both subjects. Across both subjects, a total of 60 cones were repeated during at least two different sessions.

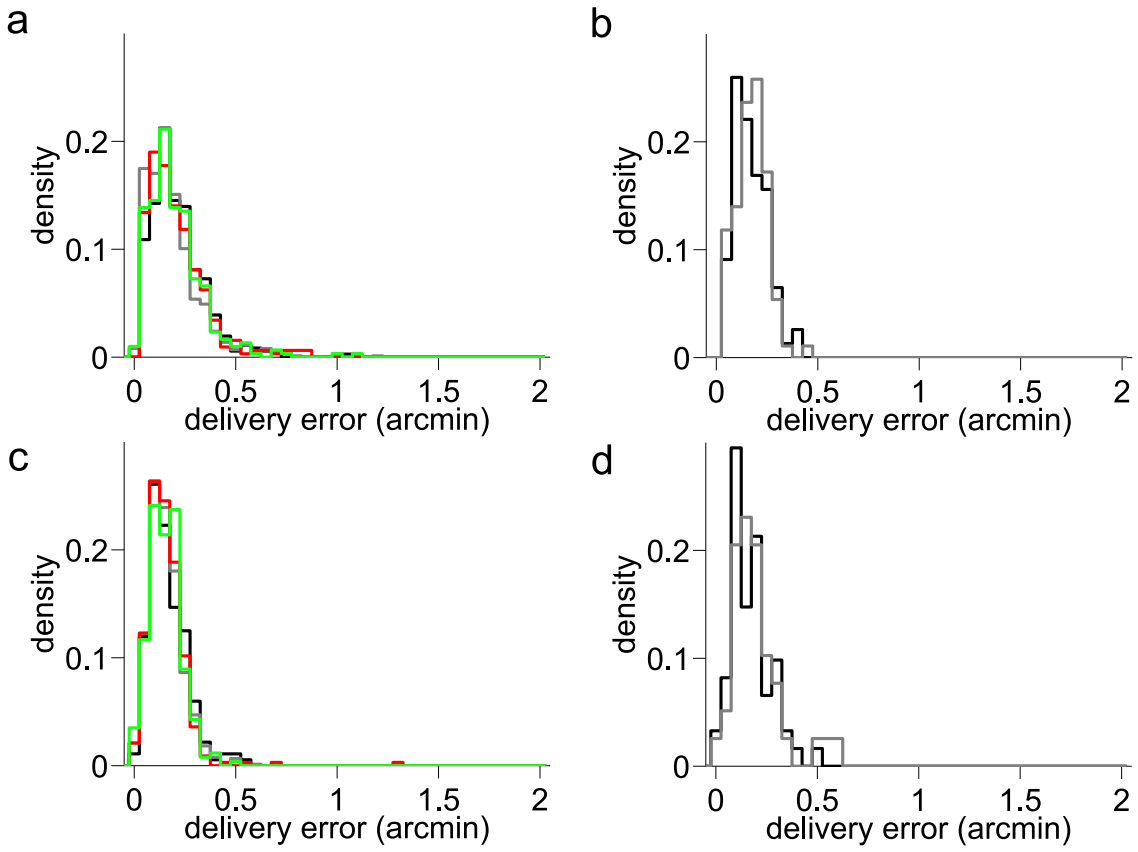

Figure 4.9: Color percepts are not influenced by errors in stimulus delivery. The accuracy of the eye tracking and light delivery system is about 0.15 arcmin (Arathorn et al., 2007). To eliminate the possible confounding factor of delivery errors in our color naming results we computed histograms of delivery errors for each trial. Separate histograms were computed for each response category. The left column contains data from all trials regardless of cone type, the right is from trials when S cones were targeted. The top row (a, b) are from subject S10001; while the bottom row are from subject S20076 (c, d). In all cases, the color responses were not biased by delivery errors. In a and c, lines correspond to red = red responses, green = green responses, gray = white responses, black = not seen. In b and d, lines black lines = not seen, gray lines = all seen categories.

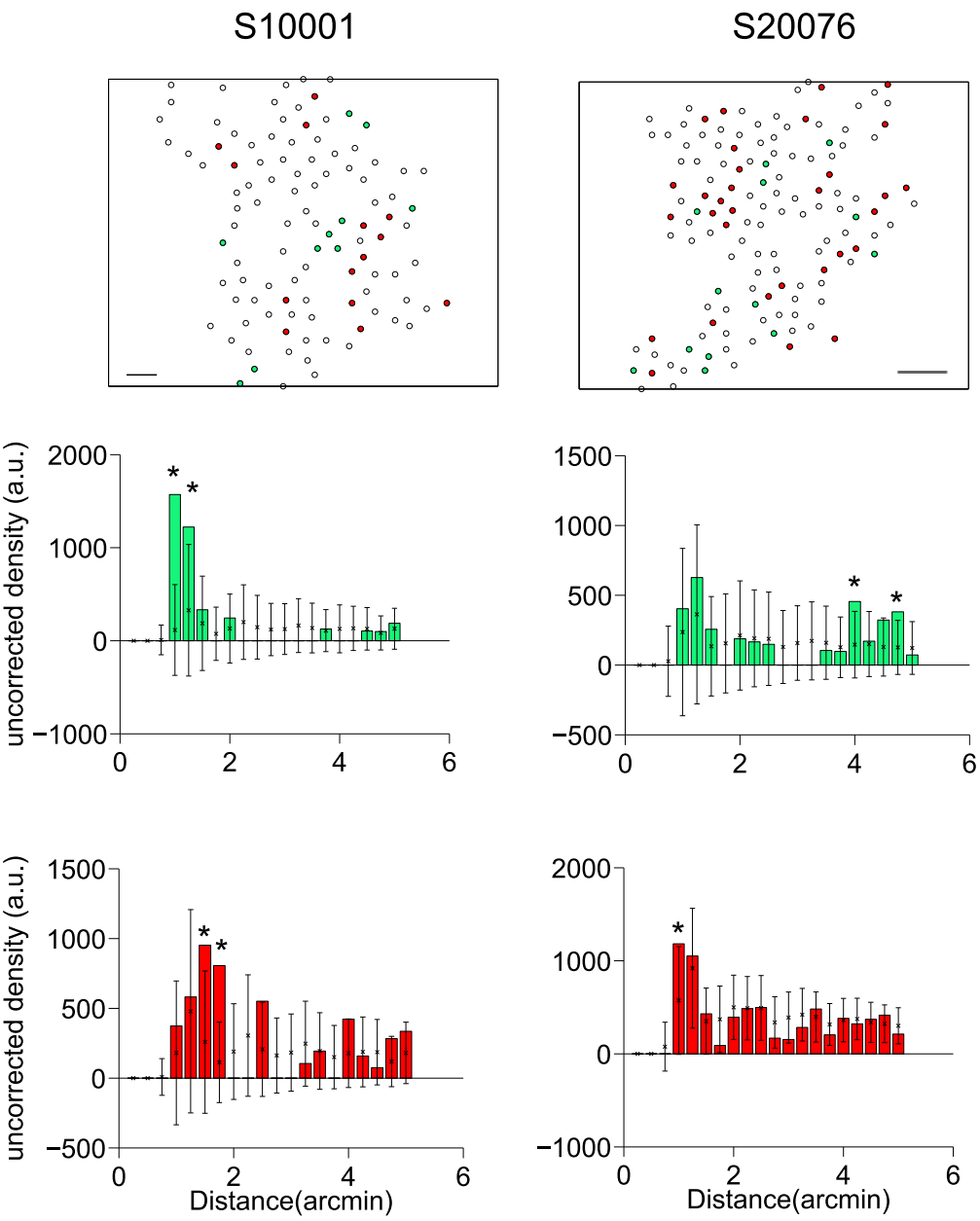

Figure 4.10: Cones signaling color are spatially clumped. A modified version of the density recovery profile analysis described by Rodieck (Rodieck, 1991a) was used to assess the degree of non-random clumping in our dataset. Top row is the mosaics used in the analysis. Cells were classified as red, green or white based on their dominant response. Cells with a response purity less than 0.6 (Monte Carlo mean) were excluded from analysis. Left column contains the results of this analysis from S10001, right column from S20076. Error bars represent 2 standard deviations from the mean Monte Carlo simulation.

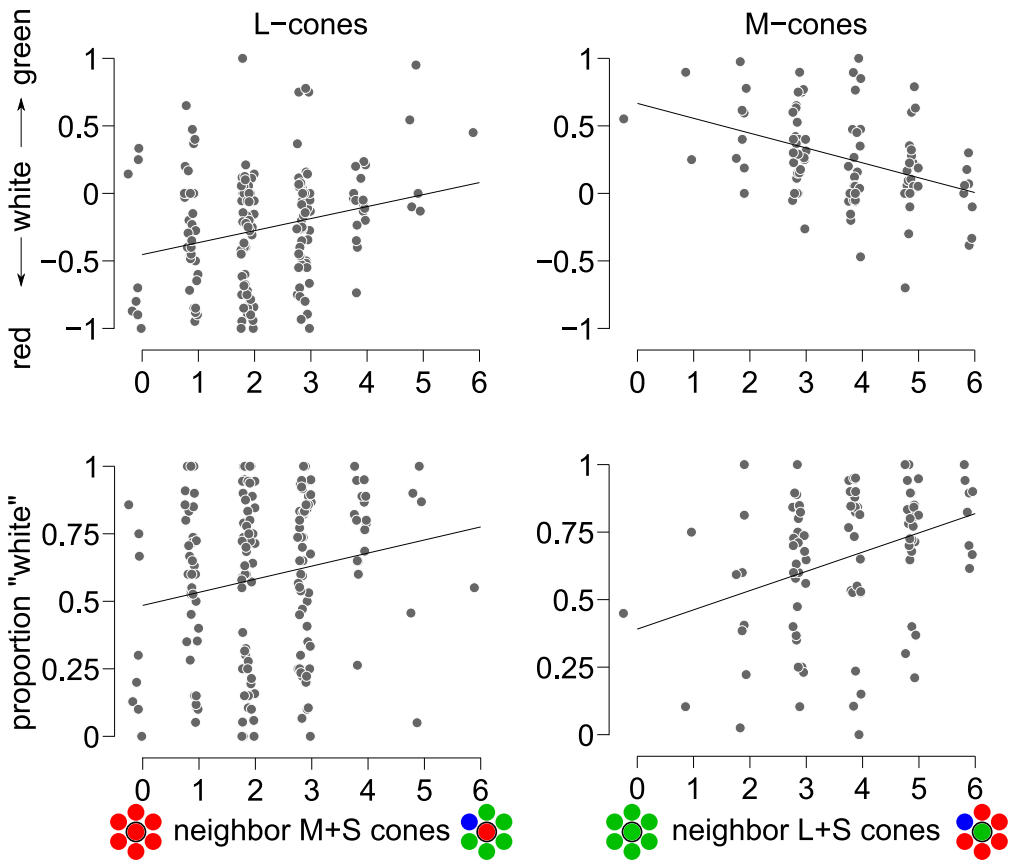

Figure 4.11: The influence of neighboring cones on color appearance. Top row: the red-green score for each L (left column) and M (middle column) cone is plotted as a function of the number of nearest neighbors of the opposite type. Solid lines represent least squares regression. L-cones: N=174, $R^2 = 0.058$, $p = 0.001$; M-cones: N=99, $R^2 = 0.17$, $p = 0.00002$. Bottom row: same as the top row, but the independent axis here represents the proportion of white responses elicited from each cone. L-cones: N=174, $R^2 = 0.034$, $p = 0.014$; M-cones: N=99, $R^2 = 0.122$, $p = 0.0004$.

Chapter 5

RULES DETERMINING THE SENSATIONS FROM SINGLE CONES

5.1 Abstract

The sensation of color begins in the cone photoreceptors of the eye. How the brain turns the activity of cones into color perception remains unresolved. We studied the colors reported by subjects in response to stimulation of individual cones. Cones were probed with adaptive-optics-corrected flashes of light and the subjects indicated the color of each flash. Reports from repeated stimulation of single cones were consistent, but were not predicted by the spectral sensitivity of the stimulated cone alone. We found both the background and the local neighborhood of the cone influenced the sensation reported. A small number of cones elicited strong color percepts, while the majority gave rise to the sensation of white regardless of background condition. Together, our results were consistent with the idea that color and achromatic sensations arise from the output of neurons located early in the visual pathway.

5.2 Introduction

The signals emanating from photoreceptors in the eye are ambiguous and redundant. Individual cones confuse fluctuations in intensity and wavelength (Rushton, 1972). The broad, overlapping sensitivities of the three cone classes (L, M, S) introduce correlations in signals across the classes (Benson et al., 2014; Wachtler et al., 2007). Spatial correlations in the visual scene produce additional redundancies in nearby photoreceptors (Tkačik et al., 2011). Yet despite these challenges, the nervous system organizes signals from the cone mosaic into a stable representation of the external world in which color, intensity and space are dis-

entangled. We studied the rules through which color is extracted from the output of the cone mosaic using stimulation of individual cones.

The simplest rule that the visual system could use to color the perceptual world would be to assign a single label (red, green, blue) to the output of the three cone classes (Figure 5.1A). This view was first communicated by Helmholtz (Helmholtz, 1924) and later implicitly adopted to account for the elementary sensations elicited during small spot experiments (Hartridge, 1946; Krauskopf, 1964, 2000; Krauskopf and Srebro, 1965; Otake et al., 2000). This line of reasoning faced trouble, however, when generalizing to larger stimuli: certain combinations of color sensations do not occur in the natural world. For example, red and green are never perceived together, yet L- and M-cones (the hypothesized red and green receptors) are often active together. Further, this theory does not provide an explanation for the appearance of white or yellow.

An alternative framework has reconsidered the problem of determining the color of objects as a statistical inference task (Brainard et al., 2008; Brainard and Williams, 1993; Williams et al., 1981b, 1991). The cone mosaic samples visual space with only one receptor at each location. This framework proposes that the brain might use the local neighborhood of each cone to estimate the activity of the missing cone types, thereby performing a trichromatic reconstruction of an under-sampled visual world. The plausibility of this type of color coding strategy was investigated by Hofer et al. (2005b) who collected small-spot color naming data from subjects with classified cone mosaics. The results from this work indicated that cones from the same spectral class were mediating different sensations – invalidating the simplest form of Helmholtzs hypothesis. A Bayesian reconstruction algorithm was shown to capture, to a first approximation, the results of Hofer et al. lending further to support to the reconstruction hypothesis (Brainard et al., 2008). It also made testable predictions about how the local structure of the cone mosaic should influence color percepts (Figure 5.1B). According to the theory, an L- or M-cone surrounded by other cones of the same spectral

class should produce white, while an M-cone surround by all L-cones, for instance, would instruct the brain about greenness. Due to technical limitations at the time, these predictions were not tested directly.

The experiments of Hofer and colleagues produced a second surprising result: using a stimulation light of either 550 or 600 nm all five of their subjects reported the sensation of blue on a fraction of trials. S-cones are classically associated with blue sensations, while L- and M-cones are thought to elicit yellow (Hurvich and Jameson, 1957). Yet S-cones were insensitive to the wavelengths used and could not have mediated the reported blue sensations. Therefore, L- or M-cones must have mediated the blue percepts their subjects reported. Hofer et al. (2005b) reasoned that in small patches of retina without S-cones, an M-cone would be most sensitive to short wavelength light and the brain might interpret the activity of such an M-cone as a blue sensation (Figure 5.1B). Alternatively, a role for M-cones in the sensation of blue has been proposed to occur via an opponent circuit that differences L-cones from the sum of M- and S-cones (Figure 5.1C) (Drum, 1989; Schmidt et al., 2014; De Valois and De Valois, 1993).

Recently, we studied the color sensations generated by targeted stimulation of single cones with a 543 nm light on a white background (Sabesan et al., 2015b). We found many L- and M-cones reliably signaled white, rather than red and green, refuting the idea of Helmholtz. The results were also counter to those predicted by the Bayesian model (Brainard et al., 2008): cones surrounded by neighbors of the opposite type were not more likely to signal hue (Sabesan et al., 2015b). However, under our experimental conditions subjects reported only green, red and white percepts (Figure 5.1D). Compared to the Hofer study, our subjects used fewer color names to describe their experience and never indicated blue or yellow percepts (Hofer et al., 2005b). One difference between the two studies is that we used a white background whereas the Hofer et al. experiments were performed in the dark.

Here we sought to understand the impact of the background on single cone percepts.

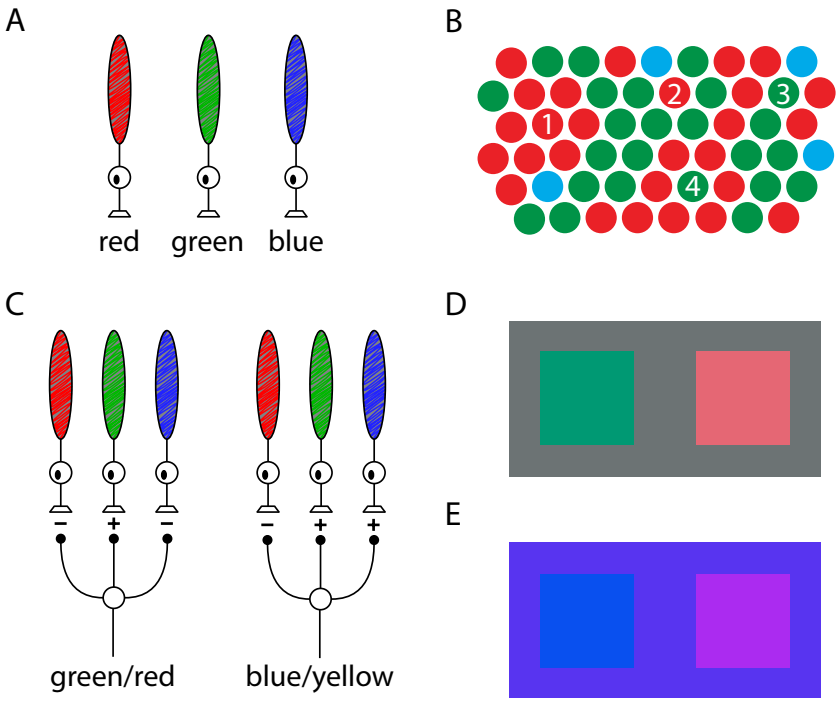

Figure 5.1: Possible sensations from single cones. (**A**) Helmholtz proposed that each type of cone gave rise to one sensation: red, green and blue (or violet). (**B**) A mosaic of cones demonstrates the predictions of a Bayesian hypothesis (Brainard et al., 2008). This hypothesis predicts the brain should learn to associate cone 1 with a white sensation, cone 2 a reddish sensation, cone 3 a greenish sensation, cone 4 a blueish sensation. (**C**) Classical red/green and blue/yellow opponent circuits that sum and difference the output of the three cone types. In this case, a single cone can feed into multiple circuits. An M-cone, for example, could mediate the sensation of both green in one circuit and blue in the other. (**D**) Approximations of the white/gray and (**E**) blue backgrounds adopted in our experiments are shown. Relative to these backgrounds a light that selectively increases activity in only L-cones (right) or M-cones (left), known as a cone isolating stimulus, produces different colors depending on the context. On a gray background the M-isolating light appears greenish or greenish-blue, while the L-isolating stimulus looks red or pink. In comparison, an M-isolating light is typically described as blue and the L-isolating light appears reddish-blue or purple.

To encourage blue responses (Figure 5.1E), we collected single cone color naming on a blue background. The influence of chromatic backgrounds on color appearance of large-spots has been studied extensively (Chichilnisky and Wandell, 1995; Shevell, 1978, 1992; Walraven, 1976; Whittle, 1973). We report here significant structure in the colors reported by subjects that are not predicted by either the Helmholtz or reconstruction models of small-spot color appearance. Through stimulation of individual cones on a blue background compared to the white background tested earlier, we discovered numerous rules the brain uses when assigning color to objects in the real world that were consistent with a spectrally opponent-neuron coding scheme.

5.3 Results

Color naming behavior on a blue background

We used adaptive-optics micro-stimulation (Arathorn et al., 2007; Bruce et al., 2015; Harmening et al., 2014; Sincich et al., 2015; Tuten et al., 2012) to present small spots against a blue background to two male subjects. With these conditions, a 0.5 degree spot (543 nm) was consistently reported by both subjects as green in appearance. When single cones were targeted, we found subjects reported white, red and blue percepts against the same blue background. In order to assess the repeatability of these percepts, a total of 44 cones across both subjects were targeted during multiple sessions. The mean correlation coefficient of the responses generated from repeated cones was 0.77 and the median was 0.94 (Figure 5.2A), confirming the reported percepts were highly repeatable.

The wavelength of the stimulus (543 nm) was ineffective at stimulating S-cones (Stockman et al., 1999). Therefore, S-cones serve as a control for the delivery accuracy of our stimulus. If the stimulus were confined to a single cone, we would expect a zero frequency of seeing in S-cones. In the 10 S-cones that were most confidently classified (see methods), we found a frequency of seeing of 45.5% (Figure 5.2B), indicating that on more than half of the

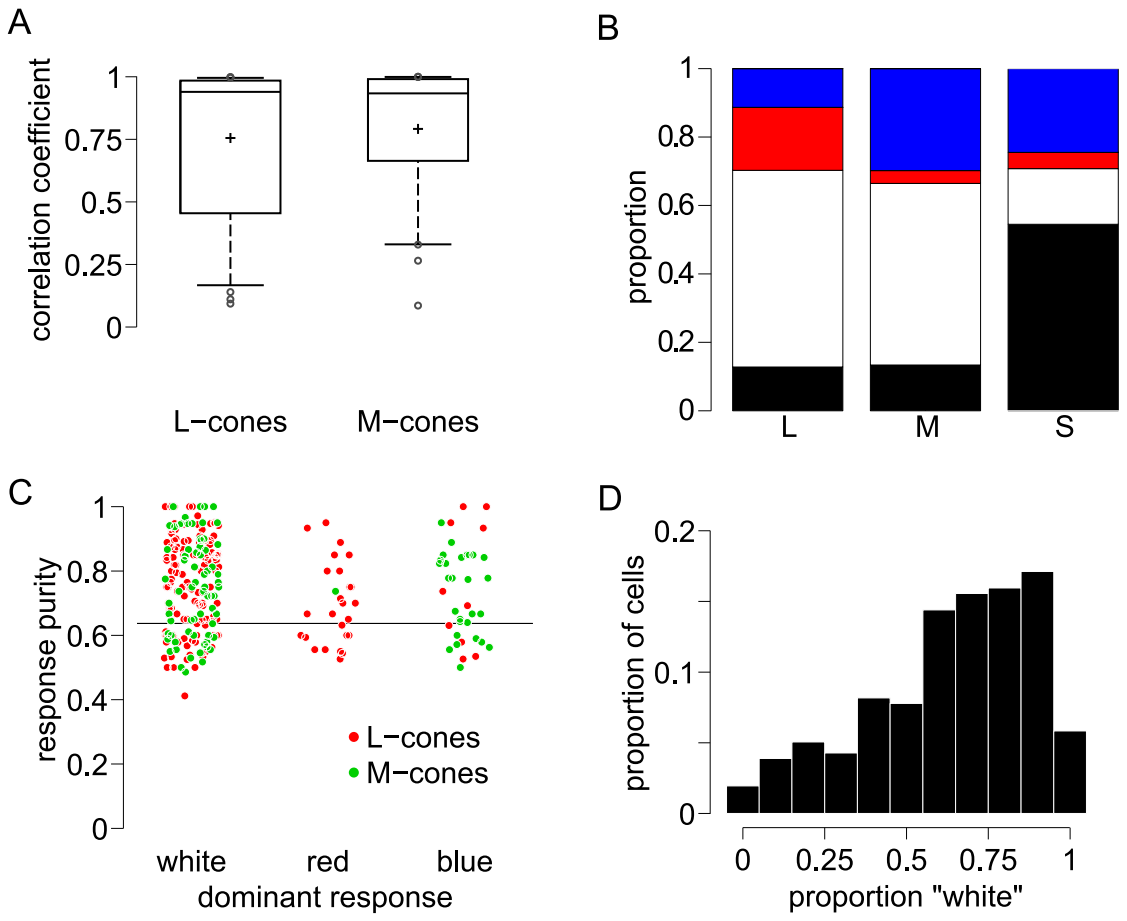

Figure 5.2: Single cone percepts on a blue background. (**A**) A subset of cones were repeated during separate sessions to assess reliability of color percepts. The box and whiskers plot represents the distribution of correlation coefficients for repeated L- and M-cones. (**B**) Proportion of responses after stimulation of L-, M- and S-cones grouped across both subjects. (**C**) Response purity of each cone separated by the dominant response color category. (**D**) Histogram of white responses across all targeted L- and M-cones.

trials the stimulating light was confined to a single cone and not seen by the subject. This number likely represents a high estimate of frequency of seeing, however, since subjects were permitted to repeat trials that were difficult to judge, which offers additional opportunities to see the flash. The remainder of analyses focused on L- and M-cones.

We next assessed the distribution of responses across L- and M-cones (Figure 5.2B). A chi-squared test on our categorical data indicated that subject responses were distributed non-randomly across the two cone types ($X^2 = 1106.2$, df=3, $p << 0.0001$). Subsequently, t-tests were computed to assess whether specific color names were associated with one cone class. Directly confirming the interpretation of Hofer et al. (2005b), we found blue percepts were more likely to be mediated by M-cones than L-cones (t_{260}=-6.05, $p = 6 \times 10^{-9}$). Meanwhile, red percepts were more likely to be driven by L-cones (t_{260}=5.94, $p = 9 \times 10^{-9}$), which was consistent with findings on a white background (Sabesan et al., 2015b). L- and M-cones were equally likely to elicit white percepts (t_{260}=0.32, $p = 0.75$).

Despite the repeatability of individual cones and apparent structure of color naming behavior across cone classes, the assignment of color within a given cone class (L, M or S) might have conformed to a random distribution. To distinguish our data from a random assignment on an individual cone level, we assessed the response purity of each cone. Response purity was defined as the number of responses in the dominant color category divided by the total number of times that cone was targeted. We performed a Monte Carlo re-sampling of our data and found the distribution of response purity in our data set was significantly different ($p << 0.0001$) from a random process (Figure 5.2C). This finding indicated that individual cones were significantly more biased towards a single color percept than would be expected by chance. Figure 5.2D further demonstrates this finding. The distribution of white responses across all cones tested consisted of two overlapping categories of cells: one large group of cells was dominated by white percepts and a smaller group elicited a low number of white responses. The latter group predominantly mediated red or blue percepts. A

chi-square goodness of fit test confirmed that the distribution did not conform to a Gaussian (X^2=36.4, df=6, $p = 2.3 \times 10^{-6}$).

The color naming behavior for each cell in our dataset is shown in Figure 5.3. A response histogram for each cone is overlaid on the subjects cone mosaic. S-cones, which serve as a control in these studies, were removed for clarity. A donut plot displays the proportion of responses reported from each targeted cone. The center of the donut indicates the type of cone targeted. Large patches of white signaling cones can be seen surrounding smaller clumps of strong color signaling cones. We found no examples of cones that strongly signaled both red and blue in high proportions. In other words, cells that strongly signaled a hue tended to have a small proportion of white responses, rather than the other hue.

White and blue backgrounds compared

We targeted many of the same cones on the blue background that were previously reported on a white background (N=252) (Sabesan et al., 2015b). We found comparable behavior under the two conditions. Frequency of seeing (Figure 5.2A) was similar under both background conditions (white: 88.2%; blue: 87.0%), confirming that the background did not affect the subjects ability to see the stimulus. The overall proportion of trials reported as white also did not change substantially (white: 54.5%; blue: 55.8%). This observation confirmed that the preponderance of white responses in the previous experiment (Sabesan et al., 2015b) was not merely a consequence of the white background.

The most substantial change between background conditions was the switch from green to blue responses and the frequency with which those names were used. Blue was reported 18.4% of the time, which was higher higher than the percentage of green (13.8%) responses on a white background. At the level of cone classes, M-cone trials were reported as blue 29.8% of the time, while green was used to describe 25.7% of M-cones trials on a white background. Surprisingly, a sizable group of L-cone trials (11.3%) also generated blue responses against

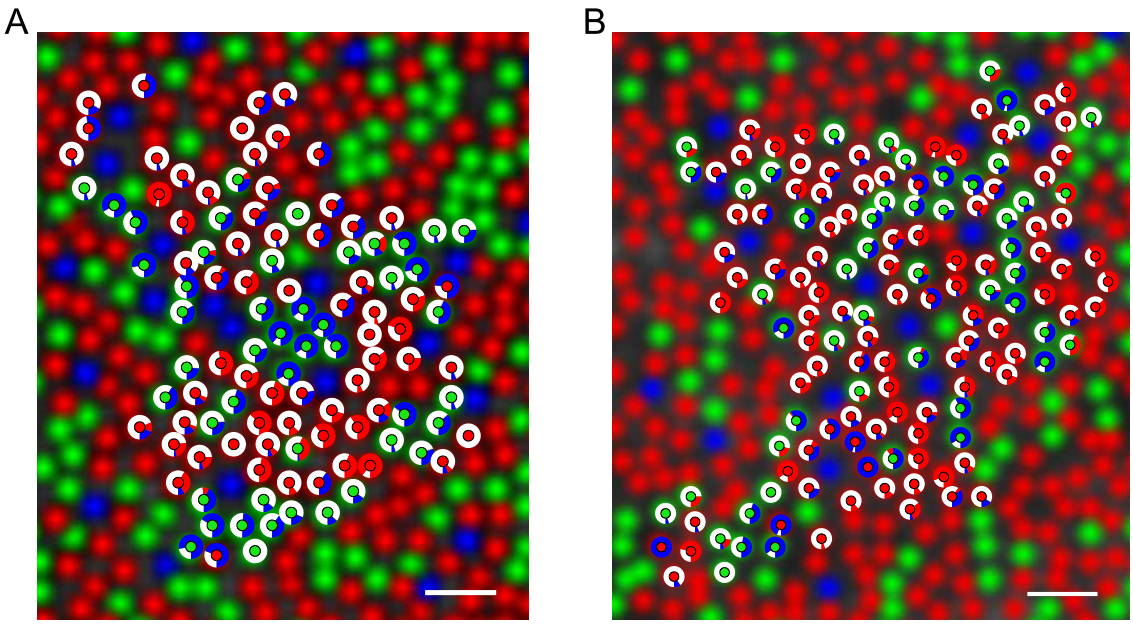

Figure 5.3: Color appearance of cone targeted stimuli on a blue background. The response to stimulation with a 543 nm light against a blue background is represented for each cone by a donut plot. The center of the donut indicates the type of cone targeted (L=red, M=green). The surrounding portion is a histogram of the color responses generated by each cone. (**A**) Subject 10001. (**B**) Subject 20076. Scale bar = 2.5 arcmin.

a blue background. Therefore, we observed a change in response preferences from both L- and M-cone trials. There was also an overall reduction in the relative number of red responses between the two background conditions (white: 19.8%; blue: 12.8%). In this case, however, the difference in naming was largely driven by a difference in red percepts reported after L-cone trials. Stimulation of L-cones on a white background elicited red responses on 28.9% of trials, while on a blue background L-cones signaled red 18.4% of the time. Part of this decrease in red responses can be attributed to the trials that elicited blue sensations. In summary, much of the change in naming behavior between the two contexts can be attributed to M-cones producing blue instead of green responses and the unexpected finding that activation of L-cones occasionally resulted in blue reports.

We next considered the degree to which individual cones change the percepts they elicit when the context was varied. Figure 5.4 displays the dominant response category for each cell tested on white and blue backgrounds and Table 5.1 summarizes the behavior of cones across contexts. The dominant response, computed in Figure 5.2C, of each cone is represented by the color of the circles. Inspection of Figure 5.4 reveals a large percentage of cones (61%) predominantly elicited white sensations regardless of backgrounds. In all cases, only a minority of cones strongly signaled hue. We found a small group of L-cones principally mediated red responses under both contexts (Table 1). A larger group of L-cones signaled white on one background and red on the other (23%). Only a single example of an M-cone exhibiting this behavior was observed. Instead, M-cones that signaled a hue mediated green or blue percepts. 14% of the M-cones in our dataset signaled green on a white background, but switch to predominantly signal blue when the background was also blue. The same behavior was observed in only 3% of L-cones. Together, these results demonstrate clear differences in the manner in which the brain interprets signals from individual L- and M-cones and clearly indicates that two different sensations can be reliably elicited from the same cone depending upon the background.

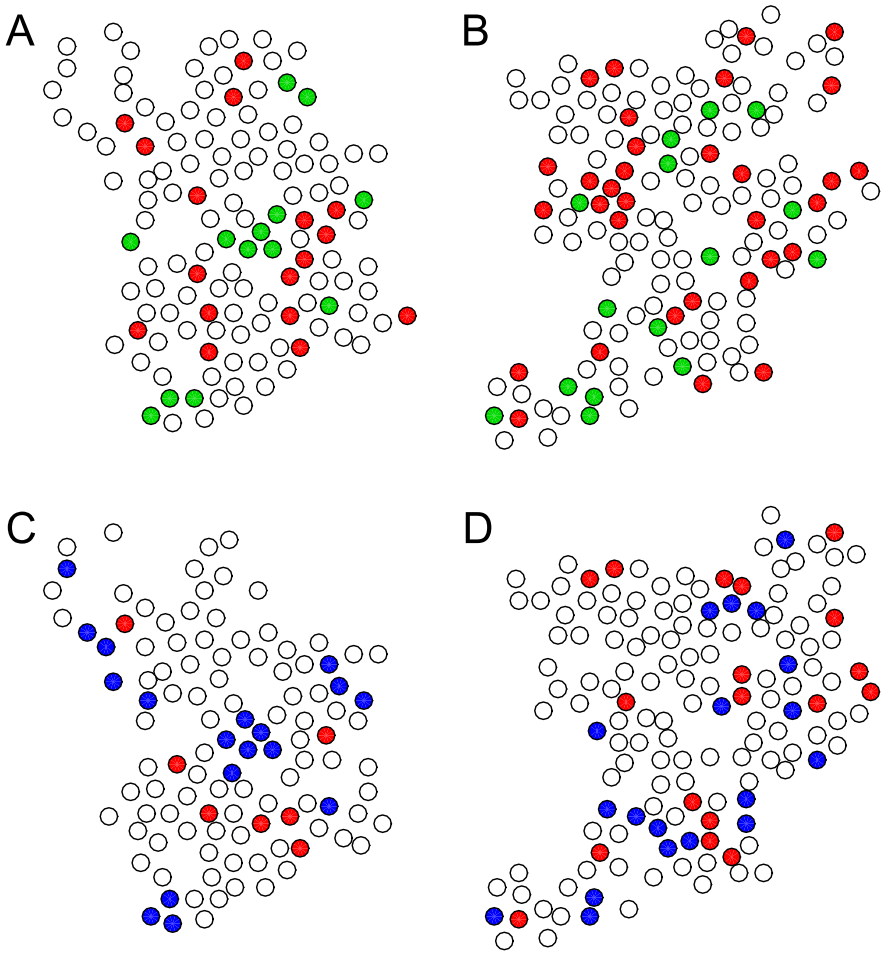

Figure 5.4: Dominant color responses on two backgrounds. Each targeted cone is represented by the color most frequently reported. (**A**&**B**) The dominant color responses on a white background are shown for each subject. (**C**&**D**) The dominant responses from cones against a blue context (**A**&**C** = subject 10001, **B**&**D** = subject 20076).

Table 5.1: Comparison of the dominant color categories on two backgrounds.

cone	w/w	r/r	g/b	w/r	w/g	w/b	r/b	total
L-cones	93	16	5	36	2	5	0	157
M-cones	61	0	13	1	6	14	0	95
total	154	16	18	37	8	19	0	252

w=white, r=red, g=green, b=blue

A more detailed quantitative comparison of the relationship between background condition and color naming is displayed in Figure 5.5. The proportion of responses named a given color was compared for each cone. The results of linear regression analysis for each condition are displayed in Supp. Table 5.2. Color naming behavior on one background predicted behavior on the other, capturing between 23 and 42% of the variance. It is worth noting that some of the unexplained variance can be attributed to unreliability in the subjects color naming between sessions (Figure 5.2A). The proportion of green responses on a white background was predictive of blue responses in both L- and M-cones (Figure 5.5A&B). Most L-cones signaled green or blue on fewer than 20% of trials, but those that frequently signaled green or blue tended to signal the other hue frequently as well (Figure 5A). As mentioned above, the proportion of red responses decreased on a blue background, which can be seen in Figure 5.5C&D. Regardless, the proportion of red responses from a given cone was correlated on both backgrounds. Lastly, white responses were reported in roughly equal proportion on both backgrounds and the likelihood a given cone signaled white was also correlated across background conditions (Figure 5.5E&F).

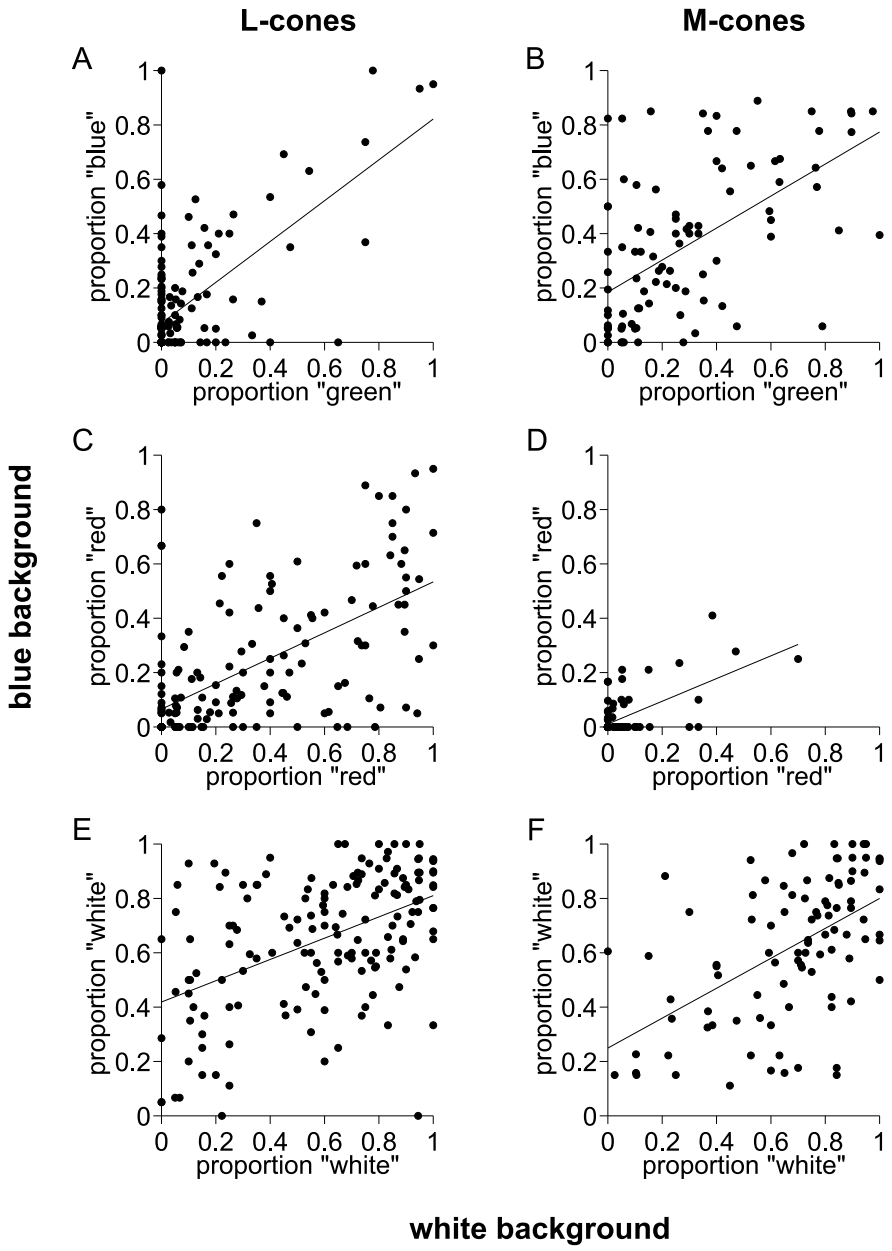

Figure 5.5: Comparison of responses from individual cones on two backgrounds. The proportion of green responses on a white background is plotted against the proportion of blue responses on a blue background for individual L- and M-cones (**A** and **B**, respectively). The plots in **C** and **D** compare the proportion of red responses from L- and M-cones. **E** and **F** represent the proportion of white responses on white and blue backgrounds. The solid lines on each plot represent the best fit linear regression line.

Predicting color responses

The local neighborhood surrounding a cone has been hypothesized to play a role in determining the percepts elicited from individual cones (Brainard et al., 2008). We determined the six nearest neighbors to each cone and analyzed the influence of this local neighborhood on color reports. In Figure 5.6 we plotted the proportion of red, green and blue responses as a function of nearest 6 neighbors that were of a different cone class. The results of regression analyses on this data are reported in Supp. Table 5.3. In most cases the effects of the local neighborhood were statistically significant, but weak. The most substantial effect of background was on the proportion of blue responses elicited after stimulation of M-cones, which captured 18% of the variance and was statistically significant. Contrary to the prediction of other models (Brainard et al., 2008) we found that M-cones were more likely to strongly signal blue when they were surrounded by other M-cones. In all cases, increasing the number of nearest neighbors beyond six decreased the relationship with the surround.

Finally, it has been hypothesized that color signals may be influenced by the presence of S-cones in the local neighborhood (Schmidt et al., 2014). In one subject we found evidence for a dependence on distance to nearby S-cones. Figure 5.7 displays the relationship between the mean distance to the nearest three S-cones and the proportion of responses named blue when M-cones were targeted. In subject 10001, we found a greater of proportion of responses named blue when an M-cone was in close proximity to S-cones (N=47, R^2=-0.246, $p = 0.0004$, SE=0.64). The distance to the single nearest, or average of the two nearest S-cones, also produced a significant prediction of proportion blue (data not shown). However, we did not observe the same trend in our second subject (N=51, R^2=0.0001, $p = 0.96$, SE=0.85). Because this analysis is sensitive to S-cones that were mis-classified as L/M-cones, one possible reason for this discrepancy is the difficult of positively identifying S-cones with our densitometry method (Sabesan et al., 2015a). For instance, one or two S-cones masquerading as an L/M-cone could be sufficient to diminish any significant trend

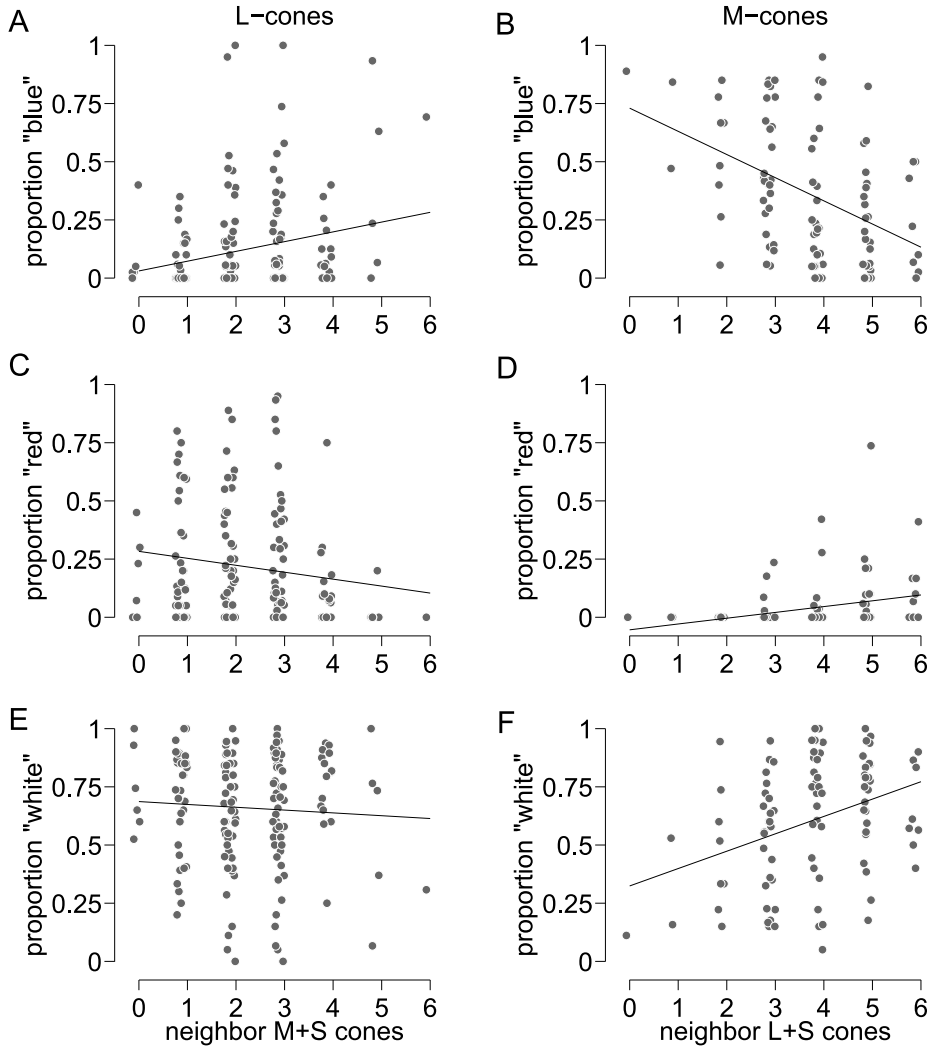

Figure 5.6: Influence of the local cone mosaic on color percepts. Each point represents an individual L- (left column) or M-cone (right column). The proportion of blue (A&B), red (C&D) and white (E&F) is represented as a function of each cones neighborhood. The solid lines represent the best fit linear regression for each plot.

in subject 20076. Indeed, the M-cone furthest from an S-cone generated ¿80% blue responses (middle right of Figure 5.7B). Should that cone actually be near an un-identified S-cone, the statistics of this relationship would shift in the direction of subject 10001.

5.4 Discussion

We studied the impact of context on the perception of cone-sized spots. These experiments led to five conclusions. (1) A large majority of cones (67%) surprisingly produced the same dominant color sensation despite a substantial change in background chromaticity. (2) Blue and green signals were often elicited from the same cone. This observation was inconsistent with Helmholtzs hypothesis that each cone class mediates a single color sensation. (3) M-cones are capable of mediating the perception of blue, which conclusively settles a long standing debate in the literature (Abramov and Gordon, 1994; Drum, 1989; Hofer et al., 2005b; Schmidt et al., 2014; De Valois and De Valois, 1993; Webster et al., 2000b; Wuerger et al., 2005; Mollon and Jordan, 1997). (4) Our results confirmed a prior observation (Brainard et al., 2008; Hofer et al., 2005b) that the spectral sensitivity of individual photoreceptor is not sufficient to predict the color it elicits and directly refuted the centuries-old notion that L-, M- and S-cone photoreceptor classes each mediate a single hue percept (Helmholtz, 1924; Krauskopf and Srebro, 1965; Otake et al., 2000). (5) Finally, we found evidence for an influence of the local neighborhood on color appearance of single cone stimulation. However, the dependence of local neighborhood was in the opposite direction predicted by a Bayesian model (Brainard et al., 2008). Below, we develop a different framework, rooted in classical opponent theory, to explain our results and discuss the implication of our results in regard to current ideas about the neural substrate of color appearance.

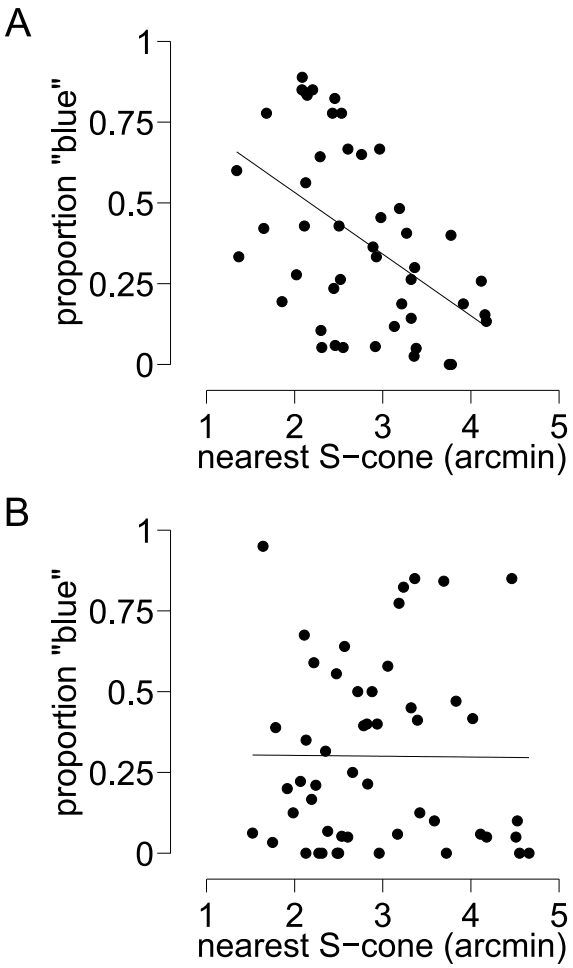

Figure 5.7: Dependence of blue percepts on distance to nearby S-cones. The proportion of blue responses when an M-cone was stimulated is plotted as a function of mean distance to the three nearest S-cones. The proportion of blue responses from L-cones did not show any significant correlation with S-cones. Each point in the plot represents an M-cone that was targeted on a blue background. The solid line represents the best-fit regression line. (A) Subject 10001. (B) Subject 20076.

Opponent theory explains our results

The chromaticity of the background altered the color naming behavior of our subjects in a predictable manner: against a white background spots were named white, red, or green, while subjects consistently substituted green in favor of blue on a blue background. In Figure 5.1D&E, the two large rectangles represent the background conditions adopted in our studies. The smaller squares are L- (right) and M-cone (left) isolating lights, relative to their respective backgrounds. From a gray background (Figure 5.1D), L-cone isolating stimuli produce a reddish color and M-cone isolating stimuli create a greenish appearing square. In comparison, from a blue background (Figure 5.1E) L-cone contrast produces a purpleish color (red and blue), while the M-cone isolating square appears only blue. The appearance of these squares is to a first approximation consistent with the trends we find for single L- and M-cones. One way these percepts could be represented in the neural code is through the classical notion of red/green and blue/yellow opponent sub-systems. In the traditional arrangement, L-cones contribute to the sensations of red, yellow or white (Hurvich and Jameson, 1957). Our results were consistent with this coding scheme. M-cones, on the other hand, are thought to participate in the sensations of yellow, green and white (Hurvich and Jameson, 1957). We did frequently observe M-cones contributing to green and white. However, our results were more consistent with the large body of evidence (Abramov and Gordon, 1994; Drum, 1989; Hofer et al., 2005b; Schmidt et al., 2014; De Valois and De Valois, 1993; Webster et al., 2000b; Wuerger et al., 2005; Mollon and Jordan, 1997) supporting a role for M-cones in the sensations of blue, rather than yellow, percepts. We found in the current experiments that the background can bias signals from cones down one of the two pathways (Figure 4): M-cones that previously signaled green, switched on a blue background to signal blue.

The logic of this framework is shown schematically in Figure 5.1C. The signal from a single M-cone contributes to both an M(L+S) (green) and an (M+S)L (blue) pathway.

When an M-cone was stimulated on a white background the signal was stronger in the M(L+S) pathway because M-cones constitute the sole excitatory drive to greenness. In the blue circuit, M-cones contribute only a portion of the drive and consequently elicited only a small amount of blue sensations. Therefore, the subjects reported a predominantly green percept, though both verbally reported a tinge of blueness to some of the greens. When a 455 nm, blue background was applied, however, S-cones activity was relatively increased, thus potentiating the neural pathway of blue (+S) and suppressing the green pathway (-S). In other words, stimulation of an M-cone contributed the same excitatory potential to both green and blue pathways, but blue percepts were stronger than green due to the steady state activity of S-cones.

This framework also provides insight into why L-cones signal less redness and more blueness on a blue background: an L-cone isolating stimulus induces the sensations of both red and blue via an M(L+S) and an L(M+S) mechanism, respectively (Figure 5.1E). Supporting this notion, we found blue responses from L-cones but far few than from M-cones (Figure 5.5; Table 5.1). A small handful of L-cones strongly signaled both green and blue and a larger group signaled white on a white background and blue on a blue background (Table 5.1). Notably, a substantial fraction of the blue responses from L-cones were from cones that predominantly signaled another color (white or red) (Figure 5.5A). This trend is reflected in the average proportion of blue from any given L-cone, which was higher than red from an M-cone. Some of these blue responses from L-cones may be explained as classification errors. The estimated rate of classification error from the densitometry technique was 3-5% and, therefore, some of the green/blue signaling L-cones may in fact be misclassified M-cones. Additionally, the difficultly inherent in the task of distinguishing blue and white percepts from a blue background might have contributed.

However, the relative preponderance of blue responses from L-cones may be indicative of a deeper point. We hypothesize that L-cones occasionally contribute to the M+S side

of the blue/yellow opponent comparison because M+S signals are generated through a surround interaction. In other words, the blue/yellow opponent equation can be rewritten as (L+M+S)L, where L is the center of an opponent neuron and (L+M+S) is its surround. Under natural conditions the L-cone component of the surround cancels and does not factor into blue color perception; L-cones instead mediate yellow percepts. But on the single cone scale probed in this study the L-cone contribution is revealed. Indeed, most L-cones elicited only a small number of blue ratings, which is consistent with the idea that the weight of the L-cone to the blue side of the equation is weak, though present none-the-less. An outer retinal circuit capable of mediating this form of opponency has been previously hypothesized (Schmidt et al., 2014), though these interactions could arise later in the visual stream as well.

Implications for the neural circuits of color vision

Midget ganglion cells are often cited as the retinal basis for red-green color vision (Mollon, 1999). Our results challenge the simplest form of this hypothesis. In the central retina, a single midget ganglion cell receives excitation from a single cone (Dacey and Petersen, 1992). This arrangement confers L-M cone opponency in a many midget ganglion cells (Sun et al., 2006). Here, we used the finest stimulus possible under diffraction limited optics to probe individual cones. If single-cone midget ganglion cells mediate the percepts of red and green, our stimulus should reveal that tendency. Instead, cones surrounded by neighbors of opposing sensitivity were no more likely to signal hue on a white background (Sabesan et al., 2015b) or the blue background reported here (Figure 5.6). On the contrary, there was a weak trend for cones to signal hue more strongly when surrounded by neighbors containing the same photopigment (Figure 5.6; Supp. Table 5.3). Notably, the majority (61%) of L/M-cones, often surrounded by opponent neighbors, predominantly elicited white sensations. This result suggested that midget ganglion cells provide a high resolution, black/white signal and the existence of spectral opponency in these cells is merely incidental (Sabesan et al., 2015b;

Schmidt et al., 2014). Classical color theory maintains that white arises when L- and M-cones are summed together (Hurvich and Jameson, 1957), which neurons in the magnocellular pathway are known to do (Lee et al., 2010). However, the spectral sensitivities of L- and M-cones are broad enough that any given L/M-cone is capable of signaling white. In addition to magnocellular neurons, the brain could additionally learn to associate midget ganglion cells that respond equally well to a black/white edge and a red/green spot with white sensations.

The current evidence also bears directly on the circuit responsible for the perception of blue. The small bistratified ganglion cell receives S-ON input from the S-cone bipolar cell (Mariani, 1984) and (L+M)-OFF signals from diffuse bipolar cells (Calkins et al., 1998; Dacey and Lee, 1994), which produces a neuron that is excited by short wavelength, blueish light, and is inhibited by longer wavelength, yellowish light (Dacey and Lee, 1994; Field et al., 2007). These observations have led to the prevailing notion that the small bistratified encodes the first stage of blue color perception in primates (Dacey and Packer, 2003; Lee et al., 2010). Our results were inconsistent with this theory. The small bistratified is inhibited by the excitation of L- and M-cones. If the small bistratified were directly informing the visual system about blueness, stimulation of L- or M-cones should predict a decrease in blue perception, not an increase as we observe. Therefore, our findings imply that either the cortex performs an operation whereby M-cones signals are combined in such a manner with the small bistratified as to act synergistically with the S-cone signal (i.e. (S+M)-L instead of S-(L+M)) or an alternative retinal substrate provides the brain with information about the appearance of blue objects in the world.

A possible alternative pathway for blue signals is suggested by the observed relationship between blue percepts in M-cones and the distance to S-cones. In one subject we found the proportion of blue responses increased when an M-cone was nearby one or more S-cones (Figure 7). This relationship could be implemented in the outer retina. The H2 horizontal cell receives robust S-cone input in addition to L/M-input (Dacey et al., 1996)

and may therefore introduce a modest S-cone signal into nearby L/M-cone pathways via lateral inhibition. Anatomical evidence points to two sites of H2 cell interaction with L/M-cone pathways: a feedback mechanism at cone terminals and a feed-forward pathway directly influencing the dendrites of L/M-cone bipolar cells (Puller et al., 2014a,b). Both pathways would produce an S+M signaling with a dependence upon proximity to S-cones. Previously, we have elaborated the hypothesis that this pathway might be the basis for blue percepts in man (Schmidt et al., 2014).

Outstanding issues

The aspect of our results that continues to present a challenge is predicting which cones will give rise to hue percepts and which will reliably produce white sensations. To begin to address this central issue, we studied the impact of local neighborhoods in the cone mosaic. Analysis of the six cones nearest to each targeted cone revealed a significant influence of the neighborhood on color percepts (Figure 5.6). The magnitude of the effect, however, was weaker than predicted by previous models, influenced color perception in the opposite direction from those predictions (Brainard et al., 2008) and mostly affected M-cones (Supp. Table 5.2). The neighborhood of L-cones exhibited little influence on the color percepts elicited with our stimulus. On the other hand, M-cones tended to signal blue more strongly when surrounded by other M-cones. These observations stand in contrast with the predictions elaborated by a Bayesian model of color appearance as well as the midget ganglion cell theory mentioned above. However, the Bayesian model was developed under the assumption of a dark background. We partially addressed this issue in the present work by changing the background and found the effects of neighborhood were unchanged from a prior study with a white background (Sabesan et al., 2015b).

Interestingly, extending our analysis beyond the six nearest cones weakened the correlation with the neighboring cones. The fact that including more than six cones diminishes the

effect points to a retinal locus of the neighborhood effects we observed. Lateral inhibition in the outer retina introduces spatial comparisons between neighboring cones. Each horizontal cell integrates signals from cones in its receptive field and in turn imposes feedback onto those cones, creating a surround component to each cones receptive field (Thoreson and Mangel, 2012). Because horizontal cells use passive conductance, the surround influence of a cone to any other is exponentially related to the distance between the two cones. In other words, the further away a neighbor sits, the weaker its influence will be on a cone of interest. Since the human cone mosaic is organized hexagonally (Curcio et al., 1990; Hofer et al., 2005a), the largest contribution to a single cones receptive field comes from its six nearest neighbors. Our results are consistent with this spatial relationship. It is theoretically possible that an influence of nearby cones could also arise in cortex. However, there is no *a priori* reason why the nearest six, rather than five or seven, cones should be particularly important at the level of V1 neurons.

A fundamental task of the visual system is to extract information about intensity and wavelength from the environment. How the visual system carries out this task is still a matter of active investigation. We have approached this topic by targeting single cones in a classified cone mosaic. Our results shed light on the rules used by the brain to produce precepts in response to fluctuations from individual cones and point to an opponent coding scheme instantiated early in the visual pathway.

5.5 Experimental procedures

Subjects

The two subjects (10001 and 20076) were both adult male Caucasians and had normal color vision (Hardy-Rand-Rittler plates and anomaloscope). Prior to experiments, drops of 1% tropicamide and 2.5% phenylephrine were administered to dilate the pupil and paralyze accommodation. Bite bars were used to stabilize the subject. Informed consent was obtained

from each subject and all experimental procedures adhered to the tenets of the Declaration of Helsinki.

Psychophysics

An adaptive optics scanning laser ophthalmoscope (AOSLO) was used in conjunction with densitometry to identify the location and spectral identity (L, M, S) of a mosaic of cones in two subjects (Sabesan et al., 2015a). The details of the experimental apparatus (Arathorn et al., 2007; Roorda et al., 2002; Stevenson and Roorda, 2005) and classification technique have been published elsewhere (Sabesan et al., 2015a).

Single cones were targeted with micro-stimulation using the same AOSLO system. The details of micro-stimulation have been reported in detail elsewhere (Arathorn et al., 2007; Bruce et al., 2015; Harmening et al., 2014). Briefly, the paradigm utilized an 842 nm (50 nm full-width at half maximum bandwidth) infrared (IR) channel for imaging and a 543 nm (24 nm full-width at half maximum bandwidth) channel for stimulation. Optical aberrations were measured in with the IR channel using a wavefront sensor. A deformable mirror was adjusted in closed loop to correct for the measured aberration, resulting in near diffraction-limited imaging and stimulus delivery (Roorda et al., 2002). IR images were used to perform real-time, high-resolution eye tracking. This system permitted targeted delivery of the diffraction-limited stimulus to within 0.15 arcmin (Arathorn et al., 2007; Stevenson and Roorda, 2005). Longitudinal chromatic aberration was corrected with standard procedures (Harmening et al., 2014). Finally, transverse chromatic aberration between the imaging and stimulating channel was measured before and after each session according to the procedures of Harmening et al. (2012) and corrected with a fixed offset term (Harmening et al., 2014). Sessions were discarded if TCA was found to change by >0.45 arcmin between the start and end of the session. The delivery location of each flash was recorded and analyzed off line.

Flashes were 3 pixels (roughly 0.45 arcmin) in diameter, which is less than half the size of

a cone inner segment at the retinal eccentricity studied (1.5 degrees), and 500 ms in duration. The subjects reported the percept associated with each flash as white, red, green, blue, yellow or not seen with a tablet device. Each cone was targeted at least 20 times. During each session, 610 cones were randomly interleaved to prevent bias in responses. Subjects were given an extended break (2-10 minutes) half way through the trial and were permitted to take additional breaks as needed during the sessions.

Background

Backgrounds were set with an external projector in Maxwellian view. In order to measure the chromaticity and luminance of the white and blue backgrounds, a patch the same size as and adjacent to the background was generated with the external projector. One subject was then given control over the chromaticity and luminance of the adjacent patch and asked to achieve a match in chromaticity and luminance to the background. This procedure was carried out two times. The patch was then measured with a PR650 spectroradiometer (Photo Research). The chromaticity of the blue background was 0.16, 0.15 in CIE 1931 xy space and the luminance was 38 cd m^{-2}. The white background had a chromaticity of 0.23, 0.30 and a luminance of 46cd m^{-2}. The luminance of both backgrounds was bright enough to eliminate any contribution from rods. Blue and white background studies were often carried out within a short time of one another. The order of the sessions was chosen at random to prevent bias between the two conditions. There was no relationship between cones tested before, after or on entirely separate days from white conditions. Further, as noted above, the selected cones for each session were randomly interleaved making it impossible to guess which cone was being targeted on any given trial.

Analysis

All analysis was carried out in Matlab (Natick, MA). Nearest neighbor analysis was performed with Matlabs "knnsearch" function. Due to the similarity in trends between our two subjects, we analyzed the data from both subjects together except where noted.

5.6 Supplementary information

Table 5.2: Linear regression analysis of color responses compared across backgrounds.

comparison	cone type	N	R^2	SE	p
blue vs green	M	95	0.335	0.225	8.3×10^{-10}
	L	157	0.416	0.138	7.4×10^{-20}
red vs red	M	95	0.396	0.087	8.5×10^{-12}
	L	157	0.365	0.260	5.8×10^{-17}
white vs white	M	95	0.291	0.216	1.8×10^{-8}
	L	157	0.233	0.266	1.5×10^{-10}

Table 5.3: Linear regression analysis of color responses compared across backgrounds.

comparison	cone type	N	R^2	SE	p
blue	M	98	0.18	1.12	1×10^{-5}
	L	159	0.054	1.13	0.0032
red	M	98	0.079	1.19	0.0050
	L	159	0.019	1.15	0.080
white	M	98	0.12	1.16	0.00046
	L	159	0.0033	1.16	0.47

Chapter 6

LATERAL INHIBITION AND SPECTRAL OPPONENCY IN THE OUTER RETINA OF PRIMATE

6.1 Abstract

Horizontal cells have been hypothesized to play important roles in gain scaling photoreceptor signals to control for fluctuations in brightness and are often assumed to play a role in color processing. However, the precise role of horizontal cells in visual perception is not fully understood. We modeled the primate fovea with a trichromatic cone mosaic, two types of horizontal cell populations and midget bipolar cells. Horizontal cell connectivity, mosaic arrangement and receptive field size of horizontal cells all had a significant influence upon the propagation of cone signals. Our analysis highlighted the potential importance of the H2 horizontal cell mediated pathway between S-cones and neighboring midget bipolar cells in color vision. Using cone isolating stimuli, we found biologically plausible parameters that would generate an S-cone signal in 2-10% of midget cells. The expectedly modest S-cone signal and relatively small number of such cells provided an explanation for why others have not routinely observed such cells. This circuit would implicate the H2 horizontal cells in blue/yellow and red/green color vision. Finally, the results offer an explanation for the preserved color vision in individuals with mutations to the ON-bipolar specific glutamate receptor, mGluR6.

6.2 Introduction

A central goal of neuroscience is to understand how neuronal circuits give rise to human perception. Studying the contribution of inhibitory inter-neurons to information processing

has been particularly limited by the tools available for modulating the activity of a single class of cells. The role of primate horizontal cells in visual processing provides one such example. Detailed anatomical descriptions have revealed the morphology and connections of this population of cells (Wässle et al., 1989; Ahnelt and Kolb, 1994a; Chan and Grünert, 1998). Single-cell electrophysiological measurements have provided a gross characterization of their biophysical properties (Dacey et al., 1996; Lee et al., 1999; Smith et al., 2001; Dacheux and Raviola, 1990; Zhang et al., 2011; Lee et al., 2003). The footprint of horizontal cells on vision, however, has been more difficult to tease apart. We have approached this problem by developing a population model of outer retinal physiology.

Lateral inhibition introduced by horizontal cells produces spatial antagonism between a cone and its neighbors. The functional impact of this lateral inhibition on vision has been considered from at least three perspectives. One has focused on the potential importance of surround inhibition on sharpening edges and enhancing contrast of the visual image. By introducing a comparison of nearby cone activities, horizontal cells remove light patterns varying slowly in time or space, effectively acting to de-blur the image. Another perspective proposes that horizontal cells contribute to the computation of controlling for local and global fluctuations in brightness across a scene (Smith et al., 2001; Masland, 2011; Dacheux and Raviola, 1990). The third aspect of vision with which horizontal cells are often associated is color opponency.

Two types of horizontal cells, known as H1 and H2, are recognized in primates. The dendrites of H1 cells contact L- and M-cone terminals, but avoid S-cones, while the axonal arbor of H1 cells receives input from rods (Rodieck, 1998; Chan and Grünert, 1998; Dacey et al., 1996; Verweij et al., 1999; Ahnelt and Kolb, 1994b). H2 cells have dendrites that collect input from all three cones types and have an axon with processes that also receives input from cones (Rodieck, 1998; Ahnelt and Kolb, 1994b). Both types of primate horizontal cells hyperpolarize in response to all wavelengths of visible light (Dacey et al., 1996; Lee et al.,

1999; Smith et al., 2001; Dacheux and Raviola, 1990; Zhang et al., 2011; Dacey et al., 2000b). Partly due to the lack of spectral opponency, early work argued that primate horizontal cells exclusively participate in achromatic vision (Dacheux and Raviola, 1990). In comparison, fish horizontal cells exhibit spectral opponency; they hyperpolarize to some wavelengths and depolarize to others (Daw, 1967; Svaetichin and MaCnichol, 1959; Kamermans et al., 1998).

Despite a lack of spectral opponency, both H1 and H2 cells have more recently been implicated in the first stages of color processing (Dacey et al., 2000b, 1996; Lee et al., 2010; Neitz and Neitz, 2011). H1 cells are likely to be involved in generating L-M opponency in midget bipolar cells through a random-wiring mechanism (Paulus and Kröger-Paulus, 1983; Crook et al., 2011). H1 cells may also mediate the aforementioned brightness regulation (Dacheux and Raviola, 1990; Smith et al., 2001; Lee et al., 2003, 1999) and could contribute to after-images and chromatic adaptation (van Hateren, 2007). H2 cells, on the other hand, may be involved in blue-yellow color vision (Schmidt et al., 2014; Kolb et al., 1997; Calkins, 2000), because they receive strong S-cone input (Dacey et al., 1996; Ahnelt and Kolb, 1994b). However, the exact role of H2 cells in blue-yellow circuitry has not been settled (Field et al., 2007; Crook et al., 2009). Field et al. (2007) have argued that the H2 contributes the major L+M inhibitory component to the small bistratified ganglion cells receptive field, which is widely thought to be the retinal basis of blue/yellow vision. On the other hand, Crook et al. (2009) contended that H2 cells serve only an indirect role in the small bistratified circuit.

The potential for H2 cells to shape the response of L- and M-cone circuits has received less attention. This is largely because they make far fewer connections with each L- and M-cone terminal (Dacey et al., 1996), which, together with the fact that H1 horizontal cells avoid contacts with S-cones, has focused attention on the role H2 cells play in S-cone processing. Yet, horizontal cell synapses are known to be reciprocal in all species studied (Thoreson and Mangel, 2012). Further motivating a consideration of this pathway is the recently discovered GABAergic feedforward pathway from H2 horizontal cells directly onto cone bipolar cells

(Puller et al., 2014a). This pathway acts in concert with the feedback pathway and would enhance the encoding of surround signals when the cone terminal is already depolarized and indifferent to further surround driven depolarization (Puller et al., 2014a).

Finally, we were additionally motivated to study the propagation of S-cone signals in the outer retina by the recent discovery of individuals with mutations to the metabotropic glutamate receptor expressed in ON-bipolar cells, mGluR6. These people are clinically diagnosed as night blind because signals from rod terminals to ON-bipolar cells are interrupted (Dryja et al., 2005) and rods do no routinely contact an OFF-bipolar cell (though a small fraction of rods may occasionally contact one type of diffuse bipolar, as noted by Tsukamoto and Omi (2014)). Similarly, physiological evidence argues against the existence of an OFF-bipolar cell dedicated to S-cones (Evers and Gouras, 1986), though again there may be occasional exceptions to this rule (Field et al., 2010; Tsukamoto and Omi, 2015; Klug et al., 2003). Therefore, these individuals were also expected to exhibit S-cone mediated color deficits. However, color vision deficits of any kind are not associated with mutations to mGluR6 (Zeitz et al., 2015). These observation led us to consider the possibility that the H2 horizontal cells provide a small number of L- and M-cones with significant signal from nearby S-cones that could be utilized by the brain to preserve normal color vision in these individuals. Using known anatomical and physiological properties of primate horizontal cells we demonstrate the plausibility of this pathway and discuss the potential implications for normal color processing.

6.3 Methods

We modified a version of the working model (WM) framework that has been previously described (Baker and Bair, 2012). WM was developed as a model of feedforward projections in the visual stream. We focused on the retinal front end of WM and further specialized the network to model color processing in the outer retina. An advantage of studying and fine

tuning this framework over other existing retinal models is that WM was designed to model cortical circuits. Therefore, the impact of parameters in the outer retina can be rapidly considered from the point of view of higher centers in the brain. For the current work, we focused on the impact of the outer retina on color processing early in the visual pathway.

Existing population models of retina do not explicitly model the cone mosaic, or horizontal cells at the detail necessary to probe specific questions about horizontal cell function (Martínez-Álvarez et al., 2013; Wohrer and Kornprobst, 2009; Pei and Qiao, 2010). Similarly, previously developed biophysical models of cones and horizontal cells, do not included a stimulus paradigm, bipolar cells or a trichromatic retina (van Hateren, 2005, 2007; Smith et al., 2008; Packer and Dacey, 2005; Wilson, 1997). Lastly, an older linear model that used measured cone mosaics to estimate receptive fields of theoretical lateral geniculate nucleus (LGN) neurons was too general in its specification. This model did not explicitly consider horizontal cells and neglected the time domain entirely (Lennie et al., 1991).

Model overview

A one-dimensional view of a signal passing through our model is shown in Fig. 6.1. A uniform white light pulse presented to the retina was filtered by the cone photoreceptors. The trichromatic cone mosaic transformed the white light stimulus (specified in RGB coordinates) into cone excitations at each time step. The activity of the cone mosaic was then propagated through two resistive meshes, which modeled the H1 and H2 horizontal cell networks. A difference between each cone and the sum of the two networks directly beneath the cone was computed to produce a bipolar cell layer.

Cones

The temporal filtering properties of cones were modeled as a biphasic low-pass filter (Schnapf et al., 1990, 1987; Smith et al., 2001). A low-pass filter was implemented as the difference

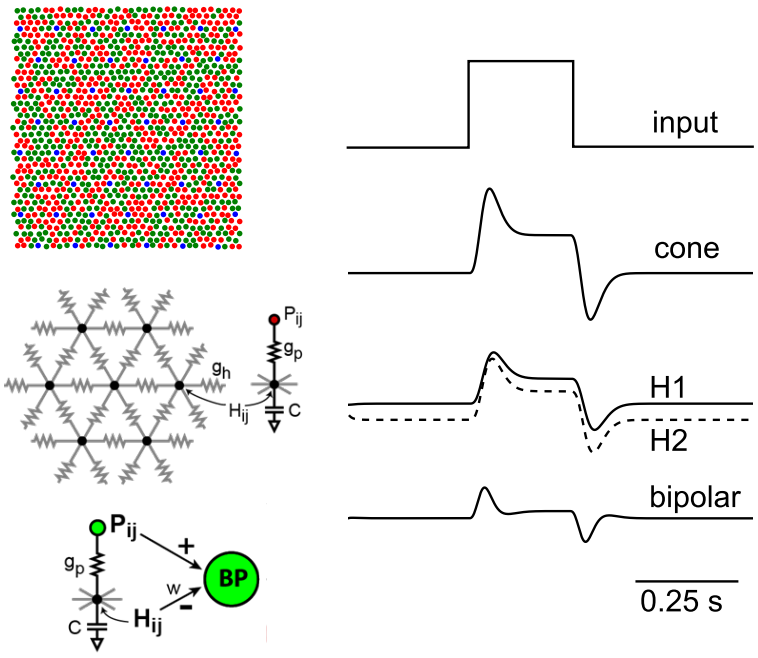

Figure 6.1: Schematic of our model. On the left is a cartoon representation of each of the major components of the model. The right is an example of a full-field flash of light propagating through a single column in our model that consists of a cone, two horizontal cell networks and a bipolar cell that takes the difference of the cone activation from the two horizontal networks.

between two Maxwell-Boltzmann distributions with a scaling constant controlling the relative height of each distribution:

$$response = M_{exc} - \alpha * M_{inh} \tag{6.1}$$

The width of each distribution, M_{exc} and M_{inh}, and the scaling constant, α, were specified to roughly reflect the kinetics described by Schnapf et al. (1990) and Schneeweis and Schnapf (1999). Recent recordings from macaque and other mammalian cone terminals by Cao et al. (2014) has convincingly demonstrated that photocurrent from cones are in fact not biphasic; directly confirming earlier studies of human electroretinogram (van Hateren and Lamb, 2006). However, inclusion of a biphasic filter does not affect the main result of our simulations and provides a convenient and efficient method for temporally filtering incoming visual stimuli in a reasonably realistic manner.

Each cone in the mosaic of about 6500 cones was designated as either an L-, M- or S-cone. In most simulations, the ratio of L- to M-cones was 1:1 and cone identities were randomly distributed. Analysis of mosaics from humans (Hofer et al., 2005a; Roorda et al., 2001) and non-human primates (Field et al., 2010; Mollon and Bowmaker, 1992) suggests the distribution of L/M-cones in the mosaic are roughly random, with a slight tendency for cone classes to clump. The overall percentage of S-cones in the mosaic was set to 4%, which is approximately the value reported in the literature for retinal locations on the foveal slope (Curcio et al., 1991; Hofer et al., 2005a). S-cones here were arranged in a perfectly crystalline mosaic. Outside of the central 1-2 degrees, where they are more disorderly, S-cones tend to be regularly spaced (Curcio et al., 1991). Finally, we also studied one mosaic of about 800 cones that had been previously classified with adaptive optics and densitometry (Sabesan et al., 2015b). The L:M cone ratio of that mosaic was 1.9:1. In order to avoid edge effects during simulation, the mosaic was placed inside a larger mosaic with the same L:M ratio.

RGB stimuli – specified in space and time ($S(x, y, t)$) – were converted into cone activa-

tions following standard colorimetry procedures (Brainard and Stockman, 2010). For simplicity, and to achieve maximal cone isolating contrast, we assumed monochromatic RGB primaries of 625, 525 and 445 nm. An example of a system that could produce monochromatic lights with spatial control, as we assume here, was recently realized with a digital light processing projector system (Bayer et al., 2015). We used the 2 degree human cone fundamentals reported by Stockman and Sharpe (2000). RGB values were then transformed into L-, M-, S- values according to:

$$\begin{bmatrix} L \\ M \\ S \end{bmatrix} = \begin{bmatrix} L_R & L_G & L_B \\ M_R & M_G & M_B \\ S_R & S_G & S_B \end{bmatrix} \begin{bmatrix} R \\ G \\ B \end{bmatrix} \tag{6.2}$$

The 3x3 matrix (L_R ...) represents the dot product of each RGB monochromatic primary with each LMS sensitivity function (Brainard and Stockman, 2010). The matrix obtained from this process is specified below:

$$\begin{bmatrix} L \\ M \\ S \end{bmatrix} = \begin{bmatrix} 0.436214 & 0.7625 & 0.057364 \\ 0.074228 & 0.914324 & 0.092431 \\ 0.0 & 0.016317 & 0.984351 \end{bmatrix} \begin{bmatrix} R \\ G \\ B \end{bmatrix} \tag{6.3}$$

In situ, photoreceptors perform a roughly logarithmic transformation on the intensity of incoming light. Here a Frobenius norm was applied to the cone system matrix (Eq. 6.3) to produce relative cone activations; thereby discarding the absolute light levels of stimuli.

For analysis of cone specific signals, we constructed cone isolating stimuli by inverting the 3x3 matrix in Eq. 6.3 and multiplying the inverted matrix with the desired vector of L-, M-, S-cone activation values (Estevez and Spekreuse, 1982). All cone isolating stimuli were computed as a change in cone activation relative to a background condition where L-, M- and S-cone activity was equated.

Horizontal cells

Horizontal cells were modeled as a resistive mesh (Naka and Rushton, 1967). The passive conductance of current through the mesh was implemented by solving the diffusion equation on a Cartesian resistive grid (or mesh). This grid has the same spatial dimensions as the stimulus, $S(x, y, t)$, but followed the hexagonal arrangement of the cone mosaic. For each grid point, the cone excitation of a single cone at the same x, y location was applied through a conductance, g_P. Connections to the six neighboring grid points influenced the node with a specified conductance, g_H. The ratio of g_P to g_H controls the space constant of the resistive mesh. For example, for a one-dimensional chain, $L = \sqrt{g_h/g_p}$, where L is the characteristic length, i.e., the distance over which an input applied (and held constant) at one point decays to $1/e$ of its value.

Bipolar cells

Bipolar cells take the difference between the excitatory signal of cones and the inhibitory signal of horizontal cells:

$$bp(t) = cone(t) - (\beta * H1(t) + \gamma * H2(t)) \tag{6.4}$$

β and γ control the strength of the horizontal surround relative to the center. Each *bp* cell is centered on a single cone, and thus its location and excitatory drive is taken to be that of the cone. Recordings of primate bipolar cells indicate that the center and surround tend to be roughly balanced (Dacey et al., 2000a), which was approximated here. Asymmetries between the ON- and OFF-bipolar pathways were not modeled.

Parameters

We focused on three parameters of our model. 1) The conductance of photoreceptor signals into each horizontal mesh network, g_P. This parameter influences both the speed at which

signals effect the horizontal networks and the spatial size of the horizontal cell receptive field. 2) The conductance between each node in the horizontal cell network, g_H, which also effects the lateral spread of signal through each horizontal cell network. 3) The weight, w, each type of horizontal cell contributed to the bipolar calculation (Eq. 6.4). The parameters assumed in our model are recorded in Table 6.1.

Table 6.1: Parameters of the model.

receptive field size	H1 g_P	H1 g_H	H1 w	H2 g_P	H2 g_H	H2 w
large	0.15	2.0	0.65	1.0	1.0	0.4
small	0.15	0.04	0.65	1.3	0.02	0.4

Analysis of model

The WM framework generates data in the ndata format (http://www.imodel.org/nd/). Responses to visual stimuli were all carried out in python (http://www.python.org) using the numpy (http://www.numpy.org/) and scipy libraries (http://www.scipy.org/).

Spatial frequency tuning curves were generated by varying the spatial frequency of achromatic drifting (8Hz) gratings at 50% contrast. The F1 response to each grating was averaged across five horizontal cells. The spatial receptive field was computed by measuring the spread of signal across each horizontal cell network in response to the activity of a single cone. Temporal constants were measured by artificially, instantaneously turning on all cones from an entirely dark stimulus to one that maximally drove all cones.

We were interested in the contribution of the outer retina to spectrally opponent neurons recorded later in the visual pathways. To facilitate a comparison with studies of LGN (Tailby et al., 2008b; Reid and Shapley, 2002; Derrington et al., 1984) and retinal ganglion cell neurons (Sun et al., 2006), we computed cone weights in our model midget bipolar

cells. Midget bipolar cells project one-to-one to midget ganglion cells (Kolb and Marshak, 2003) in the central retina and make roughly one-to-one contacts with LGN neurons (Usrey et al., 1999; Cleland et al., 1971; Reid and Shapley, 1992). Cone weights were estimated with uniform, full-field cone-isolating stimuli following the procedure outlined by Reid and Shapley (2002). The bipolar response to each cone isolating stimulus was computed and the amplitude was normalized by the cone contrast achieved with each cone-isolating stimulus. Then the three weights were further normalized such that the weights of each cone summed to 1; i.e. $L_w + M_w + S_w = 1$. All cone weights were represented in plots following the convention of (Derrington et al., 1984). Since we did not create distinct models for ON and OFF bipolar cells, the signal from our single, ON-type, bipolar cell was inverted to create OFF-type responses for display in cone weight figures.

6.4 Results

Basic characterization of the model

The connectivity of H1 and H2 cells with each cone class was set to mimic those reported for primate (Dacey et al., 1996). We computed the response of both horizontal networks to a full-field, uniform stimulus designed to isolate the activity of individual cone populations. Cone isolating conditions were computed relative to a background set to produce equal activity across cone classes. As Fig. 6.2 displays, H1 cells had input from both L- and M-cones while H2 cells received input from all three cone types with a strong contribution from S-cones. The weights of L- and M-cones into the H2 network were set to 1/10th of S-cones (Table 6.1). Despite this small contribution from each cone, L- and M-cones still contributed a significant proportion of the response because they constitute the majority of cones in the mosaic. The response to cone isolating stimuli of each horizontal network qualitatively reproduced reports from experimental recordings of these cells (Dacey et al., 1996).

Fig. 6.3 displays the results of a basic linear systems characterization of the horizontal

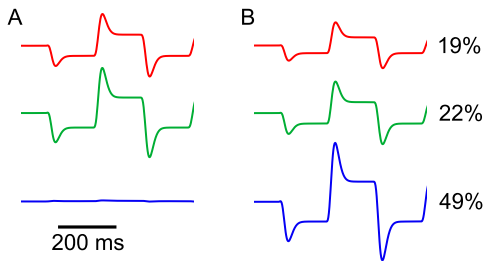

Figure 6.2: Response of modeled H1 and H2 cells to cone isolating stimuli. Increments and decrements of cone isolating stimuli relative to a background are shown for a modeled (**A**) H1 and (**B**) H2 cell. Red traces = L-cone isolating, green = M-cone isolating, blue = S-cone isolating. Cone contrast relative to the background is indicated to the right of the traces.

cells in our model. In Fig. 6.3A-C we adopted parameters that produced model cells closely mimicking the spatial receptive fields reported for H1 cells recorded from peripheral locations (Packer and Dacey, 2002). In Fig. 6.3D-F we studied the impact of considerably smaller receptive fields on processing of visual signals in the outer retina. The parameters assumed in these two models are reported in Table 6.1. In both models, the conductance of H2 horizontal cells was adjusted such that the spatial spread of light evoked signal in this population was slightly smaller than H1 cells (Fig. 6.3A&D). This choice mirrored known differences in the spatial extent of horizontal cells: H2 receptive field are smaller than those of H1 cells, at least at peripheral eccentricities (Zhang et al., 2011). The temporal dynamics of H1 and H2 cells were adjusted to be approximately equal and with a time constant of 5-6 ms (Fig. 6.3B&E). This time constant was chosen to approximate the delay between center and surround measured in higher order neurons, which has been estimated to be on the order of 7-10 ms (Benardete and Kaplan, 1997; Reid and Shapley, 2002).

The response of horizontal cells to achromatic contrast of varying spatial frequency is shown in Fig. 6.3. Both networks displayed low pass characteristics. In the case of larger receptive fields, a sharp decline in response amplitude was observed beginning around 1 cy-

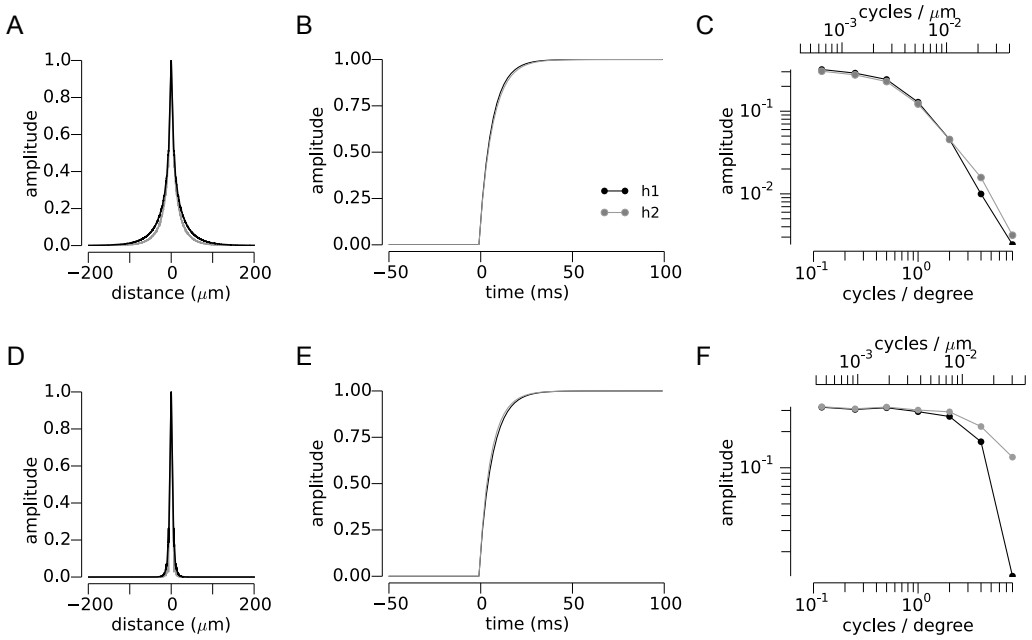

Figure 6.3: Spatial and temporal dynamics of horizontal cells. Two sets of parameters were studied for the H1 and H2 networks. **A-C** represent parameters that created behavior reflective of peripherally measured horizontal cell dynamics (Packer and Dacey, 2002). **D-F** are the results of the same analyses with parameters that produce a more spatially restricted receptive field.

cle/degree (Fig. 6.3). This relationship with spatial frequency closely agrees with experimental measurements of H1 cells at peripheral locations (Packer and Dacey, 2002). Intuitively, a low spatial frequency grating produces significant activation in all cones in the receptive field and thus elicits a strong hyperpolarization in the cell. Higher spatial frequencies drive only a subset of the cones in a given horizontal cell's receptive field and produce a weaker hyperpolarization. Following that logic, shrinking the size of the H2 receptive field still yields a low pass filter, but with a higher cut-off frequency. With fewer cones contributing to each horizontal cell receptive field, higher spatial frequencies that excite only a subset of the cones still produce strong hyperpolarizations because each cone provides a larger fraction of the overall drive into the horizontal cell (Fig.6.3).

Propagation of cone signals

We used cone isolating stimuli to explore the propagation of cone signals through the model networks. The signals in response to an S-cone isolating stimulus are shown for a single column of our model in Fig. 6.4. Bipolar cells in our model take the difference between the visually driven excitation of a single M-cone, in this example, from H1 and H2 cells. As illustrated in Fig. 6.4, an S-cone isolating stimulus produces no visually evoked response in the M-cone or the H1 network. On the other hand, the H2 network was driven strongly by the stimulus because the M-cone was positioned directly adjacent to an S-cone. The weight each horizontal network contributes to this feedback operation has not been examined experimentally, so we varied the strength that the H2 network imposed on the M-cone center bipolar cell from 0.2 to 0.8. Not surprisingly, greater weights introduced a stronger S-cone signals into the bipolar cell. However, H2 cells make far fewer contacts with each L- and M-cone than S-cones, making large weights unlikely (Dacey, 1996). Therefore, we set the weight of the H2 network at a modest 0.4 in all simulations. The effect of changing this weight would be to scale all S-cone results in subsequent figures.

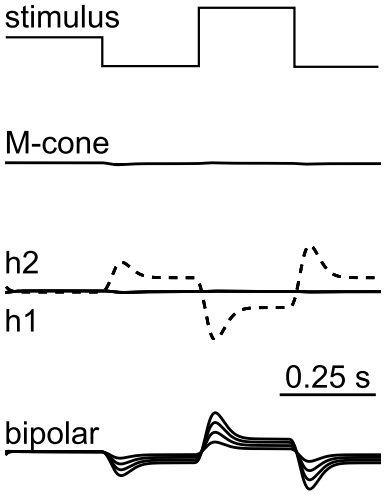

Figure 6.4: S-cone feedback onto a nearby M-cone. A single vertical column from the model is shown in response to an S-cone isolating stimulus. The M-cone and H1 cell (solid line) do not respond. The H2 cell (dotted line) is depolarized by the S-cone decrement and hyperpolarized by the S-cone increment. The impact of the horizontal cell signal is seen in the bipolar cell response, which reflects the difference between the M-cone and the H2 cell. The degree to which the H2 signal is reflected in the bipolar response is controlled by the parameter H2 w. Bipolar traces represent H2 w values ranging from 0.2 - 0.8 in increments of 0.2.

Impact of receptive field size

Technical constraints have confined experimental recordings from horizontal cells to peripheral locations. The most central eccentricity reported in the literature is about 4mm or 16-18 degrees from the fovea in the macaque (from an H1 cell). Over the peripheral areas tested, the size of H1 receptive fields scale with eccentricity (Packer and Dacey, 2002). However, whether this scaling continues to the central retina where dendritic field size of both H1 and H2 cells becomes very small is not known. It is possible that the dense gap junction coupling between cells could continue to produce effective receptive fields that extend far beyond the dendritic tree of any one horizontal cell.

The impact of receptive field size on cone weights to midget bipolar cells is explored in Fig. 6.5. We compared the signals in modeled bipolar cells under the assumption of both large and small horizontal cell receptive fields. When our model incorporated large receptive fields, cone weights did not vary substantially between bipolar cells because the surround of each bipolar pooled across many cones (Fig. 6.5A-B). In comparison, the more narrow receptive fields modeled in Fig. 6.5C-D produced substantially greater variability in the weights of L/M-cones into the surround of bipolar cells. At central eccentricities, L- and M-cone weights into parvocellular neurons are more consistent with the variability we observed with small horizontal cell receptive fields (Derrington et al., 1984; Sun et al., 2006). This finding suggests that the receptive fields of foveal horizontal cells are in fact likely to be much smaller than those recorded in the periphery; consistent with the anatomy of these cells (Wässle et al., 1989, 2000) and the size of receptive field surrounds of parvocellular neurons measured from central locations Croner and Kaplan (1995).

Impact of network density

Anatomical descriptions of horizontal cells indicate that the density of connections in the networks of H1 and H2 cells may differ (Dacey et al., 1996; Wässle et al., 1989, 2000; Chan

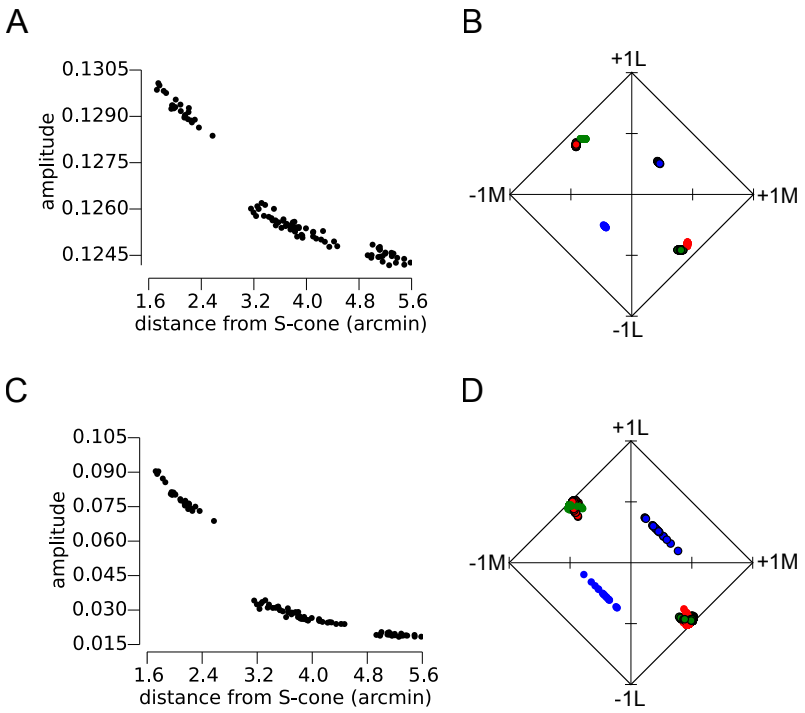

Figure 6.5: The dependence of cone weights on horizontal cell spatial receptive field. **A&B**. Horizontal cells with large spatial receptive fields are assumed. The amplitude of light evoked signal in response to an S-cone isolating stimulus was computed for 100 nodes in the H2 network and plotted as a function of that node from the nearest S-cone (**A**). There was substantial through out the H2 network with these parameters. **B**. Shows cone weights computed for bipolar cells in this model. Red dots represent L-cone centers, green=M-cone centers and blue dots indicate S-cone center bipolar cells. **C&D**. Same analysis but with much narrower spatial profile of horizontal cells. **C**. Significant S-cone signal is confined to H2 cells close to an S-cone. **D**. Same as **B** for the narrower horizontal cell receptive fields.

and Grünert, 1998). Both the number of cell bodies and the number of processes extended by H1 cells is higher than H2 cells. The consequence of a lower density of connections between H2 cells and the cone mosaic is that the electrical distance between any two cones will not always reflect their physical distance from one another. Because horizontal cells use passive conductance, two cones may occasionally be located next to each other but have less influence, via the H2 network, on one another than would be predicted by a denser network that supported the shortest path between each cone. We considered the potential impact of a lower density of processes in the H2 network by randomly eliminating connections between cones (i.e removing edges in Fig. 6.1).

Analysis of this less dense retinal network revealed fewer L/M-cone terminals receive S-cone input. Only a small smattering (11/100) of simulated cells, positioned close to an S-cones, received considerable input from S-cones (Fig. 6.6A). Importantly, roughly half the cells positioned close to an S-cone do not receive substantial S-cone input. This change in S-cone influence is also reflected in the cone weights (Fig. 6.6A). Compared to the previous example (Figure. 6.5), the majority of points fall on the edge of the diamond – indicating little influence from S-cones. Qualitatively, this plot resembles the population of LGN neurons reported by Tailby et al. (2008b) (their Fig 3B). Therefore, network density may be an important factor when considering the propagation of cone specific signals.

Impact of cone mosaic structure

The influence of the cone mosaic on color vision has drawn the attention of scientists for many decades (Williams et al., 1981b,a; Williams and Coletta, 1987; Williams et al., 1991; Roorda and Williams, 1999; Cicerone and Nerger, 1989; Carroll et al., 2002; Brainard et al., 2000; Neitz et al., 2002; Hofer et al., 2005b; Brainard, 2015). The advent of adaptive optics microscopy (Williams, 2011) and the ability to image and stimulate single cones in the living human retina have brought the fine structure of the cone mosaic into consideration once

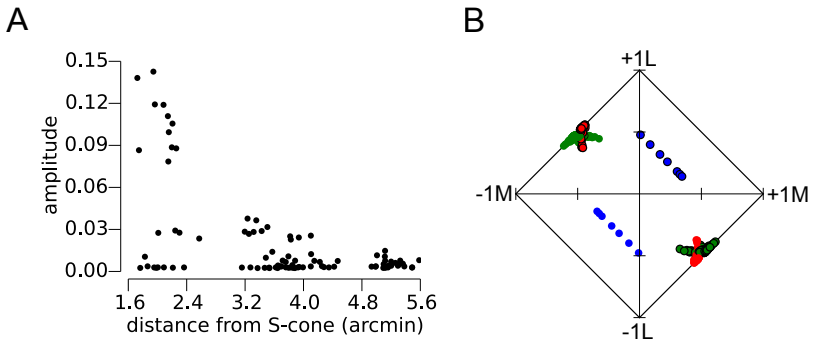

Figure 6.6: Cone inputs with a sparse H2 network. Same analysis as Fig. 6.5 for an H2 network with a lower density of connections between each node.

again (Sincich et al., 2015; Brainard, 2015). Our customizable model of the outer retina offers a simple and efficient manner for simulating responses in individual cone mosaics and propagating those signals through a population of retinal cells. The chromatic signature of modeled bipolar cells were computed for a cone mosaic measured with adaptive optics in Fig.6.7A-C (data from Sabesan et al. (2015a)). This methodology could be useful in predicting the appearance of small spots delivered to classified retinas such as the one shown here. Below we explore how parameters of the cone mosaic might influence chromatic processing in the post-synaptic circuitry using synthetic mosaics.

L:M cone ratio is known to vary widely between individuals (Carroll et al., 2002; Hofer et al., 2005a). However, the impact of L:M cone ratio on color perception is small and predominantly effects the perception of greenish appearing middle wavelengths (Neitz et al., 2002; Schmidt et al., 2014; Brainard, 2015). A previous modeling effort reported L:M ratio did not cause significant changes in LGN cone weights (Lennie et al., 1991). We changed the mosaic structure to study its potential impact on spectrally opponent cells. Changing the L:M cone ratio from 1:1 to 2:1 did not result in substantial changes in cone weights (Fig. 6.7D-

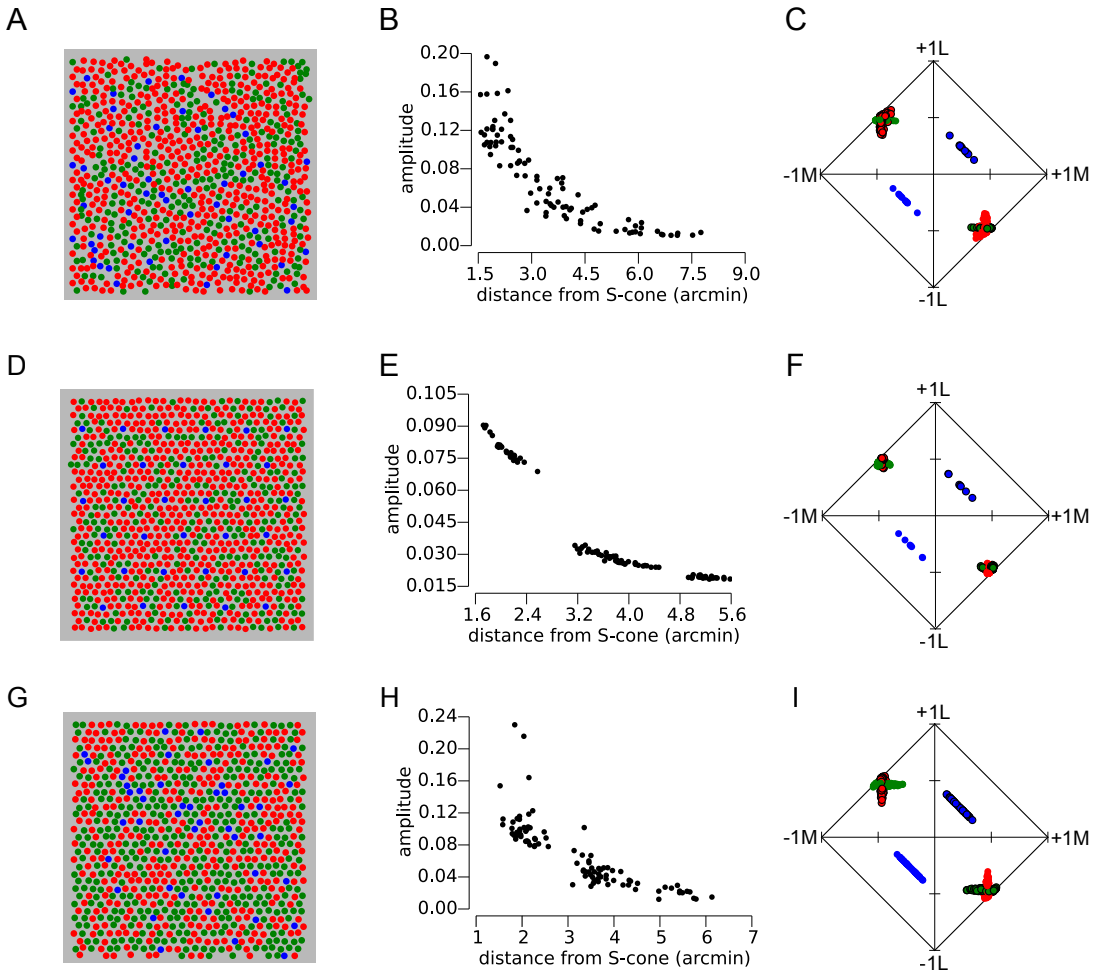

Figure 6.7: The influence of cone mosaic structure on cone weights. Cone weights were studied for three different mosaic structures. **A-C**. A mosaic measured with adaptive optics and densitometry. Analyses otherwise were the same as Fig. 6.5. **D-F**. A mosaic with 4% S-cones and an L:M ratio of 2:1. **G-I**. A mosaic containing 4% S-cones that were randomly distributed and an L:M ratio of 1:1.

F). The propagation of S-cone signals (Fig. 6.7E) was identical to Fig. 6.5F because the only difference between these two models are the L/M cone submosaics. Therefore, the impact of doubling the L:M cone ratio on the color information carried across the population of parvocellular neurons was subtle and reflected the small influence this parameter exerts on color appearance.

Near the fovea the spatial arrangement of S-cones becomes disorderly and indistinguishable from a random distribution (Curcio et al., 1991). We tested the potential influence of a random S-cone mosaic on outer retinal chromatic signaling. The results of this experiment are shown in Fig.6.7G-I. In a small number of cells (4/100), we observed large amplitude responses to S-cone isolating stimuli (Fig.6.7H). These cells resided near multiple S-cones. Due to the increased scatter of S-cone amplitudes, cone weights were also more varied than the cone weights computed from otherwise identical parameters (compare Fig.6.5G to Fig.6.7H). In particular, a small number of L/M-cone center bipolar cells fell further from the edge of the diamond (Fig.6.7H) compared to the non-random S-mosaic (Fig.6.5G), indicating significant S-cone input.

Impact of spatial structure in the stimulus

Finally, we studied the interaction between the spatial content of the stimulus and the organization of the retinal mosaic. For this analysis we used the same mosaic structure and parameters as Fig. 6.7G-I. The influence of spatial structure on S-cone signals of theoretical bipolar cells is shown in Fig. 6.8. Compared to the same model measured with full-field, uniform lights (Fig. 6.7H), a 5 cycles/degree grating produced more restricted propagation of S-cone driven signals. These results suggest that spatial structure of light impinging upon the eye could have an important relationship with the manner in which cone specific signals routinely propagate through the horizontal cell network and influence downstream neurons. Importantly, natural scenes obey specific spatial characteristics (Dong and Atick, 1995; Atick

and Redlich, 1992; Wachtler et al., 2001; Field, 1987). Therefore, the structure of light falling on the retina should have important consequences for the algorithm used by the brain to classify cells as chromatic or achromatic (Wachtler et al., 2007; Brainard et al., 2008).

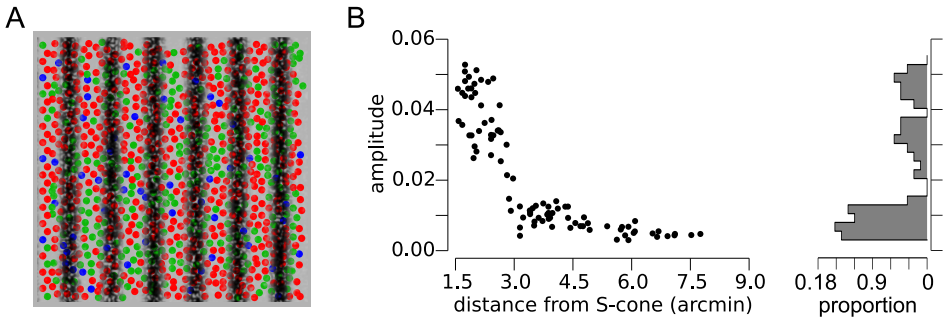

Figure 6.8: Spatial and temporal dependence of S-cone signal. An S-cone isolating grating of 5 cycles/degree was shown to the model mosaic in **A**. The amplitude of signals in H2 horizontal cells elicited by the S-isolating stimulus is recorded in **B**.

6.5 Discussion

We studied the influence horizontal cells impose on neural processing of light evoked signals in the context of color vision. Historically, unraveling the role of horizontal cells in vision has proven challenging because of the difficulty inherent in selectively modulating their activity in a behaving animal. Our motivation was to consider plausible horizontal cell networks and ask how the parameters of that model would influence color coding in the primate retina. Below we discuss our results in the context of what is know about horizontal cell physiology, the implications for color vision and the insight these studies offer for night blindness.

Horizontal cell physiology

As far as we are aware, our model represents the first time both H1 and H2 cell networks have been modeled simultaneously (Fig. 6.2). We found the connectivity patterns of these different cell types generated very different requirements for the conductances between cones and horizontal cells. Because H2 cells make fewer contacts with L- and M-cones, which make up the bulk of cones in primate mosaics, there is overall less excitatory drive into the H2 network. To compensate for this loss of excitation, we had to increase the conductance of cones, g_P, into the H2 network relative to the H1 network by roughly a factor of 10 (Table 6.1). The ratio of this parameter to the horizontal cell conductance, g_H, controls the spatial constant, or receptive field size, of the horizontal cells. The time constant of the horizontal network is also influenced by g_P and without a large increase in g_P, the time constant of the H2 cells becomes unrealistically slow. Therefore, while we did not systematically study the parameter space of our models, the results point to an important difference between H1 and H2 cells: the conductance between cones and H2 cells is higher relative to H1 cells. Uncovering the biological mechanism of this gain scaling should be an important goal for future experimental studies.

After settling on a set of parameters that reproduced the reported dynamics in the two horizontal cell networks we explored variations in known anatomical characteristics of these cells. The distribution and morphology of horizontal cells changes across the retina. The highest density of horizontal cells is in the central retina (Wässle et al., 1989; Chan and Grünert, 1998) where cone density is also highest (Curcio et al., 1990). The subtleties of this anatomical dependence on eccentricity also differs between H1 and H2 cells. Out to about 6 mm from the fovea, H1 cell are found at a higher density relative to H2 cells (Wässle et al., 1989). The size of each horizontal cell dendritic field also varies as a function of eccentricity (Packer and Dacey, 2002; Rodieck, 1998; Wässle et al., 1989). In the central retina, the dendritic trees of both H1 and H2 cells are small, contacting only a handful of nearby cones

(Wässle et al., 1989). The size of the spatial receptive fields of H1 and H2 cells also differ (Zhang et al., 2011).

We modeled the impact of these changes with eccentricity. We found that narrow receptive fields were necessary to account for the distribution of cone responses that would be expected based on cone inputs measured in macaque retinal (Sun et al., 2006) and LGN neurons (Derrington et al., 1984; Reid and Shapley, 2002; Tailby et al., 2008b). Indeed, a prior study of cone inputs to LGN cells reported a similar relationship with cone weight distribution and the space constant of the surround (Lennie et al., 1991). This conclusion is further supported by a quantitative analysis of L- and M-cone inputs to H1 cells. Dacey et al. (2000b) found large variability in the weights of each cone-type into the H1 cells that additionally varied predictably with eccentricity (Hagstrom et al., 2000). Together this evidence led to the hypothesis that H1 cells reflect the relative numerosity of cones in local regions of the retina. On the other hand if receptive fields were in fact large, the variability of cone weights into H1 cells should be very low in H1 cells from the same retinal region (Fig. 6.5A-B).

Horizontal cells are electrically coupled to cells of the same type through gap junctions (Zhang et al., 2011; Wässle et al., 2000; Chan and Grünert, 1998; Dacey et al., 1996). In fact, the degree to which they are coupled via gap junction has been hypothesized to underlie the difference in spatial receptive field size between H1 and H2 cells (Zhang et al., 2011). The potential role of gap junctions in primate outer retina on visual processing has been studied with models of cone mosaics (Hsu et al., 2000) and horizontal cells (Packer and Dacey, 2005). In the case of electrical coupling between primate horizontal cells, gap junctions are thought to introduce a second component – with a conductance distinct from the cable properties of the cells dendrites – to the receptive field that extends its spatial extent. Packer and Dacey (2005) further argued this extension added by gap junctions produced the irregularities in spatial tuning curves that they observed in some cells. Here, we assumed a simplified

continuous resistive sheet producing only a single exponentially decaying spatial receptive field (Naka and Rushton, 1967). We found that peculiarities of spacing in the cone mosaic could also contribute to irregularities observed in measured spatial frequency tuning curve (Packer and Dacey, 2005). A pure exponential receptive field would produce a perfectly smooth tuning curve. However, even in the averages shown from our models in Fig. 6.3 a hint of irregularity can be seen that is attributable to the variability in distances between neighboring cones.

The mechanism and site of horizontal cell feedback has been a source of some controversy (Hirasawa et al., 2012). Recordings from L-, M-, and S-cone terminals in monkey have revealed at least some surround antagonism is present in the cones themselves (Packer et al., 2010; Verweij et al., 2003). A second site of horizontal cell action that has persisted in the literature for many decades, but has yet to be demonstrated definitively, is a feed-forward pathway directly onto the dendritic tips of bipolar cells (Thoreson and Mangel, 2012). Historically, the evidence for this pathway has largely come from non-primate species and the existence of such a pathway in primates has been considered dubious. However, recently, the machinery necessary to support a feed-forward pathway from H2 onto cone-bipolar cells was reported in humans and non-human primates (Puller et al., 2014a,b).

In the current model, we simplified the cone-horizontal cell synapse by keeping the activity of each separate. The influence of horizontal cells was introduced only in the bipolar cells, which took the difference of these signals. Future iterations of the model will explicitly model the feedback and potential feedforward pathways of the horizontal cell network. The addition of a feedfoward pathway would serve to strengthen the surround inhibition of H2 cells and potentially add important temporal and spatial interactions between cones, bipolar cells and horizontal cells. It has been suggested that strong H1 feedback onto cone pedicles together with H2 feedforward signals into bipolar dendrites could create double opponency in the outer retina (Schmidt et al., 2014).

Kolb et al. (1997) has suggested that H2 cells do not reciprocate their signal onto L- and M-cones. The authors reason that if H2 do cells feedback, L/M-cone terminals should display S-cone opponency. Since H1 cells draw from L/M-cone terminals, an S-cone opponent signal should further be reflected in the signals of H1 cells. The consistent lack of S-opponent signal in H1 cells (Dacey et al., 1996, 2000b), they argue, offers indirect evidence that H2 cells do not feedback onto L- and M-cone terminals. Our results present one reason why H1 cells do not routinely exhibit S-opponency: S-cone driven signals in H2 cells does not propagate throughout the entire network. Only a minority of L/M-cones receive substantial S-cone input. Therefore, any S-opponent signal that might be recorded in H1 horizontal cells is swamped by the majority of L/M-cone input that does not receive S-cone signal.

Implications for night blindness

The current work focused on the propagation of S-cone signals in the outer retina. The neural circuitry that carries S-cone driven signals to the brain is distinct from that of the L- and M-cones (Calkins, 2001; Miyagishima et al., 2014). S-cone terminals are contacted by a bipolar cell that makes specific contacts with 2-3 S-cones in the fovea and avoid L- or M-cone terminals (Mariani, 1984). The S-cone bipolar cell then in turn makes robust excitatory contacts with the small bistratified ganglion cell (Calkins et al., 1998; Crook et al., 2009; Dacey and Lee, 1994), which is widely believed to serve as the retinal output of S-cone driven signals (Solomon and Lennie, 2007; Lee et al., 2010). The S-cone bipolar cell, like other ON-type bipolar cells, uses the metabotropic glutamate receptor, mGluR6, to invert the signal from hyperpolarized cone terminals – thus encoding an excitatory, ON-response, to decreased glutamate release. Application of the mGluR6 agonist L-AP4, completely abolishes the S-cone signal in small bistratified cells measured with whole cell electrophysiology (Crook et al., 2009). Since no other S-cone specific pathway has been firmly established in primate (Miyagishima et al., 2014), the absence of a functioning mGluR6 protein should produce

profound deficits in blue-yellow color vision, which is dependent upon S-cone signals.

A small group of individuals with mutations in the gene that codes for mGluR6, GRM6, have been identified. In response to light stimuli designed to isolate the ON pathway, electroretinograms confirm that signals from ON-bipolar cells are abolished in these individuals (Dryja et al., 2005). Clinically, mutations to GRM6 that result in dysfunctional mGluR6 protein are associated with incomplete congenital stationary night blindness (Zeitz et al., 2015). This behavioral deficit arises because rod photoreceptors make exclusive contacts with a rod specific ON-type bipolar cell. In the absence of rod signal, these individuals are unable to see under low light, rod mediated conditions. With no established OFF-bipolar cell specific to S-cones, a similar deficit was expected in S-cone mediated color vision. Paradoxically, the mutation in GRM6 does not produce measurable deficits in color vision. These subjects perform indistinguishably from controls on a wide range of color vision tests (Bijveld et al., 2013a; Dryja et al., 2005; Terasaki et al., 1999; Sergouniotis et al., 2012).

This finding suggests that S-cone signals are capable of exiting the retina through an alternative pathway that has yet to be characterized. Anatomical evidence has suggested an S-cone specific OFF bipolar cell may exist (Klug et al., 2003; Calkins, 2001), though these reports have been disputed (Neitz and Neitz, 2011) and physiological evidence is consistent with their absence (Evers and Gouras, 1986). Further, immunohistological double labeling of New World primate (marmoset) retina found OFF-midget bipolar cells avoided contact with S-cone terminals (Lee et al., 2005). Diffuse OFF-bipolar cells may make contacts with S-cones (Dacey et al., 2013). However, they indiscriminately sum input from L-, M- and S-cones. Therefore, they carry weak S-cone signals that are already mixed with L- and M-cone signals leaving them ill-suited to generate spectral opponency, even at higher centers in the brain.

Another potential route for S-cone signals to leave the retina, which we explored here, is through lateral inhibition via the H2 horizontal cell, which receives enhanced input from

S-cones relative to L- and M-cones (Dacey, 1996). Here we offered a second circuit capable of outputting S-cone signals in individuals with deficits in ON-bipolar signaling. Our model highlights the plausibility that a small group of L- and M-cones residing nearby an S-cone would receive enough S-cone driven signal to produce the necessary spectral opponency in L- and M-center midget pathways to preserve normal color vision in the absence of a normally functioning blue cone bipolar cell. The S-cone signal we described here would contribute to the surround of both ON and OFF midget pathways thus creating four distinct forms of spectral opponency: L-(M+S) producing a yellow signal in an L-ON center, (M+S)-L producing a blue signal in an L-OFF, M-(L+S) producing a green signal in a M-ON and (L+S)-M producing a red signal in an M-OFF center. H2 mediated propagation of S-cone signals into L/M OFF bipolar cells would be unaffected by a mutation to mGluR6. With disrupted signal between cones and ON bipolar cells, the S-cone signal could still reach the L/M-midget ON bipolar cells via cross-over inhibition from the OFF L/M-midget bipolar cells, which use ionotropic glutamate receptors and do not rely on mGluR6 (Euler et al., 2014). Another route for S-cone signals to reach L/M-midget ON bipolar cells is via the GABA mediated feedforward mechanism (Puller et al., 2014a,b), described above. In this circuit, the S-cone signal in H2 cells would be injected directly into the dendrites of both ON and OFF L/M-midget bipolar cells, bypassing the dysfunctional mGluR6 protein in the cone-to-ON-bipolar synapse.

Normal color processing

S-cone signals in central midget/parvocellular neurons have been carefully studied and are known to be rare (Sun et al., 2006; Derrington et al., 1984; Tailby et al., 2008b; Reid and Shapley, 2002; de Monasterio, 1978). Yet early reports from single units in primate retina routinely found a small population of cells, distinct from the S-(L+M) opponency of the small bistratified cell, that compared S, M and L cones as proposed here (de Monasterio, 1978;

de Monasterio et al., 1975). Recent recordings from a large number of macaque LGN neurons has also uncovered a small group of neurons with S-cone input on the order of magnitude suggested by our modeling results (Tailby et al., 2008a). Finally, S-cones signals in peripheral midget ganglion cells have also been reported by Field et al. (2010). The pathway through which S-cones traveled to generate the reported cone inputs is not know. We report here the possibility of a pathway that would be expected to produce measurable, but modest S-cone input in a small minority (perhaps 2-10%) of midget bipolar cells. We estimate the weight of S-cone input would be in the range of 10-20%, which is all that is necessary to produce cells that would be well situated to code for hue percepts (Schmidt et al., 2014). We further noted parameters of the outer retina that would influence the weights and relative numerosity of these S-opponent midget pathways.

Figure 6.9 demonstrates the spectral sensitivity of modeled cells that received modest S-cone input. The cone fundamentals (Stockman and Sharpe, 2000) were weighted according to values obtained from cone isolating stimuli and reflect the values for modeled cells that received S-cone input. For instance the small population of L- and M-center midget cells in Fig. 6.6 received modest S-cone input from the surround of about 15%. The resulting spectral sensitivity functions for those L- and M-cone center ON midget ganglion cell are shown in Fig. 6.9B and Fig. 6.9C, respectively. The L-center cell was inhibited by short wavelengths and excited by longer wavelengths with a null point at 511 nm – the wavelength most observers see as purely green (Kuehni, 2004) – making it ideally suited to code for yellow. The M-center midget was excited by middle wavelengths but was inhibited by short and long wavelengths – making it a plausible substrate for green percepts. The null points of this dichromatic system were 472 and 579 nm, which correspond to the wavelengths most observers see as purely blue and yellow. Analogous OFF-center midget cells would produce inverted functions that could mediate blue and red hue percepts. Therefore this small group of cells is well matched with human hue perception (Schmidt et al., 2014).

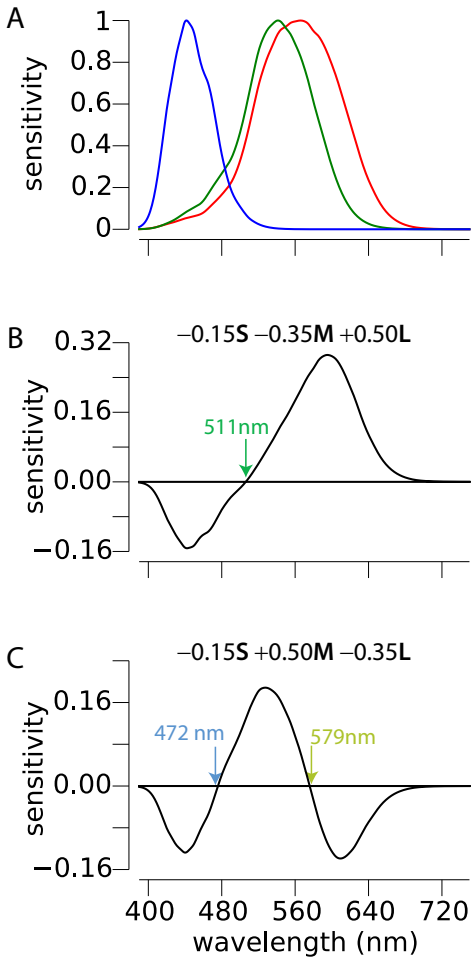

Figure 6.9: Theoretical spectral sensitivity functions of midget ganglion cells with S-cone input. **A**. S-, M- and L-cone fundamentals normalized to peak at one (Stockman and Sharpe, 2000). **B**. An L-center ganglion cell that received M- and S-cone inhibition via horizontal cells. The null point of this theoretical cell makes it well matched with the human blue-yellow sensitivity function. **C**. An M-center ganglion cell that received L- and S-cone inhibition. The two null points of this cell make it suited to code for red and green percepts.

However, the idea that a majority of midget ganglion cells, with measurable L-M spectral opponency, contribute to a black/white pathway is on the surface untenable (De Valois and De Valois, 1993). The notion that all cells containing spectral opponency participate in color processing is inherent in almost every study of color processing. Yet, most parvocellular neurons often confuse red/green spots with black/white edges leaving them poorly suited to code for color appearance (Wiesel and Hubel, 1966). The L-M opponency carried by these cells does, however, likely contribute to chromatic detection (Eskew, 2009). As for color appearance, we propose here that a combination of spatial structure in the input (Fig. 6.8), lower density of H2 network (Fig. 6.6) and irregularities of S-cone mosaic (Fig. 6.7D-I) could give rise to a small population of parvocellular neurons that would receive S-cone input and be ideally suited to signal color. The fact that parvocellular neurons provide robust projections to the ventral stream would allow higher cortical areas to categorize the output of these neurons as chromatic or achromatic based on experience. Learning which cells most reliably signal hue as opposed to those that confuse hue with black/white edges could be achieved with a cortical learning algorithm similar to the one proposed by Brainard et al. (2008). The majority of parvocellular neurons would provide a pathway for high resolution black and white, while activity of small few would elicit red, green, blue or yellow.

Chapter 7

CONCLUSIONS

The salience of color in our visual experience has inspired curiosity about how color is constructed in the mind for centuries. Modern techniques of neuroscience have resolved many features of the neural circuitry, but the story of color science continues to be written. The importance of understanding this neural code extends beyond the mysteries of hue. To borrow from the keen eye of John Mollon, "It is clear that if we understood the status of unique hues we should probably understand something useful about the general question of neural representation and its relationship to conscious experience" (Mollon and Jordan, 1997).

The prevailing theories of color representation in the retina nearly unanimously focus on the small bistratified ganglion cell (SBC) and midget ganglion cell (MGC) pathways. Throughout this work I have detailed many outstanding issues with theories based around these cell types. Some of these issues have been noted before. Others, such as the provocative finding that individuals with abnormal SBC circuits experience normal color vision, were considered in detail here for the first time.

More than merely taking issue with established thought, the work contained in this document developed and examined an alternative framework for considering color vision. The most notable features of this framework are: (1) The notion that conscious experience of color is part of an evolutionarily recent specialization of the primate brain primarily concerned with the recognition of objects – a capacity that far outstrips related systems in other animals. (2) On the other hand, the SBC is part of an ancient system that converses primarily with the oldest centers of our brain. The spectral sensitivity of these cells predict a role in color

appearance, but experimental results do not agree with this prediction. Presumably, the anatomical connectivity of SBCs evolved for a purpose distinct from the conscious perception of color.

(3) Midget ganglion cells, the dominant source of input to the object recognition centers of the ventral visual stream, mediate a high resolution, black/white pathway. The L-M cone opponency carried by this pathway provides spectral information that might be useful for tasks requiring chromatic discriminations. However, the color appearance of visible light is not determined by these cells. (4) The essential computations necessary for color sensation are computed by just a small subset of midget ganglion cells that receive a modest input from S-cones. (5) The brain learns through experience which midget ganglion cells most reliably indicate the color of objects in the world. Other cells, that are less selective in chromaticity space, are categorized as white and reflect the average distribution of spectra in the environment. This assertion provides a parsimonious explanation for the rapid adoption of trichromacy in primates both during evolution and after introduction of novel photopigments in the laboratory.

Throughout this document I have reported evidence from numerous experimental and theoretical paradigms to support these claims. I first developed a mathematical model that made predictions about the appearance of visible light based on a theorized circuitry. The most surprising of these predictions was that the experience of middle wavelengths should dependent upon the ratio of L- and M-cones, while the appearance of shorter and longer wavelengths should be less so. Here I reported that carefully measured color appearance data supported this prediction in a group of fourteen subjects with measured L:M ratios.

The idea that only a subset of MGCs participate in hue perception implies that the brain disregards the spectral information in the signals of other MGCs when assigning color to objects. This notion is untenable to many who have considered the problem of color. However, I described results from single cone studies which were consistent with this idea.

The majority of cones reliably produced the sensation of white, while only a minority (about 25%) reported repeatable hue percepts. Black and white vision has long been recognized as higher resolution than either of our two color subsystems. MGCs are necessary to account for our achromatic visual acuity and the results from single cone studies were consistent with the hypothesis that the brain relies on only a subset of midget ganglion cells to assign color to objects.

I also presented evidence that M-cones participate in the sensation of blue not yellow – another important prediction of the framework examined here. Modern color scientist routinely point out that the axes of color neurons early in the visual pathway do not align with the content of our visual experience. Specifically, it is often asserted that signals from the SBC must be combined in unknown proportions with the signals from the midget ganglion cells to account for color appearance. Yet the fundamental implication of this observation – that M-cones drive the sensation of blue, not yellow – remains under-appreciated, even by those pointing out the failure of the SBC model. The work here has been explicit about this point. Beginning with a theory principled with known entities in the retina, I theorized a neural circuit capable of bring together S- and M-cone signals that is both simple and experimentally falsifiable. Subsequent chapters tested predictions of this model. In perhaps the most convincing demonstration to date, targeted stimulation of single cones was used to elicit color sensations. This work provided direct evidence of M-cones participation in the sensation of blue and challenged the idea that the SBC mediates this sensation.

Finally, I described a model of the neural circuits that constitute the outer retina in monkey and man. Through an exploration of the parameters of this model I described how a relatively small, but physiologically significant signal from S-cones might plausibly find its way into a subset of MGC circuits. The expectedly modest S-cone signal and relatively small number of such cells provided an explanation for why others have not routinely observed such cells.

Yet the success of this work was not without flaws. In my estimation, the most glaringly unresolved issue facing this theory is the lack of physiological evidence to support the modeling and psychophysical results described in this document. Our lab has begun to address this critical issue with *in vitro* recordings from primate retina. A central focus of this work will be unraveling the contribution of H2 horizontal cells to visual processing.

Secondly, future work will need to relate this color theory with more complex visual scenes that define the ethological relevance of color vision. Similarly, the relationship between the retinal neurons examined here and higher order neurons, often suggested to play a role in complex color tasks, needs to be resolved. Dating back to the classic work of Semir Zeki, workers in extra-striate visual areas have regularly reported cells with sharp color tunings, distinct from the opponent cells common in earlier areas. The importance of these cells in color vision and their relationship to the retinal circuits probed here are both outstanding issues. One possibility is that the color tuned neurons of V4, for instance, are red herrings, whose primary concern is with other features of the visual scene. Another possibility is that the features of relatively primitive color appearance tasks – monocular small spot experiments, single wavelength studies, etc – that are nicely predicted by the output of retinal circuits do not engage these higher-order neurons. This would imply that both cells are important for a complete understanding of color vision.

In any event, the enigmatic relationship between color preferring neurons, both retinal and cortical, and the complex tasks of judging hue, saturation and lightness in scenes composed of objects at various distances, positioned in shadow and relief, and reflecting the light from an ever changing illuminant should continue to tease curious minds for some time to come.

REFERENCES

Abney, W. (1909). On the change in hue of spectrum colours by dilution with white light. *Proceedings of the Royal Society of London. Series A.*, 83(560):120–127.

Abramov, I. and Gordon, J. (1994). Color appearance: on seeing red - or yellow, or green, or blue. *Annual Review of Psychology*, 45:451–85.

Abramov, I. and Gordon, J. (2005). Seeing unique hues. *Journal of the Optical Society of America. A*, 22(10):2143–53.

Abramov, I., Gordon, J., and Chan, H. (1991). Color appearance in the peripheral retina: effects of stimulus size. *Journal of the Optical Society of America. A*, 8(2):404–14.

Ahnelt, P. and Kolb, H. (1994a). Horizontal cells and cone photoreceptors in human retina: a Golgi-electron microscopic study of spectral connectivity. *Journal of Comparative Neurology*, 343(3):406–27.

Ahnelt, P. and Kolb, H. (1994b). Horizontal cells and cone photoreceptors in primate retina: a Golgi-light microscopic study of spectral connectivity. *Journal of Comparative Neurology*, 343(3):387–405.

Aho, A. C., Donner, K., Hyden, C., O, L. L., and T, R. (1988). Low retinal noise in animals with low body temperature allows high visual sensitivity. *Nature*, 334:348–350.

Albers, J. (2013). *Interaction of color*. Yale University Press, New Haven, 4th edition.

Anstis, S. (2006). White's effect in lightness, color and motion. In Harris, L. and Jenkins, M., editors, *Seeing spatial form*, chapter 1. Oxford University Press, Oxford, UK.

Arathorn, D. W., Yang, Q., Vogel, C. R., Zhang, Y., Tiruveedhula, P., and Roorda, A. (2007). Retinally stabilized cone-targeted stimulus delivery. *Optics Express*, 15(21):13731–44.

Asenjo, A. B., Rim, J., and Oprian, D. D. (1994). Molecular determinants of human red/green color discrimination. *Neuron*, 12(5):1131–8.

Atick, J. J. and Redlich, A. N. (1992). What does the retina know about natural scenes? *Neural Computation*, 210:196–210.

Avant, L. L. (1965). Vision in the Ganzfeld. *Psychological Bulletin*, 64(4):246–258.

Ayama, M., Nakatsue, T., and Kaiser, P. K. (1987). Constant hue loci of unique and binary balanced hues at 10, 100, and 1000 Td. *Journal of the Optical Society of America. A*, 4(6):1136–44.

Baker, P. M. and Bair, W. (2012). Inter-Neuronal Correlation Distinguishes Mechanisms of Direction Selectivity in Cortical Circuit Models. *The Journal of Neuroscience*, 32(26):8800–8816.

Bayer, F. S., Paulun, V. C., Weiss, D., and Gegenfurtner, K. R. (2015). A tetrachromatic display for the spatiotemporal control of rod and cone stimulation. *Journal of Vision*, 15(11):1–16.

Baylor, D. A. (1987). Photoreceptor Signals and Vision. Proctor lecture. *Investigative Ophthalmology & Visual Science*, 28(1):34–49.

Baylor, D. A., Fuortes, M. G. F., and O'Bryan, P. M. (1971). Receptive fields of cones in the retina of the turtle. *Journal of Physiology*, 214:265–294.

Behnia, R. and Desplan, C. (2015). Visual circuits in flies: beginning to see the whole picture. *Current Opinion in Neurobiology*, 34:125–132.

Belmore, S. C. and Shevell, S. K. (2008). Very-long-term chromatic adaptation : Test of gain theory and a new method. *Visual Neuroscience*, 25:411–414.

Benardete, E. A. and Kaplan, E. (1997). The receptive field of the primate P retinal ganglion cell, I: Linear dynamics. *Visual Neuroscience*, 14(1):169–85.

Benardete, E. A. and Kaplan, E. (1999). Dynamics of primate P retinal ganglion cells: responses to chromatic and achromatic stimuli. *Journal of Physiology*, 519 Pt 3:775–90.

Benson, N. C., Manning, J. R., and Brainard, D. H. (2014). Unsupervised learning of cone spectral classes from natural images. *PLoS Computational Biology*, 10(6):e1003652.

Bijveld, M. M. C., Florijn, R. J., Bergen, A. a. B., van den Born, L. I., Kamermans, M., Prick, L., Riemslag, F. C. C., van Schooneveld, M. J., Kappers, A. M. L., and van Genderen, M. M. (2013a). Genotype and phenotype of 101 dutch patients with congenital stationary night blindness. *Ophthalmology*, 120(10):2072–81.

Bijveld, M. M. C., van Genderen, M. M., Hoeben, F. P., Katzin, A., van Nispen, R. M. A., Riemslag, F. C. C., and Kappers, A. M. L. (2013b). Assessment of night vision problems in patients with congenital stationary night blindness. *PLoS ONE*, 8(5):e62927.

Bok, M., Porter, M., Place, A., and Cronin, T. (2014). Biological Sunscreens Tune Polychromatic Ultraviolet Vision in Mantis Shrimp. *Current Biology*, pages 1–7.

Bosten, J. M. and Boehm, A. E. (2014). Empirical evidence for unique hues? *Journal of the Optical Society of America A*, 31(4):A385.

Bosten, J. M. and Lawrance-Owen, A. J. (2014). No difference in variability of unique hue selections and binary hue selections. *Journal of the Optical Society of America A*, 31(4):357–364.

Bowmaker, J. K., Heath, L. A., Wilkie, S. E., and Hunt, D. M. (1997). Visual pigments and oil droplets from six classes of photoreceptor in the retinas of birds. *Vision Research*, 37(16):2183–2194.

Boycott, B. and Wässle, H. (1999). Parallel Processing in the Mammalian Retina The Proctor Lecture. *Investigative Ophthalmology & Visual Science*, 40(7).

Boycott, B. B., Dowling, J. E., and Kolb, H. (1969). Organization of the primate retina: light microscopy. *Philosophical Transactions of the Royal Society of London. B*, 255:110–181.

Boycott, B. B. and Wässle, H. (1991). Morphological Classification of Bipolar Cells of the Primate Retina. *European Journal of Neuroscience*, 3:1069–1088.

Brainard, D. H. (2015). Color and the Cone Mosaic. *Annual Review of Vision Science*, 1:1–28.

Brainard, D. H., Roorda, A., Yamauchi, Y., Calderone, J. B., Metha, A., Neitz, M., Neitz, J., Williams, D. R., and Jacobs, G. H. (2000). Functional consequences of the relative numbers of L and M cones. *Journal of the Optical Society of America. A*, 17(3):607–14.

Brainard, D. H. and Stockman, A. (2010). Colorimetry. In Bass, M., editor, *Vision and Vision Optics*, chapter 10, pages 1–56. McGraw-Hill, New York, 3 edition.

Brainard, D. H. and Williams, D. R. (1993). Spatial reconstruction of signals from short-wavelength cones. *Vision Research*, 33(1):105–116.

Brainard, D. H., Williams, D. R., and Hofer, H. (2008). Trichromatic reconstruction from the interleaved cone mosaic: Bayesian model and the color appearance of small spots. *Journal of Vision*, 8(5):1–23.

Bruce, K. S., Harmening, W. M., Langston, B. R., Tuten, W. S., Roorda, A., and Sincich, L. C. (2015). Normal Perceptual Sensitivity Arising From Weakly Reflective Cone Photoreceptors. *Investigative Ophthalmology & Visual Science*, 56(8):4431.

Buzás, P., Blessing, E. M., Szmajda, B. A., and Martin, P. R. (2006). Specificity of M and L cone inputs to receptive fields in the parvocellular pathway: random wiring with functional bias. *The Journal of Neuroscience*, 26(43):11148–61.

Caine, N. G. and Mundy, N. I. (2000). Demonstration of a foraging advantage for trichromatic marmosets (Callithrix geoffroyi) dependent on food colour. *Proceedings of the Royal Society of London. Series B.*, 267(1442):439–444.

Calkins, D. J. (2000). Representation of cone signals in the primate retina. *Journal of the Optical Society of America A*, 17(3):597.

Calkins, D. J. (2001). Seeing with S cones. *Progress in retinal and eye research*, 20(3):255–87.

Calkins, D. J. and Sterling, P. (1996). Absence of spectrally specific lateral inputs to midget ganglion cells in primate retina. *Nature*, 381:613–615.

Calkins, D. J. and Sterling, P. (1999). Evidence that circuits for spatial and color vision segregate at the first retinal synapse. *Neuron*, 24(2):313–21.

Calkins, D. J., Tsukamoto, Y., and Sterling, P. (1998). Microcircuitry and mosaic of a blue-yellow ganglion cell in the primate retina. *The Journal of Neuroscience*, 18(9):3373–85.

Cao, L.-H., Luo, D.-G., and Yau, K.-W. (2014). Light responses of primate and other mammalian cones. *Proceedings of the National Academy of Sciences of the United States of America*, 111(7):2752–7.

Carandini, M. and Heeger, D. (2012). Normalization as a canonical neural computation. *Nature Reviews. Neuroscience*, 13:51–62.

Carroll, J., McMahon, C., Neitz, M., and Neitz, J. (2000). Flicker-photometric electroretinogram estimates of L:M cone photoreceptor ratio in men with photopigment spectra derived from genetics. *Journal of the Optical Society of America. A*, 17(3):499–509.

Carroll, J., Neitz, J., and Neitz, M. (2002). Estimates of L:M cone ratio from ERG flicker photometry and genetics. *Journal of Vision*, 2(8):531–542.

Chan, T. L. and Grünert, U. (1998). Horizontal cell connections with short wavelength-sensitive cones in the retina: a comparison between New World and Old World primates. *Journal of Comparative Neurology*, 393(2):196–209.

Chatterjee, S. and Callaway, E. M. (2003). Parallel colour-opponent pathways to primary visual cortex. *Nature*, 426(6967):668–71.

Chen, S. and Li, W. (2012). A color-coding amacrine cell may provide a blue-Off signal in a mammalian retina. *Nature Neuroscience*, 15(7):954–6.

Chichilnisky, E. J. and Wandell, B. A. (1995). Photoreceptor sensitivity changes explain color appearance shifts induced by large uniform backgrounds in dichoptic matching. *Vision Research*, 35(2):239–254.

Cicerone, C. M. and Nerger, J. L. (1989). The relative numbers of long-wavelength-sensitive to middle-wavelength-sensitive cones in the human fovea centralis. *Vision Research*, 29(1):115–28.

Cleland, B. G., Dubin, M. W., and Levick, W. R. (1971). Simultaneous recording of input and output of lateral geniculate neurones. *Nature: New biology*, 231(23):191–192.

Conway, B. R. (2001). Spatial structure of cone inputs to color cells in alert macaque primary visual cortex (V-1). *The Journal of Neuroscience*, 21(8):2768–83.

Conway, B. R. (2009). Color vision, cones, and color-coding in the cortex. *The Neuroscientist*, 15(3):274–90.

Conway, B. R. (2013). Color signals through dorsal and ventral visual pathways. *Visual Neuroscience*, pages 1–13.

Conway, B. R. and Livingstone, M. S. (2006). Spatial and temporal properties of cone signals in alert macaque primary visual cortex. *The Journal of Neuroscience*, 26(42):10826–46.

Conway, B. R., Moeller, S., and Tsao, D. Y. (2007). Specialized color modules in macaque extrastriate cortex. *Neuron*, 56(3):560–73.

Crognale, M. A., Webster, M. A., and Fong, A. Y. (2009). Application of digital micromirror devices to vision science: shaping the spectrum of stimuli. *Proceedings of SPIE*, 7210:7210–4.

Croner, L. J. and Kaplan, E. (1995). Receptive fields of P and M ganglion cells across the primate retina. *Vision Research*, 35(1):7–24.

Cronin, T. W. and Marshall, J. N. (1989). A retina with at least ten spectral types of photoreceptors in a mantis shrimp. *Nature*, 339:137–140.

Crook, J. D., Davenport, C. M., Peterson, B. B., Packer, O. S., Detwiler, P. B., and Dacey, D. M. (2009). Parallel ON and OFF cone bipolar inputs establish spatially coextensive receptive field structure of blue-yellow ganglion cells in primate retina. *The Journal of Neuroscience*, 29(26):8372–87.

Crook, J. D., Manookin, M. B., Packer, O. S., and Dacey, D. M. (2011). Horizontal cell feedback without cone type-selective inhibition mediates "red-green" color opponency in midget ganglion cells of the primate retina. *The Journal of Neuroscience*, 31(5):1762–72.

Curcio, C. A., Allen, K. A., Sloan, K. R., Lerea, C. L., Hurley, J. B., Klock, I. B., and Milam, A. H. (1991). Distribution and morphology of human cone photoreceptors stained with anti-blue opsin. *Journal of Comparative Neurology*, 312:610–624.

Curcio, C. A., Sloan, K. R., Kalina, R. E., and Hendrickson, A. E. (1990). Human photoreceptor topography. *Journal of Comparative Neurology*, 292(4):497–523.

Dacey, D., Packer, O. S., Diller, L., Brainard, D., Peterson, B., and Lee, B. (2000a). Center surround receptive field structure of cone bipolar cells in primate retina. *Vision Research*, 40(14):1801–11.

Dacey, D. M. (1994). Physiology, morphology and spatial densities of identified ganglion cell types in primate retina. In *Higher-order processing in the visual system.*

Dacey, D. M. (1996). Circuitry for color coding in the primate retina. *Proceedings of the National Academy of Sciences of the United States of America*, 93:582–588.

Dacey, D. M., Crook, J. D., and Packer, O. S. (2013). Distinct synaptic mechanisms create parallel S-ON and S-OFF color opponent pathways in the primate retina. *Visual Neuroscience*, pages 1–13.

Dacey, D. M., Diller, L. C., Verweij, J., and Williams, D. R. (2000b). Physiology of L- and M-cone inputs to H1 horizontal cells in the primate retina. *Journal of the Optical Society of America. A*, 17(3):589–96.

Dacey, D. M. and Lee, B. B. (1994). The 'blue-on' opponent pathway in primate retina originates from a distinct bistratified ganglion cell type. *Nature*, 367:731–735.

Dacey, D. M., Lee, B. B., Stafford, D. K., Pokorny, J., and Smith, V. C. (1996). Horizontal cells of the primate retina: cone specificity without spectral opponency. *Science*, 271(5249):656–9.

Dacey, D. M., Liao, H.-W., Peterson, B. B., Robinson, F. R., Smith, V. C., Pokorny, J., Yau, K.-W., and Gamlin, P. D. (2005). Melanopsin-expressing ganglion cells in primate retina signal colour and irradiance and project to the LGN. *Nature*, 433:749–754.

Dacey, D. M. and Packer, O. S. (2003). Colour coding in the primate retina: diverse cell types and cone-specific circuitry. *Current Opinion in Neurobiology*, 13(4):421–427.

Dacey, D. M. and Petersen, M. R. (1992). Dendritic field size and morphology of midget and parasol ganglion cells of the human retina. *Proceedings of the National Academy of Sciences of the United States of America*, 89(20):9666–70.

Dacey, D. M., Peterson, B. B., and Robinson, F. R. (2002). Identification of an S-cone opponent OFF pathway in the Macaque monkey retina: Morphology, physiology and possible circuitry. *Investigative Ophthalmology & Visual Science*, pages E–abstract 2983.

Dacey, D. M., Peterson, B. B., Robinson, F. R., and Gamlin, P. D. (2003). Fireworks in the Primate Retina : Neurotechnique LGN-Projecting Ganglion Cell Types. *Neuron*, 37:15–27.

Dacheux, R. F. and Raviola, E. (1990). Physiology of HI horizontal cells in the primate retina. *Proceedings of the Royal Society of London. Series B.*, 239(1295):213–230.

Danilova, M. V. and Mollon, J. D. (2012a). Cardinal axes are not independent in color discrimination. *Journal of the Optical Society of America A*, 29(2):1–8.

Danilova, M. V. and Mollon, J. D. (2012b). Foveal color perception: Minimal thresholds at a boundary between perceptual categories. *Vision Research*, 62:162–172.

Daw, N. W. (1967). Goldfish Retina: Organization for Simultaneous Color Contrast Author. *Science*, 158(3803):942–944.

de Monasterio, F. M. (1978). Signals from blue cones in "red-green" opponent-colour ganglion cells of the macaque retina. *Vision Research*, 19:441–449.

de Monasterio, F. M. and Gouras, P. (1977). Responses of macaque ganglion cells to far violet lights. *Vision Research*, 17(10):1147–56.

de Monasterio, F. M., Gouras, P., and Tolhurst, D. J. (1975). Trichromatic colour opponency in ganglion cells of the rhesus monkey. *Journal of Physiology*, 251:197–216.

De Valois, R. L., Abramov, I., and Jacobs, G. H. (1966). Analysis of response patterns of LGN cells. *Journal of the Optical Society of America*, 56(7):966–977.

De Valois, R. L. and De Valois, K. K. (1993). A Multi-Stage Color Model. *Vision Research*, 33(8):1053–1065.

De Valois, R. L., De Valois, K. K., Switkes, E., and Mahon, L. (1997). Hue scaling of isoluminant and cone-specific lights. *Vision Research*, 37(7):885–97.

De Vries, H. L. (1946). Luminosity curve of trichromats. *Nature*, 157:736–7.

Deeb, S. S., Diller, L. C., Williams, D. R., and Dacey, D. M. (2000). Interindividual and topographical variation of L:M cone ratios in monkey retinas. *Journal of the Optical Society of America. A*, 17(3):538–44.

Delahunt, P. B., Webster, M. A., Ma, L., and Werner, J. S. (2004). Long-term renormalization of chromatic mechanisms following cataract surgery. *Visual Neuroscience*, 21(3):301–7.

Derrington, A. M., Krauskopf, J., and Lennie, P. (1984). Chromatic mechanisms in lateral geniculate nucleus of macaque. *Journal of Physiology*, 357:241–65.

Dominy, N. J. and Lucas, P. W. (2001). Ecological importance of trichromatic vision to primates. *Nature*, 410(6826):363–366.

Dong, D. and Atick, J. (1995). Statistics of natural time-varying images. *Network: Computation in Neural Systems*, 6(3):345–358.

Dowling, J. E. and Boycott, B. B. (1966). Organization of the Primate Retina : Electron Microscopy. *Proceedings of the Royal Society of London. Series B.*, 166(1002):80–111.

Drum, B. (1989). Hue signals from short- and middle-wavelength-sensitive cones. *Journal of the Optical Society of America. A*, 6(1):153–7.

Dryja, T. P., Mcgee, T. L., Berson, E. L., Fishman, G. A., Sandberg, M. A., Alexander, K. R., Derlacki, D. J., and Rajagopalan, A. S. (2005). Night blindness and abnormal cone electroretinogram ON responses in patients with mutations in the GRM6 gene encoding mGluR6. *Proceedings of the National Academy of Sciences of the United States of America*, 102(12):4884–4889.

Duebel, J., Haverkamp, S., Schleich, W., Feng, G., Augustine, G. J., Kuner, T., and Euler, T. (2006). Two-photon imaging reveals somatodendritic chloride gradient in retinal ON-type bipolar cells expressing the biosensor Clomeleon. *Neuron*, 49(1):81–94.

Eskew, R. T. (2009). Higher order color mechanisms: a critical review. *Vision Research*, 49:2686–2704.

Estevez, O. and Spekreuse, H. (1982). The "silent substitution" method in visual research. *Vision Research*, 22:681–691.

Euler, T., Haverkamp, S., Schubert, T., and Baden, T. (2014). Retinal bipolar cells: elementary building blocks of vision. *Nature Reviews Neuroscience*, 15(8):507–519.

Evers, H. U. and Gouras, P. (1986). Three cone mechanisms in the primate electroretinogram: two with, one without off-center bipolar responses. *Vision research*, 26(2):245–54.

Fedigan, L. M., Melin, A. D., Addicott, J. F., and Kawamura, S. (2014). The heterozygote superiority hypothesis for polymorphic color vision is not supported by long-term fitness data from wild neotropical monkeys. *PLoS ONE*, 9(1):e84872.

Field, D. J. (1987). Relations between the statistics of natural images and the response properties of cortical cells. *Journal of the Optical Society of America. A*, 4(12):2379–94.

Field, G. D. and Chichilnisky, E. J. (2007). Information processing in the primate retina: circuitry and coding. *Annual Review of Neuroscience*, 30:1–30.

Field, G. D., Gauthier, J. L., Sher, A., Greschner, M., Machado, T. A., Jepson, L. H., Shlens, J., Gunning, D. E., Mathieson, K., Dabrowski, W., Paninski, L., Litke, A. M., and Chichilnisky, E. J. (2010). Functional connectivity in the retina at the resolution of photoreceptors. *Nature*, 467(7316):673–7.

Field, G. D., Sher, A., Gauthier, J. L., Greschner, M., Shlens, J., Litke, A. M., and Chichilnisky, E. J. (2007). Spatial properties and functional organization of small bistratified ganglion cells in primate retina. *The Journal of Neuroscience*, 27(48):13261–72.

Garrigan, P., Ratliff, C. P., Klein, J. M., Sterling, P., Brainard, D. H., and Balasubramanian, V. (2010). Design of a trichromatic cone array. *PLoS Computational Biology*, 6(2):e1000677.

Gegenfurtner, K. R. and Rieger, J. (2000). Sensory and cognitive contributions of color to the recognition of natural scenes. *Current Biology*, 10(13):805–8.

Gordon, J. and Abramov, I. (1977). Color vision in the peripheral retina. II. Hue and saturation. *Journal of the Optical Society of America*, 67(2):202–7.

Gordon, J., Abramov, I., and Chan, H. (1994). Describing color appearance: Hue and saturation scaling. *Perception & psychophysics*, 56(I):27–41.

Grünert, U., Martin, P. R., and Wässle, H. (1994). Immunocytochemical analysis of bipolar cells in the macaque monkey retina. *Journal of Comparative Neurology*, 348(4):607–27.

Guth, S. L. (1991). Model for color vision and light adaptation. *Journal of the Optical Society of America. A*, 8(6):976–93.

Hagstrom, S. A., Neitz, M., and Neitz, J. (2000). Cone pigment gene expression in individual photoreceptors and the chromatic topography of the retina. *Journal of the Optical Society of America. A*, 17(3):527–37.

Hansen, T. and Gegenfurtner, K. R. (2006). Higher level chromatic mechanisms for image segmentation. *Journal of Vision*, 6(3):239–59.

Hansen, T., Olkkonen, M., Walter, S., and Gegenfurtner, K. R. (2006). Memory modulates color appearance. *Nature Neuroscience*, 9(11):1367–8.

Harmening, W. M., Tiruveedhula, P., Roorda, A., and Sincich, L. C. (2012). Measurement and correction of transverse chromatic offsets for multi-wavelength retinal microscopy in the living eye. *Biomedical Optics Express*, 3(9):1268–1270.

Harmening, W. M., Tuten, W. S., Roorda, A., and Sincich, L. C. (2014). Mapping the Perceptual Grain of the Human Retina. *The Journal of Neuroscience*, 34(16):5667–5677.

Hartridge, H. (1946). Colour receptors of the human fovea. *Nature*, 158:97–98.

Helmholtz, H. (1924). *Treatise on Physiological Optics. Vol 2.* Optical Society of America, Rochester, 1 edition.

Hendrickson, A. (2005). Organization of the Adult Primate Fovea. In Penfold, P. L. and Provis, J. M., editors, *Macular degeneration*, pages 1–23. Springer Berlin Heidelberg.

Hering, E. (1878). *Zur Lehre vom Lichtsinne. Sechs Mittheilungen an die Kaiserliche Akademie der Wissenschaften in Wien.* Carl Gerolds Sohn, Vienna.

Hering, E. (1964). *Outlines of a theory of the light sense.* Harvard University Press, Cambridge, MA.

Hirasawa, H., Yamada, M., and Kaneko, A. (2012). Acidification of the synaptic cleft of cone photoreceptor terminal controls the amount of transmitter release, thereby forming the receptive field surround in the vertebrate retina. *The Journal of Physiological sciences*, 62(5):359–75.

Hofer, H., Carroll, J., Neitz, J., Neitz, M., and Williams, D. R. (2005a). Organization of the human trichromatic cone mosaic. *The Journal of Neuroscience*, 25(42):9669–79.

Hofer, H., Singer, B., and Williams, D. R. (2005b). Different sensations from cones with the same photopigment. *Journal of Vision*, 5:444–454.

Hoon, M., Okawa, H., Della Santina, L., and Wong, R. O. L. (2014). Functional architecture of the retina: Development and disease. *Progress in Retinal and Eye Research*, 42:44–84.

Horwitz, G. D., Chichilnisky, E. J., and Albright, T. D. (2007). Cone inputs to simple and complex cells in V1 of awake macaque. *Journal of neurophysiology*, 97(4):3070–81.

Horwitz, G. D. and Hass, C. A. (2012). Nonlinear analysis of macaque V1 color tuning reveals cardinal directions for cortical color processing. *Nature Neuroscience*, 15(6):913–9.

Hsu, A., Smith, R. G., Buchsbaum, G., and Sterling, P. (2000). Cost of cone coupling to trichromacy in primate fovea. *Journal of the Optical Society of America A*, 17(3):635.

Hurvich, L. M. and Jameson, D. (1955). Some quantitative aspects of an opponent-colors theory. II. Brightness, saturation, and hue in normal and dichromatic vision. *Journal of the Optical Society of America*, 45(8):602–16.

Hurvich, L. M. and Jameson, D. (1957). An opponent-process theory of color vision. *Psychological Review*, 64(6):384–404.

Ingling Jr., C. R. and Martinez, E. (1983). The spatio-chromatic signal of the r-g channels. *Vision Research*, 23(12):1495–1500.

Jacobs, G. H. (2008). Primate color vision: a comparative perspective. *Visual Neuroscience*, 25(5-6):619–33.

Jacobs, G. H. (2009). Evolution of colour vision in mammals. *Philosophical Transactions of the Royal Society of London. B*, 364(1531):2957–67.

Jacobs, G. H. (2014). The Discovery of Spectral Opponency in Visual Systems and its Impact on Understanding the Neurobiology of Color Vision. *Journal of the History of the Neurosciences*, pages 1–28.

Jadzinsky, P. D. and Baccus, S. a. (2013). Transformation of visual signals by inhibitory interneurons in retinal circuits. *Annual Review of Neuroscience*, 36:403–28.

Joo, H. R., Peterson, B. B., Haun, T. J., and Dacey, D. M. (2011). Characterization of a novel large-field cone bipolar cell type in the primate retina: evidence for selective cone connections. *Visual Neuroscience*, 28(1):29–37.

Jordan, G. and Mollon, J. D. (1995). Rayleigh Matches and Unique Green. *Vision Research*, 35(5):613–620.

Jordan, G. and Mollon, J. D. (1997). Unique hues in heterozygotes for protan and deutan deficiencies. In Cavonius, C., editor, *Colour Vision Deficiencies XIII*, pages 67–76. Kluwer Academic Publishers, Dordrecht.

Joselevitch, C. and Kamermans, M. (2009). Retinal parallel pathways: seeing with our inner fish. *Vision Research*, 49(9):943–59.

Judd, D. B. (1966). Fundamenta studies of color vision from 1860 to 1960. *Proceedings of the National Academy of Sciences of the United States of America*, 55:1313–1330.

Kamermans, M., Kraaij, D. A., and Spekreijse, H. (1998). The cone/horizontal cell network: a possible site for color constancy. *Visual Neuroscience*, 15(5):787–97.

Kaplan, E. and Shapley, R. M. (1986). The primate retina contains two types of ganglion cells, with high and low contrast sensitivity. *Proceedings of the National Academy of Sciences of the United States of America*, 83(April):2755–2757.

Kelber, A. and Osorio, D. (2010). From spectral information to animal colour vision: experiments and concepts. *Proceedings of the Royal Society of London. Series B.*, 277(1688):1617–1625.

Klug, K., Herr, S., Ngo, I. T., Sterling, P., and Schein, S. (2003). Macaque retina contains an S-cone OFF midget pathway. *The Journal of Neuroscience*, 23(30):9881–7.

Kolb, H., Goede, P., Roberts, S., McDermott, R., and Gouras, P. (1997). Uniqueness of the S-cone pedicle in the human retina and consequences for color processing. *Journal of Comparative Neurology*, 386(3):443–60.

Kolb, H., Linberg, K. A., and Fisher, S. K. (1992). Neurons of the human retina: a Golgi study. *Journal of Comparative Neurology*, 318(2):147–87.

Kolb, H. and Marshak, D. (2003). The midget pathways of the primate retina. *Documenta Ophthalmologica*, 106:67–81.

Krauskopf, J. (1964). Color Appearance of Small Stimuli and the Spatial Distribution of Color Receptors. *Journal of the Optical Society of America*, 54(9):1171.

Krauskopf, J. (2000). Relative number of long- and middle-wavelength-sensitive cones in the human fovea. *Journal of the Optical Society of America A*, 17(3):510.

Krauskopf, J. and Srebro, R. (1965). Spectral Sensitivity of Color Mechanisms: Derivation from Fluctuations of Color Appearance near Threshold. *Science*, 150(3702):1477–1479.

Krauskopf, J., Williams, D. R., and Heeley, D. W. (1982). Cardinal directions of color space. *Vision Research*, 22(9):1123–31.

Kuchenbecker, J. A., Neitz, J., and Neitz, M. (2014). Ethnic variation in the ratio of long- to middle-wavelength sensitive cones. *Association for Research in Vision and Ophthalmology*.

Kuehni, R. G. (2004). Variability in Unique Hue Selection: A Surprising Phenomenon. *Color Research & Application*, 29(2):158–162.

Lamb, T. D. (1995). Photoreceptor spectral sensitivities: Common shape in the long-wavelength region. *Vision Research*, 35(22):3083–3091.

Lee, B. B. (2004). Paths to colour in the retina. *Clinical and experimental optometry*, 87(4-5):239–248.

Lee, B. B., Dacey, D. M., Smith, V. C., and Pokorny, J. (1999). Horizontal cells reveal cone type-specific adaptation in primate retina. *Proceedings of the National Academy of Sciences of the United States of America*, 96(25):14611–6.

Lee, B. B., Dacey, D. M., Smith, V. C., and Pokorny, J. (2003). Dynamics of sensitivity regulation in primate outer retina: the horizontal cell network. *Journal of Vision*, 3(7):513–26.

Lee, B. B., Martin, P. R., and Grünert, U. (2010). Retinal connectivity and primate vision. *Progress in Retinal and Eye Research*, 29(6):622–39.

Lee, S. C. S., Telkes, I., and Grünert, U. (2005). S-cones do not contribute to the OFF-midget pathway in the retina of the marmoset, Callithrix jacchus. *The European Journal of Neuroscience*, 22(2):437–47.

Lennie, P., Haake, P. W., and Williams, D. R. (1991). The Design of Chromatically Opponent Receptive Fields. In Landy, M. and Movshon, J. A., editors, *Computational Models of Visual Processing*, pages 71–82. The MIT Press.

Li, M., Liu, F., Juusola, M., and Tang, S. (2014a). Perceptual Color Map in Macaque Visual Area V4. *The Journal of Neuroscience*, 34(1):202–217.

Li, P. H., Field, G. D., Greschner, M., Ahn, D., Gunning, D. E., Mathieson, K., Sher, A., Litke, A. M., and Chichilnisky, E. (2014b). Retinal Representation of the Elementary Visual Signal. *Neuron*, 81(1):130–139.

Liang, J., Williams, D. R., and Miller, D. T. (1997). Supernormal vision and high-resolution retinal imaging through adaptive optics. *Journal of the Optical Society of America. A*, 14(11):2884–2892.

Lindsey, D. T. and Brown, A. M. (2006). Universality of color names. *Proceedings of the National Academy of Sciences of the United States of America*, 103(44):16608–13.

Lindsey, D. T. and Brown, A. M. (2009). World Color Survey color naming reveals universal motifs and their within-language diversity. *Proceedings of the National Academy of Sciences of the United States of America*, 106(47):19785–90.

Lindsey, D. T. and Brown, A. M. (2014). The color lexicon of American English. *Journal of Vision*, 14(2):1–25.

Linhares, J. M. M., Pinto, P. D., and Nascimento, S. M. C. (2008). The number of discernible colors in natural scenes. *Journal of the Optical Society of America. A*, 25:2918–2924.

Livingstone, M. and Hubel, D. (1988). Segregation of form, color, movement, and depth: anatomy, physiology, and perception. *Science*, 240(4853):740–9.

Logvinenko, A. D. (2012). A theory of unique hues and colour categories in the human colour vision. *Color Research & Application*, 37(2):109–116.

Logvinenko, A. D. and Beattie, L. L. (2011). Partial hue-matching. *Journal of Vision*, 11(8):1–16.

Logvinenko, A. D. and Geithner, C. (2013). Unique hues as revealed by unique-hue selecting versus partial hue-matching. *Attention, perception & psychophysics*.

Logvinenko, A. D. and Hutchinson, S. J. (2007). Evidence for the existence of colour mechanisms producing unique hues as derived from a colour illusion based on spatio-chromatic interactions. *Vision Research*, 47(10):1315–1334.

Lucas, P. W., Dominy, N. J., Riba-Hernandez, P., Stoner, K. E., Yamashita, N., Loria-Calderon, E., Petersen-Pereira, W., Rojas-Duran, Y., Salas-Pena, R., Solis-Madrigal, S., Osorio, D., and Darvell, B. W. (2003). Evolution and function of routine trichromatic vision in primates. *Evolution*, 57(11):2636–2643.

Makous, W. (2007). Comment on "Emergence of novel color vision in mice engineered to express a human cone photopigment". *Science*, 318(5848):196; author reply 196.

Mancuso, K., Hauswirth, W. W., Li, Q., Connor, T. B., Kuchenbecker, J. A., Mauck, M. C., Neitz, J., and Neitz, M. (2009). Gene therapy for red-green colour blindness in adult primates. *Nature*, 461(7265):784–7.

Mancuso, K., Mauck, M. C., Kuchenbecker, J. A., Neitz, M., and Neitz, J. (2010). A multi-stage color model revisited: implications for a gene therapy cure for red-green colorblindness. *Advances in Experimental Medicine and Biology*, 664:631–638.

Mariani, A. P. (1984). Bipolar cells in monkey retina selective for the cones likely to be blue-sensitive. *Nature*, 308:184–186.

Marshall, J., Carleton, K. L., and Cronin, T. (2015). Colour vision in marine organisms. *Current Opinion in Neurobiology*, 34:86–94.

Marshall, J. and Oberwinkler, J. (1999). The colourful world of the mantis shrimp. *Nature*, 401(6756):873–874.

Martínez-Álvarez, A., Olmedo-Payá, A., Cuenca-Asensi, S., Ferrández, J. M., and Fernández, E. (2013). RetinaStudio: A bioinspired framework to encode visual information. *Neurocomputing*, 114:45–53.

Masland, R. H. (2011). Cell populations of the retina: the Proctor lecture. *Investigative Ophthalmology & Visual Science*, 52(7):4581–91.

Masland, R. H. (2012). The neuronal organization of the retina. *Neuron*, 76(2):266–80.

Maximov, V. V. (2000). Environmental factors which may have led to the appearance of colour vision. *Philosophical Transactions of the Royal Society of London. B*, 355(1401):1239–1242.

Maxwell, J. C. (1855). Experiments on colour, as perceived by the eye, with remarks on colour-blindness. *Transactions of the Royal Society of Edinburgh*, XXI:275–298.

McMahon, C., Carroll, J., Awua, S., Neitz, J., and Neitz, M. (2008). The L:M cone ratio in males of African descent with normal color vision. *Journal of Vision*, 8(2):1–9.

McMahon, M. J., Packer, O. S., and Dacey, D. M. (2004). The classical receptive field surround of primate parasol ganglion cells is mediated primarily by a non-GABAergic pathway. *The Journal of Neuroscience*, 24(15):3736–45.

Meister, M. (2015). On the dimensionality of odor space. *eLife*, 4:e07865.

Merigan, W. H. and Maunsell, J. H. R. (1993). How parallel are the primate visual pathways? *Annual Review of Neuroscience*, 16:369–402.

Miyagishima, K. J., Grünert, U., and Li, W. (2014). Processing of S-cone signals in the inner plexiform layer of the mammalian retina. *Visual Neuroscience*, 31(2):153–163.

Miyahara, E., Pokorny, J., Smith, V. C., Baron, R., and Baron, E. (1998). Color vision in two observers with highly biased LWS/MWS cone ratios. *Vision Research*, 38(4):601–12.

Mollon, J. (2006). Monge: The Verriest Lecture, Lyon, July 2005. *Visual Neuroscience*, 23:297–309.

Mollon, J. D. (1989). "tho' she kneel'd in that place where they grew..." The uses and origins of primate colour vision. *Journal of Experimental Biology*, 38:21–38.

Mollon, J. D. (1999). Color vision : Opsins and options. *Proceedings of the National Academy of Sciences of the United States of America*, 96:4743–4745.

Mollon, J. D. (2003). The Origins of Modern Color Science. In Shevell, S. K., editor, *The Science of Color*. Elsevier, Oxford, Uk, 2nd edition.

Mollon, J. D. and Bowmaker, J. K. (1992). The spatial arrangement of cones in the primate fovea. *Nature*, 360:677–679.

Mollon, J. D. and Jordan, G. (1997). On the Nature of Unique Hues. In Dickenson, C., Murray, I., and Carden, D., editors, *John Dalton's Colour Vision Legacy*, pages 381–392. Taylor & Francis., London.

Mullen, K. T. (1985). The contrast sensitivity of human colour vision to red-green and blue-yellow chromatic gratings. *Journal of Physiology*, 359:381–400.

Muller, G. E. (1930). *Uber Die Farbenempfindungen. Psychophys. Unters.* Barth, Leipzig.

Naka, K. I. and Rushton, W. A. H. (1967). The generation and spread of S-potentials in fish (Cyprinidae). *Journal of Physiology*, 192:437–461.

Nathans, J. (1999). The evolution and physiology of human color vision: insights from molecular genetic studies of visual pigments. *Neuron*, 24(2):299–312.

Nathans, J., Piantanida, T. P., Eddy, R. L., Shows, T. B., and Hogness, D. S. (1986a). Molecular genetics of inherited variation in human color vision. *Science*, 232:203–210.

Nathans, J., Thomas, D., and Hogness, D. S. (1986b). Molecular genetics of human color vision: the genes encoding blue, green, and red pigments. *Science*, 232:193–202.

Neitz, J., Carroll, J., Yamauchi, Y., Neitz, M., and Williams, D. R. (2002). Color perception is mediated by a plastic neural mechanism that is adjustable in adults. *Neuron*, 35(4):783–92.

Neitz, J. and Neitz, M. (2008). Colour vision: the wonder of hue. *Current Biology*, 18(16):R700–2.

Neitz, J. and Neitz, M. (2011). The genetics of normal and defective color vision. *Vision Research*, 51(7):633–51.

Neitz, J., Neitz, M., He, J. C., and Shevell, S. K. (1999). Trichromatic color vision with only two spectrally distinct photopigments. *Nature Neuroscience*, 2(10):884–8.

Neitz, J., Neitz, M., and Kainz, P. M. (1996). Visual pigment gene structure and the severity of color vision defects. *Science*, 274(5288):801–4.

Neitz, M. and Neitz, J. (2014). Curing Color Blindness Mice and Nonhuman Primates. *Cold Spring Harb Perspect Med*, 4:a017418.

Neitz, M., Neitz, J., and Jacobs, G. H. (1991). Spectral Tuning of Pigments Underlying Red-Green Color Vision. *Nature*, 252:971–971974.

Nerger, J. L., Volbrecht, V. J., and Ayde, C. J. (1995). Unique hue judgments as a function of test size in the fovea and at 20-deg temporal eccentricity. *Journal of the Optical Society of America. A*, 12(6):1225–32.

Norrsell, U., Finger, S., and Lajonchere, C. (1999). Cutaneous sensory spots and the "law of specific nerve energies": history and development of ideas. *Brain research bulletin*, 48(5):457–65.

O'Connor, E., Allen, L. E., Bradshaw, K., Boylan, J., Moore, A. T., and Trump, D. (2006). Congenital stationary night blindness associated with mutations in GRM6 encoding glutamate receptor MGluR6. *The British journal of ophthalmology*, 90:653–654.

O'Neil, S. F., McDermott, K. C., Mizokami, Y., Werner, J. S., Crognale, M. a., and Webster, M. a. (2012). Tests of a functional account of the Abney effect. *Journal of the Optical Society of America. A*, 29(2):A165–73.

Osorio, A. D., Smith, A. C., Vorobyev, M., Smith, H. M. B., and Osorio, D. (2004). Detection of Fruit and the Selection of Primate Visual Pigments for Color Vision. *The American Naturalist*, 164(6):696–708.

Osorio, D. and Vorobyev, M. (1996). Colour vision as an adaptation to frugivory in primates. *Proceedings of the Royal Society of London. Series B.*, 263(1370):593–599.

Otake, S., Gowdy, P. D., and Cicerone, C. M. (2000). The spatial arrangement of L and M cones in the peripheral human retina. *Vision Research*, 40:677–693.

Packer, O. S. and Dacey, D. M. (2002). Receptive field structure of H1 horizontal cells in macaque monkey retina. *Journal of Vision*, 2(4):272–92.

Packer, O. S. and Dacey, D. M. (2005). Synergistic center-surround receptive field model of monkey H1 horizontal cells. *Journal of Vision*, 5(11):1038–54.

Packer, O. S., Verweij, J., Li, P. H., Schnapf, J. L., and Dacey, D. M. (2010). Blue-yellow opponency in primate S cone photoreceptors. *The Journal of Neuroscience*, 30(2):568–72.

Paulus, W. and Kröger-Paulus, A. (1983). A new concept of retinal colour coding. *Vision Research*, 23(5):529–40.

Pei, Z. and Qiao, Q. (2010). An approximate retina model with cascade structures. *Proceedings - 2010 6th International Conference on Natural Computation, ICNC 2010*, 4(Icnc):2009–2012.

Philipona, D. L. and Regan, J. K. O. (2006). Color naming, unique hues, and hue cancellation predicted from singularities in reflection properties. *Visual Neuroscience*, 23:331–339.

Pokorny, J. and Smith, V. C. (1987). L/M cone ratios and the null point of the perceptual red/green opponent system. *Die Farbe*, 34:53–57.

Pokorny, J., Smith, V. C., and Lutze, M. (1987). Aging of the human lens. *Applied Optics*, 26(8):1437–40.

Poppel, E. (1986). Long-range colour-generating interactions across the retina. *Nature*, 320:523–525.

Puller, C., Haverkamp, S., Neitz, M., and Neitz, J. (2014a). Synaptic elements for GABAergic feed-forward signaling between HII horizontal cells and blue cone bipolar cells are enriched beneath primate S-cones. *PLoS ONE*, 9(2):e88963.

Puller, C., Manookin, M. B., Neitz, M., and Neitz, J. (2012). Syntaxin-4 is highly enriched beneath S-cone pedicles in the primate retina. In *Association for Research in Vision and Ophthalmology*, page 6323.

Puller, C., Manookin, M. B., Neitz, M., and Neitz, J. (2014b). A specialized synaptic pathway for chromatic signals beneath S-cone photoreceptors is common to human, Old and New World primates. *Journal of the Optical Society of America*, 31(4):A189–A194.

Regan, B. C., Julliot, C., Simmen, B., Viénot, F., Charles-Dominique, P., and Mollon, J. D. (2001). Fruits, foliage and the evolution of primate colour vision. *Philosophical Transactions of the Royal Society of London. B*, 356(1407):229–283.

Reid, R. C. and Shapley, R. M. (1992). Spatial structure of cone inputs to the receptive fields in primate lateral geniculate nucleus. *Nature*, 356(6371):716–718.

Reid, R. C. and Shapley, R. M. (2002). Space and time maps of cone photoreceptor signals in macaque lateral geniculate nucleus. *The Journal of Neuroscience*, 22(14):6158–75.

Rodieck, R. W. (1991a). The density recovery profile: a method for the analysis of points in the plane applicable to retinal studies. *Visual Neuroscience*, 6(2):95–111.

Rodieck, R. W. (1991b). Which cells code for color? In Valberg, A. and Lee, B. B., editors, *From Pigments to Perception*, pages 83–93. Lee, Plenum Press, New York, NY.

Rodieck, R. W. (1998). *The First Steps in Seeing*. Sinauer Associates Inc, Sunderland, Massachusetts, 1 edition.

Roorda, A. (2011). Adaptive optics for studying visual function : A comprehensive review. *Journal of Vision*, 11(5):1–21.

Roorda, A., Metha, A. B., Lennie, P., and Williams, D. R. (2001). Packing arrangement of the three cone classes in primate retina. *Vision Research*, 41(10-11):1291–306.

Roorda, A., Romero-Borja, F., Donnelly, III, W., Queener, H., Hebert, T., and Campbell, M. (2002). Adaptive optics scanning laser ophthalmoscopy. *Optics Express*, 10(9):405.

Roorda, A. and Williams, D. R. (1999). The arrangement of the three cone classes in the living human eye. *Nature*, 397(6719):520–2.

Rossi, E. A. and Roorda, A. (2010). The relationship between visual resolution and cone spacing in the human fovea. *Nature Neuroscience*, 13(2):156–7.

Rushton, W. A. H. (1972). Pigments and signals in colour vision. *Journal of Physiology*, 220:1–31.

Sabbah, S., Zhu, C., Hornsby, M. A. W., Kamermans, M., and Hawryshyn, C. W. (2013). Feedback from horizontal cells to cones mediates color induction and may facilitate color constancy in rainbow trout. *PLoS ONE*, 8(6):e66216.

Sabesan, R., Hofer, H., and Roorda, A. (2015a). Characterizing the human cone photoreceptor mosaic via dynamic photopigment densitometry. *PLoS ONE*, in press.

Sabesan, R., Schmidt, B. P., Tuten, W. S., and Roorda, A. (2015b). Representation of color and achromatic percepts in the human cone mosaic. (in preparation).

Sanes, J. R. and Masland, R. H. (2015). The Types of Retinal Ganglion Cells: Current Status and Implications for Neuronal Classification. *Annual Review of Neuroscience*, 38:221–246.

Saunders, B. A. C. (1997). Are there nontrivial constraints on colour categorization ? *Behavioral and Brain Sciences*, 20:167–228.

Schefrin, B. E. and Werner, J. S. (1990). Loci of spectral unique hues throughout the life span. *Journal of the Optical Society of America. A*, 7(2):305–11.

Schmidt, B. P., Neitz, M., and Neitz, J. (2014). Neurobiological hypothesis of color appearance and hue perception. *Journal of the Optical Society of America A*, 31(4):A195–A207.

Schnapf, J. L., Kraft, T. W., and Baylor, D. A. (1987). Spectral sensitivity of human cone photoreceptors. *Nature*, 352:439–441.

Schnapf, J. L., Nunn, B. J., Meister, M., and Baylor, D. A. (1990). Visual transduction in cones of the monkey Macaca fasciularis. *Journal of Physiology*, 427:681–713.

Schneeweis, D. M. and Schnapf, J. L. (1999). The photovoltage of macaque cone photoreceptors: adaptation, noise, and kinetics. *The Journal of Neuroscience*, 19(4):1203–16.

Sekiguchi, N., Williams, D. R., and Brainard, D. H. (1993a). Aberration-free measurements of the visibility of isoluminant gratings. *Journal of the Optical Society of America. A*, 10(10):2105–17.

Sekiguchi, N., Williams, D. R., and Brainard, D. H. (1993b). Efficiency in detection of isoluminant and isochromatic interference fringes. *Journal of the Optical Society of America. A*, 10(10):2118–33.

Sergouniotis, P. I., Robson, A. G., Li, Z., Devery, S., Holder, G. E., Moore, A. T., and Webster, A. R. (2012). A phenotypic study of congenital stationary night blindness (CSNB) associated with mutations in the GRM6 gene. *Acta Ophthalmologica*, 90(3).

Shamey, R., Sawatwarakul, W., and Kuehni, R. G. (2015). Cognitive comparison of unique and intermediate hues. *Color Research & Application*, 40(3):264–269.

Shapley, R. and Hawken, M. J. (2011). Color in the Cortex : single- and double-opponent cells. *Vision Research*, 51:701–717.

Shapley, R. and Hugh Perry, V. (1986). Cat and monkey retinal ganglion cells and their visual functional roles. *Trends in Neurosciences*, 9(May):229–235.

Sharpe, L. T., Stockman, A., Jagla, W., and Jägle, H. (2005). A luminous efficiency function, V*(lambda), for daylight adaptation. *Journal of Vision*, 5(11):948–68.

Sharpe, L. T., Stockman, A., Jägle, H., and Nathans, J. (1999). Opsin genes, cone photopigments, color vision, and color blindness. In Gegenfurtner, K. R. and Sharpe, L. T., editors, *Color vision: from genes to perception*, pages 3–52. Cambridge University Press, Cambridge.

Sher, A. and DeVries, S. H. (2012). A non-canonical pathway for mammalian blue-green color vision. *Nature Neuroscience*, 15(7):952–3.

Shevell, S. K. (1978). The dual role of chromatic backgrounds in color perception. *Vision Research*, 19:1649–1661.

Shevell, S. K. (1992). Color Perception Within a Chromatic Context : Changes in Red / Green Equilibria Caused by. *Vision Research*, 32(9):1623–1634.

Shevell, S. K. and Kingdom, F. A. A. (2008). Color in complex scenes. *Annual Review of Psychology*, 59:143–66.

Shevell, S. K. and Wei, J. (2000). A central mechanism of chromatic contrast. *Vision Research*, 40(23):3173–3180.

Sincich, L. C., Sabesan, R., Tuten, W. S., Roorda, A., and Harmening, W. M. (2015). Functional Imaging of Cone Photoreceptors. In Kremers, J., Baraas, R., and Marshal, J., editors, *Human Color Vision*, chapter 4. Springer, New York.

Sincich, L. C., Zhang, Y., Tiruveedhula, P., Horton, J. C., and Roorda, A. (2009). Resolving single cone inputs to visual receptive fields. *Nature Neuroscience*, 12(8):967–9.

Smith, V. C., Pokorny, J., Lee, B. B., and Dacey, D. M. (2001). Primate Horizontal Cell Dynamics : An Analysis of Sensitivity Regulation in the Outer Retina. *Journal of Physiology*, 85:545–558.

Smith, V. C., Pokorny, J., Lee, B. B., and Dacey, D. M. (2008). Sequential processing in vision: The interaction of sensitivity regulation and temporal dynamics. *Vision Research*, 48(26):2649–56.

Solomon, S. G. and Lennie, P. (2007). The machinery of colour vision. *Nature Reviews. Neuroscience*, 8(4):276–86.

Sternheim, C. E. and Boynton, R. M. (1966). Uniqueness of perceived hues investigated with a continuous judgemental technique. *Journal of Experimental Psychology*, 72(5):770–776.

Stevenson, S. B. and Roorda, a. (2005). Correcting for miniature eye movements in high resolution scanning laser ophthalmoscopy. *Ophthalmic Technologies XV*, 5688:145–151.

Stockman, A. and Brainard, D. H. (2010). Color Vision Mechanisms. In Bass, M., editor, *Vision and Vision Optics*, chapter 11, pages 1–104. McGraw-Hill, New York, 3rd edition.

Stockman, A. and Sharpe, L. T. (2000). The spectral sensitivities of the middle- and long-wavelength-sensitive cones derived from measurements in observers of known genotype. *Vision Research*, 40(13):1711–37.

Stockman, A., Sharpe, L. T., and Fach, C. C. (1999). The spectral sensitivity of the human short-wavelength sensitive cones derived from thresholds and color matches. *Vision Research*, 39:2901–2927.

Stoughton, C. M. and Conway, B. R. (2008). Neural basis for unique hues. *Current Biology*, 18(16):R698–9.

Sun, H., Smithson, H. E., Zaidi, Q., and Lee, B. B. (2006). Specificity of Cone Inputs to Macaque Retinal Ganglion Cells. *Journal of Neurophysiology*, 95:837–849.

Svaetichin, G. and MaCnichol, E. F. (1959). Retinal mechanisms for chromatic and achromatic vision. *Annals of the New York Academy of Sciences*, 74(2):385–404.

Tailby, C., Solomon, S. G., Dhruv, N. T., and Lennie, P. (2008a). Habituation reveals fundamental chromatic mechanisms in striate cortex of macaque. *The Journal of Neuroscience*, 28(5):1131–9.

Tailby, C., Solomon, S. G., and Lennie, P. (2008b). Functional asymmetries in visual pathways carrying S-cone signals in macaque. *The Journal of Neuroscience*, 28(15):4078–87.

Terasaki, H., Miyake, Y., Nomura, R., Horiguchi, M., Suzuki, S., and Kondo, M. (1999). Blue-on-Yellow Perimetry in the Complete Type of Congenital Stationary Night Blindness. *Investigative Ophthalmology & Visual Science*, 40(11):2761–2764.

Thoen, H. H., How, M. J., Chiou, T.-H., and Marshall, J. (2014). A different form of color vision in mantis shrimp. *Science*, 343(6169):411–3.

Thoreson, W. B. and Mangel, S. C. (2012). Lateral interactions in the outer retina. *Progress in retinal and eye research*, 31(5):407–41.

Tkačik, G., Garrigan, P., Ratliff, C., Milčinski, G., Klein, J. M., Seyfarth, L. H., Sterling, P., Brainard, D. H., and Balasubramanian, V. (2011). Natural images from the birthplace of the human eye. *PLoS ONE*, 6(6):e20409.

Tsukamoto, Y. and Omi, N. (2014). Some OFF bipolar cell types make contact with both rods and cones in macaque and mouse retinas. *Frontiers in neuroanatomy*, 8(September):105.

Tsukamoto, Y. and Omi, N. (2015). OFF bipolar cells in macaque retina: type-specific connectivity in the outer and inner synaptic layers. *Frontiers in Neuroanatomy*, 9(October).

Tuten, W. S., Tiruveedhula, P., and Roorda, A. (2012). Adaptive Optics Scanning Laser Ophthalmoscope-Based Microperimetry. *Optometry and Vision Science*, 89(5):563–574.

Ungerleider, L. G. and Mishkin, M. (1982). Two cortical visual systems. In Ingle, D. J., Goodale, M. A., and Mansfield, R. J. W., editors, *Analysis of Visual Behavior*, pages 549–586. MIT Press, Cambridge.

Usrey, W. M., Reppas, J. B., and Reid, R. C. (1999). Specificity and strength of retinogeniculate connections. *Journal of neurophysiology*, 82(6):3527–3540.

Valberg, A. (2001). Unique hues: an old problem for a new generation. *Vision Research*, 41(13):1645–57.

van Hateren, J. H. (2005). A cellular and molecular model of response kinetics and adaptation in primate cones and horizontal cells. *Journal of Vision*, 5(4):331–347.

van Hateren, J. H. (2007). A model of spatiotemporal signal processing by primate cones and horizontal cells. *Journal of Vision*, 7(3):3.

van Hateren, J. H. and Lamb, T. D. (2006). The photocurrent response of human cones is fast and monophasic. *BMC Neuroscience*, 7(1):34.

Van Leeuwen, M. T., Joselevitch, C., Fahrenfort, I., and Kamermans, M. (2007). The contribution of the outer retina to color constancy: a general model for color constancy synthesized from primate and fish data. *Visual Neuroscience*, 24(3):277–90.

Vardi, N., Duvoisin, R., Wu, G., and Sterling, P. (2000). Localization of mGluR6 to dendrites of ON bipolar cells in primate retina. *Journal of Comparative Neurology*, 423(3):402–12.

Varela, C., Blanco, R., and De la Villa, P. (2005). Depolarizing effect of GABA in rod bipolar cells of the mouse retina. *Vision Research*, 45(20):2659–67.

Verweij, J., Dacey, D. M., Peterson, B. B., and Buck, S. L. (1999). Sensitivity and dynamics of rod signals in H1 horizontal cells of the macaque monkey retina. *Vision Research*, 39(22):3662–72.

Verweij, J., Hornstein, E. P., and Schnapf, J. L. (2003). Surround antagonism in macaque cone photoreceptors. *The Journal of Neuroscience*, 23(32):10249–57.

Volbrecht, V. J. and Nerger, J. L. (2012). Color appearance at 10 along the vertical and horizontal meridians. *Journal of the Optical Society of America. A*, 29(2):A44–51.

Volbrecht, V. J., Nerger, J. L., and Harlow, C. E. (1997). The bimodality of unique green revisited. *Vision Research*, 37(4):407–16.

von Kries, J. (1905). Die Gesichtsempfindungen. In Nagel, W. A., editor, *Handbuch der Physiologie der Mensche*, chapter 3.

Vorobyev, M. (2003). Coloured oil droplets enhance colour discrimination. *Proceedings of the Royal Society of London. Series B.*, 270(1521):1255–1261.

Vorobyev, M., Osorio, D., Bennett, a. T. D., Marshall, N. J., and Cuthill, I. C. (1998). Tetrachromacy, oil droplets and bird plumage colours. *Journal of Comparative Physiology. A.*, 183(5):621–633.

Vos, J. J. (1986). Are unique and invariant hues coupled? *Vision Research*, 26(2):337–342.

Wachtler, T., Doi, E., Lee, T.-w., and Sejnowski, T. J. (2007). Cone selectivity derived from the responses of the retinal cone mosaic to natural scenes. *Journal of Vision*, 7(8):1–14.

Wachtler, T., Lee, T.-W., and Sejnowski, T. J. (2001). Chromatic structure of natural scenes. *Journal of the Optical Society of America A*, 18(1):65–77.

Walraven, J. (1976). Discounting the background: The missing link in the explanation of chromatic induction. *Vision Research*, 16(3):289–295.

Walraven, J. and Werner, J. S. (1991). The invariance of unique white; a possible implication for normalizing cone action spectra. *Vision Research*, 31(12):2185–93.

Wässle, H. (2004). Parallel processing in the mammalian retina. *Nature Reviews. Neuroscience*, 5(10):747–57.

Wässle, H., Boycott, B. B., and Rohrenbeck, J. (1989). Horizontal cells in the monkey retina: cone connections and dendritic network. *European Journal of Neuroscience*, 1:421–435.

Wässle, H., Dacey, D. M., Haun, T., Haverkamp, S., Grünert, U., and Boycott, B. B. (2000). The mosaic of horizontal cells in the macaque monkey retina: with a comment on biplexiform ganglion cells. *Visual Neuroscience*, 17(4):591–608.

Webster, M. (2012). Evolving concepts of sensory adaptation. *F1000 Biology Reports*, 4(November):1–7.

Webster, M. A. (2011). Adaptation and visual coding. *Journal of Vision*, 11(5):1–23.

Webster, M. A. and Kay, P. (2012). Color categories and color appearance. *Cognition*, 122(3):375–92.

Webster, M. A. and Kay, P. (2014). Individual and Population Differences in Focal Colors. In MacLaury, R., Paramei, G. V., and Dedrick, D., editors, *The Anthropology of Color*, number 1. John Benjamins.

Webster, M. A., Miyahara, E., Malkoc, G., and Raker, V. E. (2000a). Variations in normal color vision. I. Cone-opponent axes. *Journal of the Optical Society of America. A*, 17(9):1535–44.

Webster, M. A., Miyahara, E., Malkoc, G., and Raker, V. E. (2000b). Variations in normal color vision. II. Unique hues. *Journal of the Optical Society of America. A*, 17(9):1545–55.

Welbourne, L. E., Morland, A. B., and Wade, A. R. (2015). Human colour perception changes between seasons. *Current Biology*, 25(15):R646–R647.

Welbourne, L. E., Thompson, P. G., Wade, A. R., and Morland, A. B. (2013). The distribution of unique green wavelengths and its relationship to macular pigment density. *Journal of Vision*, 13:1–10.

Werner, J. S. (1996). Visual problems of the retina during ageing: Compensation mechanisms and colour constancy across the life span. *Progress in Retinal and Eye Research*, 15(2):621–645.

Werner, J. S. and Schefrin, B. E. (1993). Loci of achromatic points throughout the life span. *Journal of the Optical Society of America. A*, 10(7):1509–16.

Werner, J. S. and Wooten, B. R. (1979). Opponent chromatic mechanisms: Relation to photopigments and hue naming. *Journal of the Optical Society of America*, 69(3):422–434.

White, M. (1979). A new effect of pattern on perceived lightness. *Perception*, 8(June):413–416.

White, M. (2010). The Early History of White's Illusion. *Colour : Design & Creativity*, 5(7):1–7.

Whittle, P. (1973). The brightness of coloured flashes on backgrounds of various colours and luminances. *Vision Research*, 13(3):621–638.

Wichmann, F. A., Sharpe, L. T., and Gegenfurtner, K. R. (2002). The contributions of color to recognition memory for natural scenes. *Journal of Experimental Psychology: Learning, Memory, and Cognition*, 28(3):509–520.

Wiesel, T. N. and Hubel, D. H. (1966). Spatial and chromatic interactions in the lateral geniculate body of the rhesus monkey. *Journal of Neurophysiology*, 29(6):1115–56.

Williams, D. R. (1988). Topography of the foveal cone mosaic in the living human eye. *Vision Research*, 28(3):433–454.

Williams, D. R. (2011). Imaging single cells in the living retina. *Vision Research*, 51(13):1379–96.

Williams, D. R. and Coletta, N. J. (1987). Cone spacing and the visual resolution limit. *Journal of the Optical Society of America. A*, 4(8):1514–23.

Williams, D. R., Macleod, D. A., and E, M. M. H. (1981a). Punctate sensitivity of the blue sensitive mechanism. *Vision Research*, 21:1357–1375.

Williams, D. R., Macleod, D. A., and Hayhoe, M. M. (1981b). Foveal tritanopia. *Vision Research*, 21:1241–1256.

Williams, D. R., Sekiguchi, N., Haake, W., Brainard, D., and Packer, O. (1991). The cost of trichromacy for spatial vision. In Valber, A. and Lee, B. B., editors, *From Pigments to Perception*, pages 11–21. Plenum Press, New York.

Wilson, H. R. (1997). A neural model of foveal light adaptation and afterimage formation. *Visual neuroscience*, 14(3):403–423.

Witzel, C. and Franklin, A. (2014). Do focal colours look particularly "colourful"? *Journal of the Optical Society of America A*, 31(4):365–374.

Wohrer, A. and Kornprobst, P. (2009). Virtual Retina: A biological retina model and simulator, with contrast gain control. *Journal of Computational Neuroscience*, 26(2):219–249.

Wool, L. E., Komban, S. J., Jansen, M., and Alonso, J.-m. (2015). Salience of unique hues and implications for color theory. *Journal of Vision*, 15(2):1–11.

Wooten, B. R., Hammond, B. R., Land, R. I., and Snodderly, D. M. (1999). A practical method for measuring macular pigment optical density. *Investigative Ophthalmology & Visual Science*, 40(11):2481–9.

Wuerger, S. M., Atkinson, P., and Cropper, S. (2005). The cone inputs to the unique-hue mechanisms. *Vision Research*, 45(25-26):3210–23.

Wurm, L. H., Legge, G. E., Isenberg, L. M., and Luebker, A. (1993). Color improves object recognition in normal and low vision. *Journal of Experimental Psychology. Human perception and performance*, 19(4):899–911.

Young, T. (1801). The Bakerian Lecture. On the Theory of Ligh and Colours. *Philosophical Transactions of the Royal Society of London*, 92:12–48.

Zaidi, Q., Marshall, J., Thoen, H., and Conway, B. R. (2014). Evolution of neural computations: Mantis shrimp and human color decoding. *i-Perception*, 5(6):492–496.

Zeitz, C., Robson, A. G., and Audo, I. (2015). Congenital stationary night blindness: An analysis and update of genotypephenotype correlations and pathogenic mechanisms. *Progress in Retinal and Eye Research*, 45:58–110.

Zeki, S. (1980). The representation of colours in the cerebral cortex. *Nature*, 284:412–418.

Zhang, A.-J., Jacoby, R., and Wu, S. M. (2011). Light- and dopamine-regulated receptive field plasticity in primate horizontal cells. *Journal of Comparative Neurology*, 519(11):2125–34.

Zurek, D. B., Cronin, T. W., Taylor, L. a., Byrne, K., Sullivan, M. L., and Morehouse, N. I. (2015). Spectral filtering enables trichromatic vision in colorful jumping spiders. *Current Biology*, 25(10):R403–R404.